2018

Combining Observations Of Soils And Streams To Investigate Trends Caused By Reduced Acid Depositon In The Sleepers River Watershed

Jesse Armfield
University of Vermont

COMBINING OBSERVATIONS OF SOILS AND STREAMS TO INVESTIGATE TRENDS CAUSED BY REDUCED ACID DEPOSITON IN THE SLEEPERS RIVER WATERSHED

A Thesis Presented

by

Jesse R. Armfield

to

The Faculty of the Graduate College

of

The University of Vermont

In Partial Fulfillment of the Requirements
for the Degree of Master of Science
Specializing in Geology

October, 2018

Defense Date: August 10, 2018
Thesis Examination Committee:

Julia N. Perdrial, Ph.D., Advisor
Donald S. Ross, Ph.D., Chairperson
Nicolas Perdrial, Ph.D.
Cynthia J. Forehand, Ph.D., Dean of the Graduate College

ABSTRACT

Acid deposition forms when emission-derived sulfur dioxide and nitrogen oxides interact with precipitation and was particularly severe in the northeastern US. Effects of acid deposition include declining soil quality due to low pH and base cation leaching, which subsequently altered the composition of soil solution, ground water (GW) and eventually stream water. Because of the high buffering capacity of carbonates, watersheds underlain by carbonate rich rocks have received limited attention in acid deposition studies, however, carbonate weathering by strong anthropogenic acids can increase atmospheric CO_2 levels. Emission reductions due to the Clean Air Act and Amendments has led to a substantial reduction of acid deposition and many ecosystems are now recovering and stream water contains contain lower concentrations of acid anions and base cations. However, the effects of recovery on watershed soil, soil solution, and GW composition, which potentially varies with landscape position, are not well constrained. The objective of this study was therefore to investigate links between soils and water composition in a watershed with important carbonate contents in the underlying rock, the Sleepers River Research Watershed (SRRW). Using long-term datasets that span the recovery period, temporal trends (1991-2015) for acid anions (sulfate and nitrate), pH, base cations (Ca, Na) and Si were investigated for stream water. Trends with time, depth, and landscape position (hilltop, hillslope, and riparian zone) were assessed for the same solutes in GW and soil solution (2004-2013). Furthermore, soil elemental composition and mineralogy in archived (1996) and modern (2017) soil samples were analyzed to investigate changes in soil composition due to base cation leaching and carbonate weathering with time and landscape position. Results indicate that SRRW is indeed recovering from acidification as evidenced by declining sulfate content and rising pH in stream water, GW, and soil solution. Additionally, Ca typically derived from carbonate weathering decreased progressively with time in GW and decreased in soil solution at various landscape positions due to reduced leaching. However, Ca in stream water shows slight increases, likely due to Ca released from riparian soil stores. Spatial heterogeneity is especially pronounced in headwater catchments with steep topography as evidenced by changes in solution and soil composition along hillslopes.

In addition to the paper submitted for publication (Chapter 2) to Frontiers in Earth Science – Biogeochemistry this thesis includes i) a background and literature review to inform the reader on pertinent topics, ii) an appendix containing additional soil data with figures, iii) and an appendix with additional aqueous phase data with figures.

CITATION PAGE

Material from this thesis has been submitted for publication to Frontiers in Earth Science on July 27, 2018 in the following form:

Armfield J.R., Perdrial J.N., Gagnon A., Ehrenkranz J., Perdrial N., Cincotta M., Ross D., Shanley J., Underwood K.L., Ryan P.. (2018). Does stream water composition at Sleepers River in Vermont reflect dynamic changes in soils during recovery from acidification? Frontiers in Earth Science

ACKNOWLEDGEMENTS

First off, I'd like to thank my advisor, Julia Perdrial for the endless guidance, support, and wisdom she provided throughout this research. Julia, I can't thank you enough for everything. I would also like to thank my committee members, Don Ross and Nico Perdrial, for their thoughtful feedback and input throughout this process. I would also like to thank Alex Gagnon and Jack Ehrenkranz for their help completing fieldwork, sample processing, and lab analyses. I had a great time working with Alex and Jack in the field and in the lab, they made this part of my research much more enjoyable and I have the utmost respect for you guys. Jamie Shanley, thank you for your numerous contributions to this research including data, advice, samples and for being so generally helpful when I had questions. Scott Bailey, thanks for the samples you provided as well as the valuable advice you gave me when I was starting this project. Kristen Underwood thank you for taking the time to help me with understand and perform statistical analyses as well as for the example scripts you provided. I would also like to extend my gratitude to Peter Ryan and Jody Smith for allowing me to use their lab facilities at Middlebury College, which generated important data for this research. Finally, I'd like to thank the Geology department at UVM for their continued support throughout my time at UVM.

TABLE OF CONTENTS

LIST OF FIGURES

Chapter 1: Comprehensive Literature Review

Chapter 2: Paper for Submission

Appendix A: ADDITIONAL SOIL DATA

CHAPTER 1: COMPREHENSIVE LITERATURE REVIEW

1.1 What is Weathering?

Weathering, i.e. the breakdown of bedrock and regolith through physical and chemical processes, is a key process shaping the terrestrial critical zone (CZ). This zone spans from the top of the tree canopy to the actively cycled groundwater and is often termed the zone of life, because life-sustaining ecosystem services are provided. For example, through the weathering process lithogenic nutrients are provided, soils developed, and CO_2 can be sequestered (Brantley et al., 2007; Perdrial et al., 2015; Spence and Telmer, 2002).

Physical weathering, such as frost wedging, fractures and abrades rocks into smaller fragments increasing the surface area to volume ratio. Chemical weathering occurs through multiple types of reactions such as oxidation/reduction (typical for sulfides and oxides), dissolution (typical for carbonates), and hydrolysis (typical for silicates). Weathering reactions can be congruent, such as the complete dissolution of calcite, or incongruent like the weathering of a feldspar to a clay and a dissolved component (Strawn et al., 2015). In congruent weathering reactions weathering-derived solutes are present in solution with the same stoichiometry as the mineral and reactant (e.g. $CaCO_3 + H_2CO_3 \rightarrow Ca^{2+} + 2HCO_3^-$;Strawn et al., 2015). However, incongruent weathering changes the stoichiometry of reactant vs. dissolved products because a solid phase is formed as well (e.g. $2KAlSi_3O_8 + 9H_2O + 2H^+ \rightarrow Al_2Si_2O_5(OH)_4 + 4H_4SiO_4 + 2K^+$; White et al., 2001). Chemical weathering through proton attack is strongly driven by the presence of organic and inorganic acids in aqueous solution (Berner and Berner, 2012). One important inorganic

acid supplying protons is carbonic acid, that forms when CO_2 dissolves in water according to $CO_2 + H_2O \rightarrow H_2CO_3$ (Strawn et al., 2015). Because most of the CO_2 for carbonic acid formation ultimately comes from the atmosphere, carbonic acid weathering of silicate minerals is a primary mechanism by which global atmospheric CO_2 is regulated on geologic time scales (Spence and Telmer, 2002). For example, in the weathering of orthoclase to kaolinite (i.e. $2KAlSi_3O_8 + 11H_2O + 2CO_2 \rightarrow Al_2Si_2O_5(OH)_4 + 4H_4SiO_4 + 2K^+ + 2HCO_3$), 2 moles of CO_2 are transferred into bicarbonate, an aqueous carbon species that can be sequestered in marine carbonates and only releases 1 mole of CO_2 during this process (i.e. $Ca^{2+} + 2HCO_3^- \rightarrow CaCO_3 + CO_2 + H_2O$). The net effect is therefore a sequestration of CO_2 on geologic timescales. However, when carbonates (not silicates) are weathered, especially when weathering is not driven by carbonic acid but by anthropogenic acids, CO_2 is produced and not consumed (e.g. $2CaCO_3 + H_2SO_4 \rightarrow 2Ca^{2+} + 2HCO_3^- + SO_4^{2-} \rightarrow CaCO_3 + CO_2 + SO_4^{2-} + Ca^{2+}$; Amiotte-Suchet et al., 1999; Huang et al., 2013; Liu et al., 2008).

1.2 Weathering and Soil Formation

The soil forming process is dependent on the five soil forming factors: time, climate, biology, relief, and parent material (Fanning and Fanning, 1989; Jenny, 1941). The weathering of bedrock and other soil parent materials (till, colluvium, alluvium, loess, etc.) is therefore an important factor controlling soil development (Fanning and Fanning, 1989). Bedrock is broken down into saprolite at the first phase of soil formation and retains much of the original rock structure but is mildly depleted of minerals that are unstable at earth's surface and secondary oxides can accumulate in fractures (Pavich et al., 1989). A

previously physically weathered medium (i.e. till) deposited over bedrock has different grain size and hydraulic conductivity than underlying bedrock and can therefore affect the pedogenic process.

Depending on each of the soil forming factors saprolite or a physically weathered media can weather further into a variety of developed soils through the weathering out of progressively more stable minerals towards the surface, the formation and translocation of pedogenic minerals, and the addition of organics (Pavich et al., 1989). Relief, one of the soil forming factors, plays an important role in weathering because dissolved weathering products are often transferred to low lying landscape positions, especially in regions with steep relief. In locations where weathering-derived solutes accumulate, e.g. in swales, secondary minerals can form. In contrast, secondary minerals from incongruent weathering can be left behind at hilltops and slopes, increasing the compositional heterogeneity of the near surface environment. The long-term effect of this process can be observed in soil catenas where landscape position is the primary control on soil composition (Fig. 1-1; Bonifacio et al., 1997; Olson et al., 2003; Schimel D. et al., 1985; Wiekenkamp et al., 2016). For example, work by Bonifacio et al. (1997) exemplifies the effect of landscape position and differences in soil drainage on a slope about 100m in length where 4 USDA soil orders were represented.

Relief also plays a large role in determining hydrologic flowpaths, fluid residence time, and soil drainage class which relates landscape position to weathering (Maher, 2011). Longer fluid residence times in the substrate allows the solution to approach equilibrium with the weathering front leading to higher concentrations of weathering-derived solutes

in solutions with longer fluid residence times (Maher, 2011). Solution in well drained hilltop soils is usually undersaturated with respect to the mineral assemblage, allowing weathering to progress, while soils downslope are closer to equilibrium and show fewer signs of weathering (Kim, 1999). For example, Lidman et al. (2017) showed that natural waters are progressively enriched in some weathering-derived solutes along flowpaths (Ca, K, Mg) but other solutes (Sr, Na, Rb, Cs, Si) have relatively uniform concentrations along flowpaths suggesting they are in equilibrium with the weathering front (Fig. 1-2).

1.2.1 Measuring Weathering

Because weathering leads to i) the breakdown of primary minerals and the formation of secondary minerals and ii) liberates dissolved species that can either accumulate in place or elsewhere and iii) leads to the transfer of solutes out of the CZ via streams, weathering is typically assessed by i) investigating the primary and secondary mineralogy of soils ii) comparing soils normalized to the composition of parent material and iii) monitoring the solute export of streams (Brantley et al., 2007; Johnson et al., 1981).

For example, the type of pedogenic (secondary) minerals such as illite vs. the primary muscovite content can be used to qualitatively assess the degree to which a soil horizon is weathered. (Hawkins and Graham, 2017; Strawn et al., 2015). Mineralogical investigations also track mineral transformations by horizon or landscape position, as demonstrated by Hawkins and Graham (2017) where kaolin group minerals dominated the clay fraction of the well-drained upper slopes soils while smectites dominated the lower slope soils and precipitated due to excess weathering-derived solutes sourced from upslope.

Comparing soils normalized to the composition of parent material and an immobile element with depth allows for the conceptualization of vertical chemical gradients (Brantley et al., 2007). The shape of the pattern produced by the values on these normalized chemical gradients, termed "tau values" (see eq. 1), can be used to understand the long-term evolution of a soil profile (Fig. 1-3; Brantley et al., 2007). A negative tau value of a given element indicates that it was removed from a soil and a positive tau value indicates an accumulation (Fig. 1-3; Brantley et al., 2007). Plotting tau values versus depth allows for an assessment of the cycling of an element and a quantification of the degree of weathering of that element relative to parent material while accounting for volume changes and apparent dilution/enrichment (Brantley et al., 2007; Brimhall and Dietrich, 1987). Investigations of many soils led to the definition of 5 end-member types of soil profiles including immobile (i.e. no change), depletion (i.e. all horizons depleted), depletion-enrichment (i.e. upper horizons depleted, lower horizons enriched), addition (i.e. shallow horizons enriched), and biogenic (i.e. enriched at the surface, depleted at depth; Brantley et al., 2007). However, most soils show some combination of these end-member patterns.

Monitoring solute export from streams is a classic comprehensive approach to quantify weathering while accounting for the interconnectedness of the CZ and has been used extensively (Berner and Berner, 2012; Johnson et al., 1981; Taylor and Velbel, 1991; Vebel, 1985). This approach requires computing chemical flux out of the watershed, inputs from precipitation, as well as estimating biological uptake and release (Berner and Berner, 2012) and is a common approach to quantify weathering and base cation leaching in acid deposition studies (Garmo et al., 2014; Johnson et al., 1981; Newell and Skjelkvåle, 1997;

Skjelkvåle et al., 2001; Skjelkvåle, 2003; Skjelkvåle et al., 2005). Once additional factors (e.g. biological uptake/release, wet/dry inputs) are accounted for an increase in solute export is considered to indicate increased weathering and a decrease in this export indicates decreased weathering (Johnson et al., 1981; Peters and Aulenback, 2009; Vebel, 1985).

1.3 Acid Deposition

Because of the importance of proton proliferation for most chemical weathering processes and soil leaching, the deposition of strong anthropogenic acids on many ecosystems in the northeastern US, central Europe and more recently China, is relevant (Rice and Herman, 2012). This acid deposition, or "acid rain", was first recognized in the United States at the Hubbard Brook Experimental Forest by Gene Likens (Likens et al., 1972) and causes as well as effects have been studied extensively since (Driscoll et al., 2001).

Technology invented during the Industrial Revolution caused a rapid increase in fossil fuel emissions which generated SO_2, NO_x, and CO_2 in excess of background conditions leading to acidic precipitation throughout many industrialized regions (Newell & Skjelkvåle, 1997). The interaction between atmospheric N and S oxides with precipitation leads to the formation of strong acids such as H_2SO_4 and HNO_3 which are subsequently deposited on earth's surface (Fig. 1-4; Berner and Berner, 2012). Strong acid deposition supplies additional protons to the CZ increasing weathering rates, leaching rates, and mobilizing Al (Driscoll et al., 2001; Johnson et al., 1981; Matzner and Murach, 1995; Raddum et al., 2007). Acid deposition can increase weathering rates and free lithogenic nutrients, however, this process also accelerates soil leaching so that soils become depleted albeit increased weathering (Peters and Aulenback, 2009). The ensuing ecological effects

of acid deposition are systemic and include reduced tree growth, increased tree mortality, a reduced species diversity and a reduced abundance of aquatic wildlife (Driscoll et al., 2001; Matzner and Murach, 1995; Raddum et al., 2007).

1.3.1 Recovery from Acidification

Acid deposition peaked in the US in 1969 prompting emission abatement strategies, such as the Clean Air Act of 1970 and the Clean air amendments of 1990, which have rapidly reduced the amount of SO_2 released into the atmosphere (Fig. 1-5; Rice and Herman, 2012; Smith et al., 2010). In turn, reduced emissions have led to a reversal of many of the changes caused by acidification such as an increase in the pH of precipitation and a decrease in the quantity of acid anions deposited, i.e. chemical recovery (Fig. 1-6; Driscoll et al., 2001; Garmo et al., 2014; Kopáček et al., 2016).

Although early work showed only limited signs of recovery due to watershed storage of acids (Likens et al., 1996) recent meta-data studies have documented important wide-spread decreases in sulfate, aluminum, and base cations concentrations in waters of recovering regions (Fig. 1-7; Garmo et al., 2014; Rogora et al., 2013). Despite wide-spread signs of chemical recovery, biological recovery is slow and is currently limited to less acid sensitive systems (de Wit et al., 2007). Data from the Hubbard Brook Experimental Forest suggests that further emissions reductions will be necessary to allow for full recovery of sensitive ecosystems (Driscoll et al., 2001).

1.4 The Sleepers River Research Watershed (SRRW)

Sensitivity to acidification is a function of the buffering capacity of bedrock and soils. For example, watersheds that are underlain by bedrock containing carbonates can buffer soil pH much more effectively, potentially offsetting some of the detrimental effects of acid inputs. The SRRW watershed in northeastern Vermont (Fig. 1-8) is one example of a well-buffered system because it is underlain by the laterally extensive Waits River Formation which contains variable amounts of carbonates (Ferry, 1991; Ratcliffe et al., 2011). At SRRW bedrock is covered by 1-4 m of dense, silty till from the last glaciation (Wisconsinan; Shanley, 2000), which is primarily composed of the Waits River Formation, but contains lesser amounts of the Gile Mountain Formation, the Missisquoi Formation, and undifferentiable Devonian granites (Hornbeck et al., 1997). Importantly, the till contains a mix of silicates and carbonates, which exert and important control on the chemistry of the watershed (Hornbeck et al., 1997; Shanley, 2000).

Elevation and landscape position are the primary controls on soil composition in the SRRW watershed: Spodosols are developed primarily in the well-drained upland and are the most prevalent soil type above ~ 600m of elevation (Kendall et al., 1999). Below this threshold Inceptisols are the dominant soil order (Kendall et al., 1999) while Histosols are prevalent only in the riparian zone (Shanley et al., 2004). Typical vegetation at SRRW is northern hardwood including sugar maple, yellow birch, white ash, and American beech trees with lesser amounts of conifers (balsam fir and red spruce; Shanley, 2000; Shanley et al., 2004).

SRRW is an ideal testbed to investigate how bedrock weathering, topography and flowpaths interact to shape the CZ response to acid deposition, because the watershed

received acid deposition, presents an undulating topography with landscape position controls on soil order, contains important amounts of carbonates that weather readily, and has provided records of data on stream water composition and discharge as well as soil solution and GW composition data.

1.5 Figures

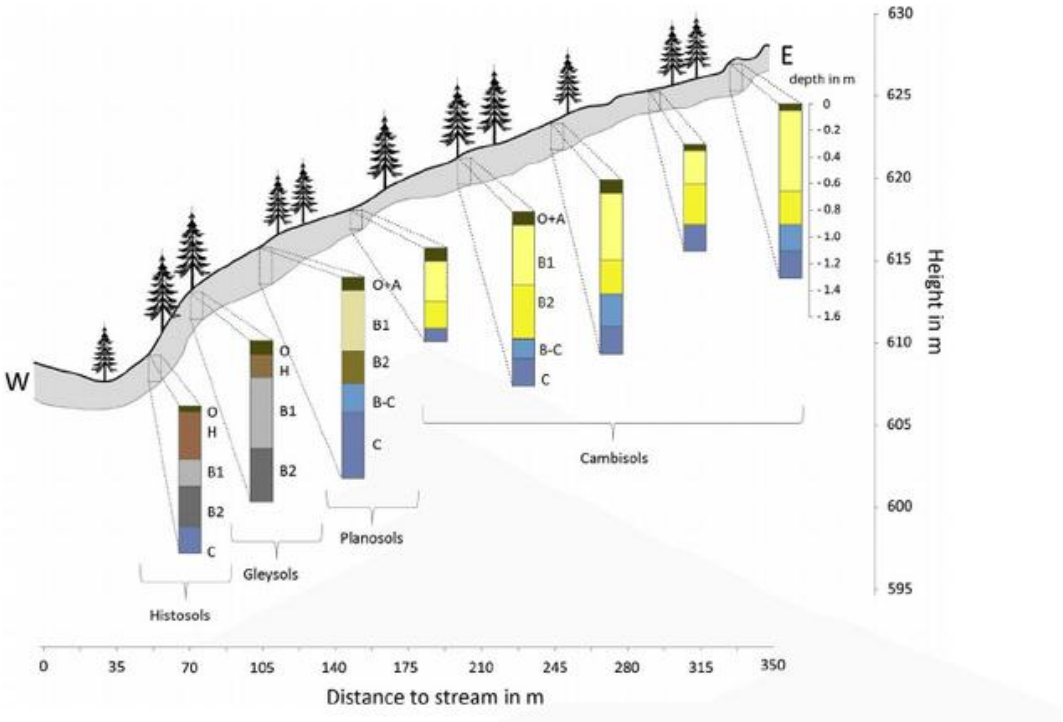

Figure 1-1. The catena in the Wüstebach catchment in Germany exemplifying landscape position controls on soil order (Wiekenkamp et al., 2016).

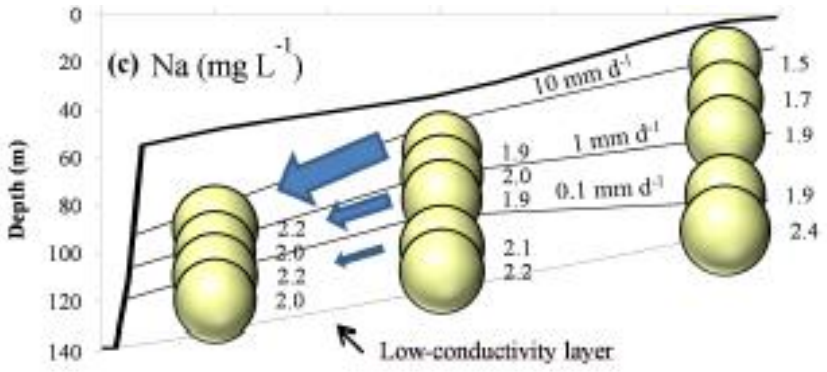

Figure 1-2. Chemostatic conditions for Na along a hillslope in the Krycklan catchment in northern Sweden. Blue arrows show flow direction and magnitude of hydraulic conductivity measurements (mm d^{-1}; Modified from: Lidman et al., 2017).

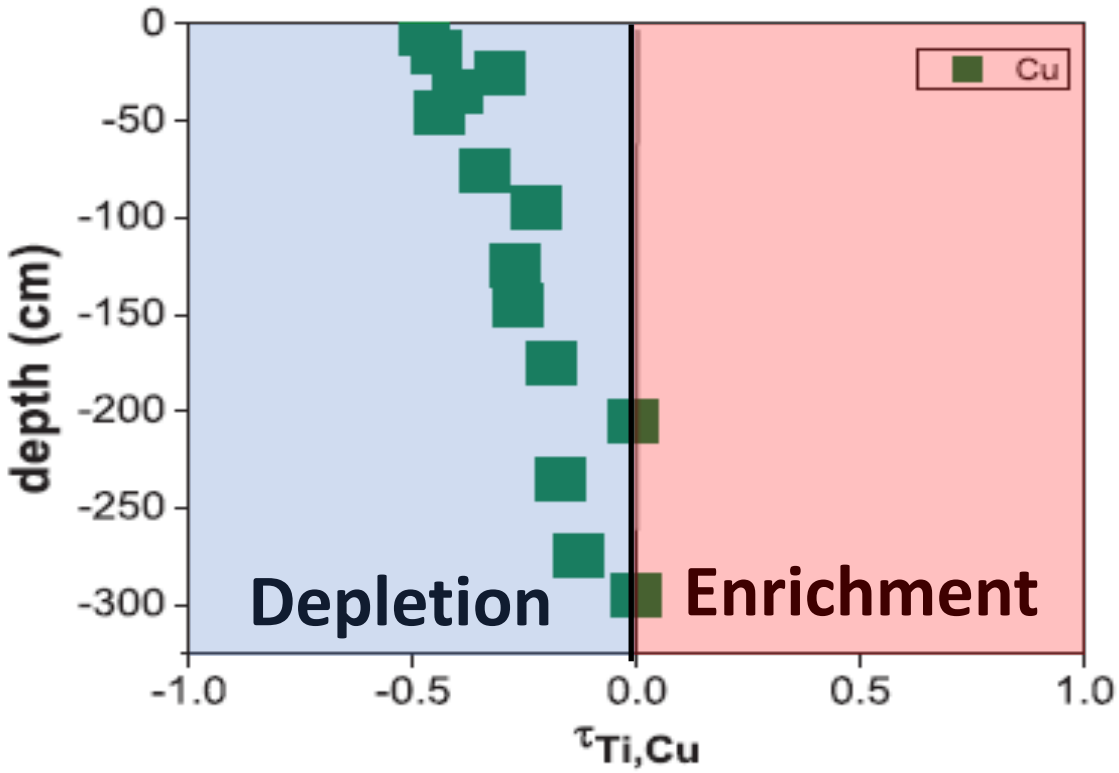

Figure 1-3. Tau plot of a typical depletion profile where negative tau values (blue shading) indicate soil copper (Cu) content is relatively depleted with respect to the underlying parent materials (Modified from Brantley et al., 2007).

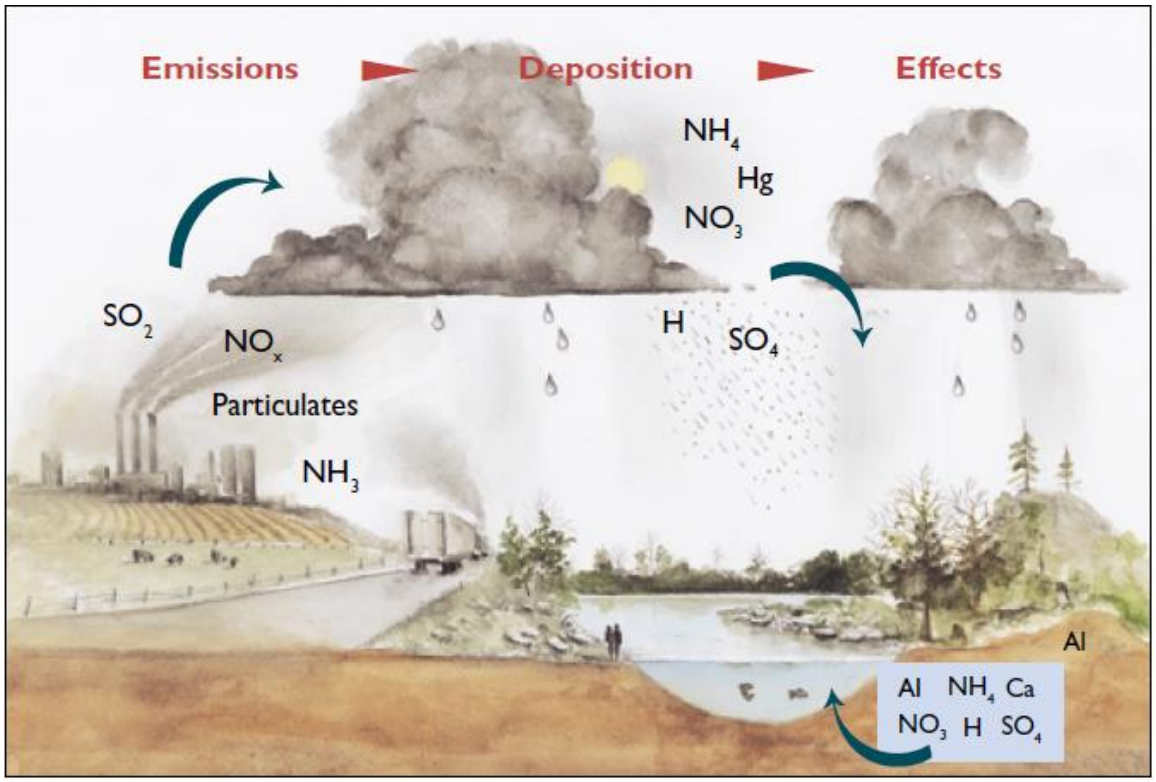

Figure 1-4. Generation of strong, anthropogenic acids from emission and subsequent deposition downwind leading to soil leaching (Driscoll et al., 2001).

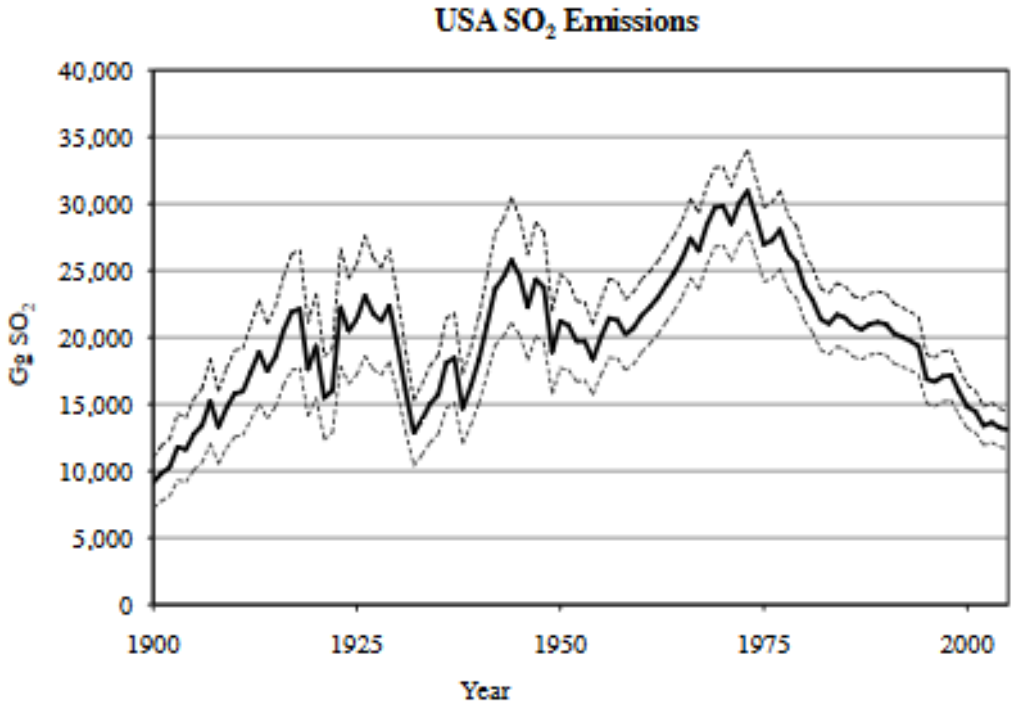

Figure 1-5. Total SO_2 emissions in the USA have declined significantly since the implementation of the Clean Air Act in 1970 (Smith et al., 2010).

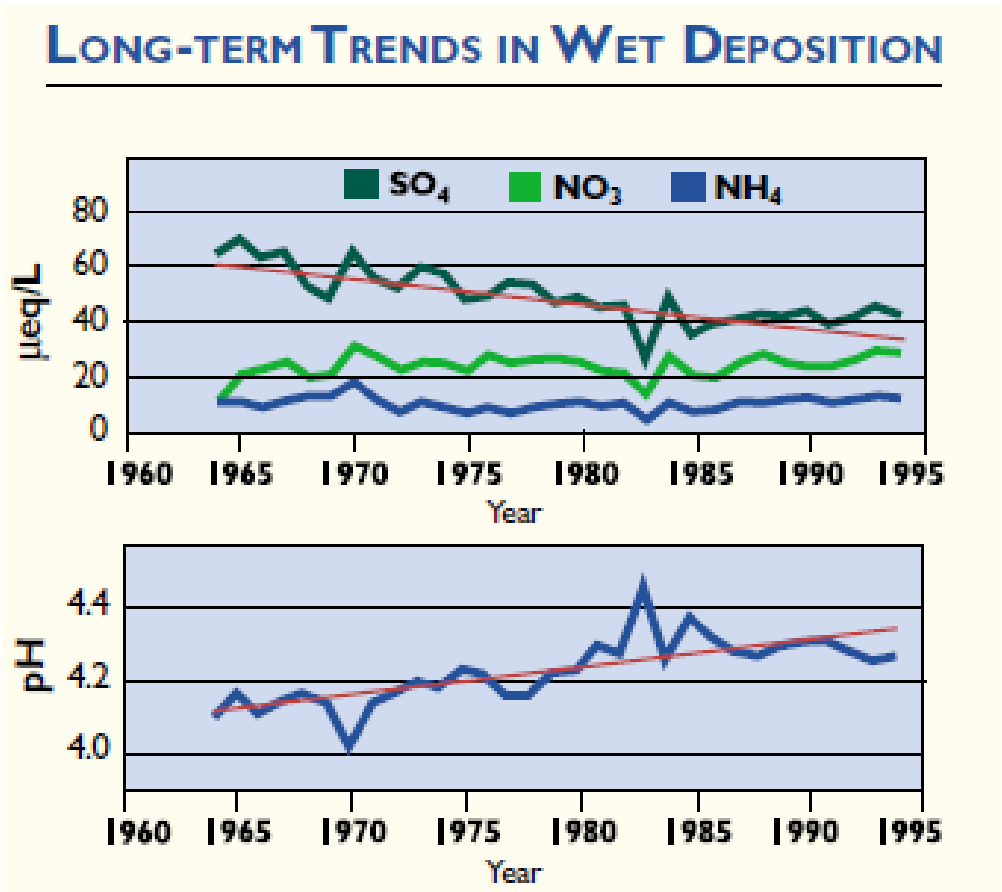

Figure 1-6. Long-term trends in precipitation chemistry at the recovering Hubbard Brook Experimental Forest (Driscoll et al., 2001). Red linear fits indicate statistically significant trends.

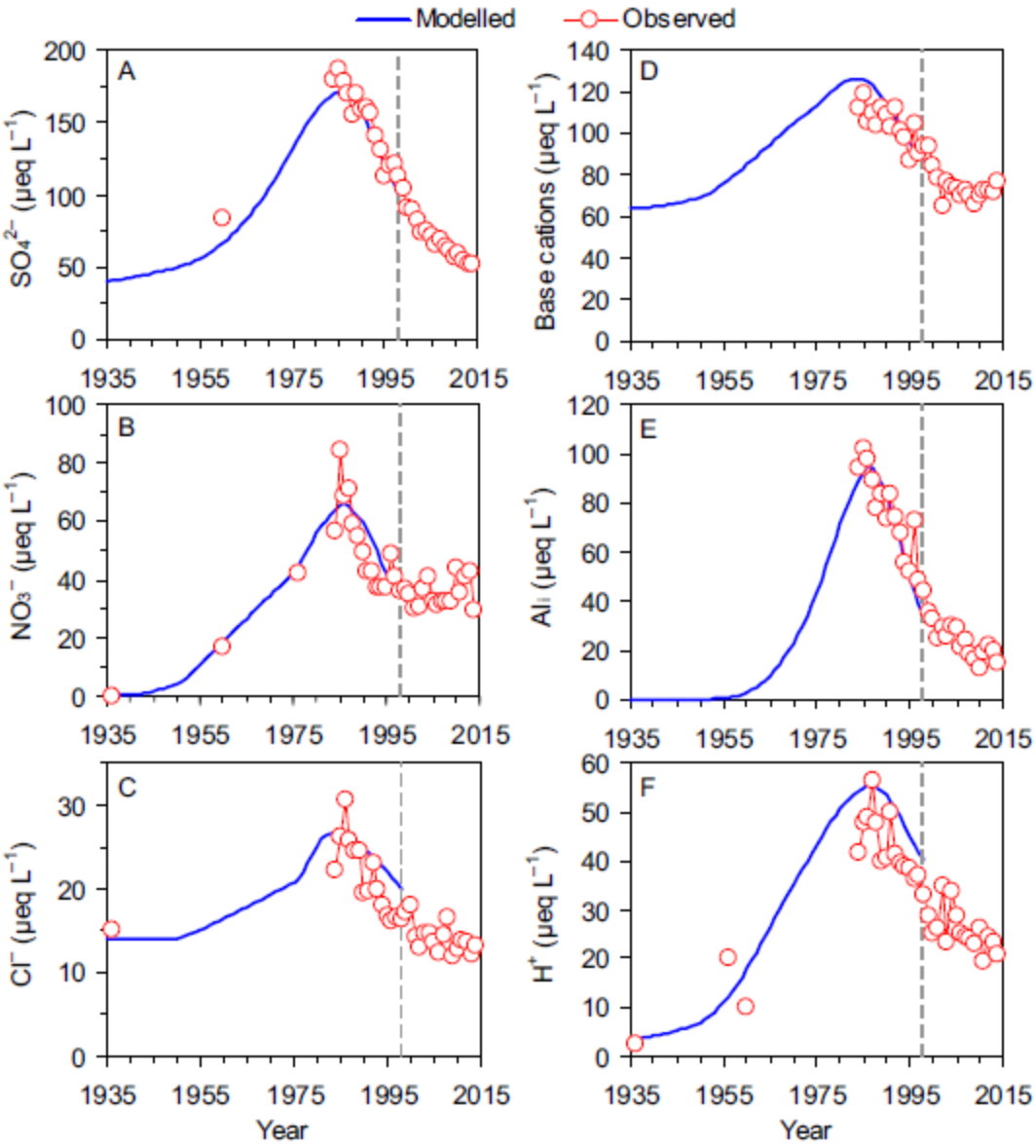

Figure 1-7. Modeled (blue line) and observed (dots) concentrations of dissolved species and protons associated with acidification and recovery in Certovo Lake in the Czech Republic. Trends in this lake show clear signals of recovery from anthropogenic acid deposition (Kopáček et al., 2016).

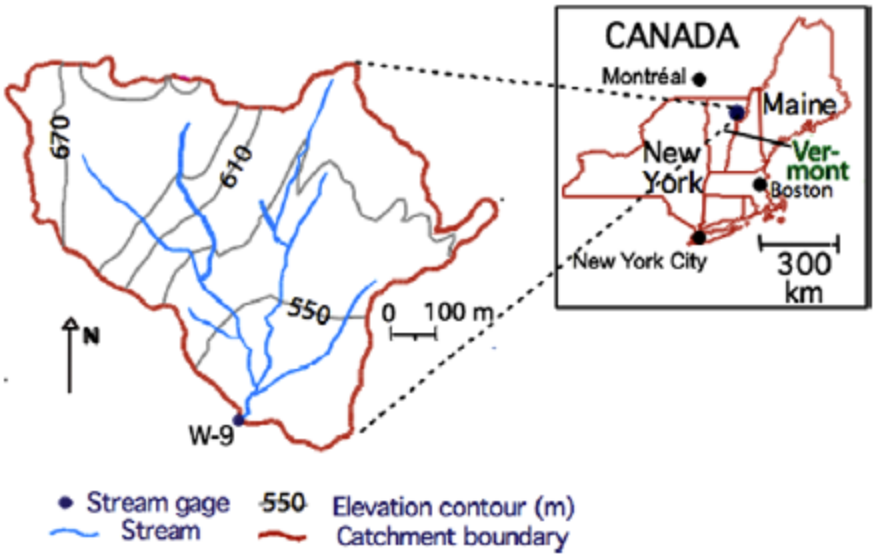

Figure 1-8. location of the forested head watershed of Sleeper River (W-9) in northeastern Vermont (Modified from Mayer et al., 2010).

1.6 References

Amiotte-Suchet, P., Aubert, D., Probst, J.L., Gauthier-Lafaye, F., Probst, A., Andreux, F., Viville, D., 1999. δ13C pattern of dissolved inorganic carbon in a small granitic catchment: the Strengbach case study (Vosges mountains, France). Chem. Geol. 159, 129–145. https://doi.org/10.1016/S0009-2541(99)00037-6

Appling, A.P., Leon, M.C., McDowell, W.H., 2015. Reducing bias and quantifying uncertainty in watershed flux estimates: the R package loadflex., Ecosphere 6(12):269.

Bailey, S.W., Brousseau, P.A., McGuire, K.J., Ross, D.S., 2014. Influence of landscape position and transient water table on soil development and carbon distribution in a steep, headwater catchment. Geoderma 226–227, 279–289. https://doi.org/10.1016/j.geoderma.2014.02.017

Berner, E.K., Berner, R.A., 2012. Chemical Weathering: Minerals, Plants, and Water Chemistry, in: Global Environment: Water, Air, and Geochemical Cycles. Princeton University Press, pp. 151–184.

Bishop, K., Seibert, J., Köhler, S., Laudon, H., 2004. Resolving the Double Paradox of rapidly mobilized old water highly variable responses in runoff chemistry. Hydrol. Process. 18, 185–189. https://doi.org/10.1002/hyp.5209

Bonifacio, E., Zanini, E., Boero, V., Franchini-Angela, M., 1997. Pedogenesis in a soil catena on serpentinite in north-western Italy. Geoderma 75, 33–51. https://doi.org/10.1016/S0016-7061(96)00076-6

Brantley, S.L., Goldhaber, M.B., Ragnarsdottir, K.V., 2007. Crossing Disciplines and Scales to Understand the Critical Zone. Elements 3, 307–314.

Brimhall, G.H., Dietrich, W.E., 1987. Constitutive mass balance relations between chemical composition, volume, density, porosity, and strain in metasomatic hydrochemical systems: Results on weathering and pedogenesis. Geochim. Cosmochim. Acta 51, 567–587. https://doi.org/10.1016/0016-7037(87)90070-6

Burns, D.A., McHale, M.R., Driscoll, C.T., Roy, K.M., 2005. Response of Surface Water Chemistry to Reduced Levels of Acid Precipitation: Comparison of Trends in Two regions of New York, USA. Hydrol. Process. 20, 1611–1627.

Cerling, T.E., 1984. The stable isotopic composition of modern soil carbonateand its relationship to climate. Earth Planet. Sci. Lett. 71, 229–240.

Cronan, C.S., Schofield, C.L., 1979. Aluminum leaching response to Acid precipitation: effects on high-elevation watersheds in the northeast. Science 204, 304–306.

Dawson, J.J., Bakewell, C., Billett, M.F., 2001. Is in-stream processing an important control on spatial changes in carbon fluxes in headwater catchments? Sci Total Env. 265, 153–67.

de Wit, H., Skjelkvåle, B.L., Høgåsen, T., Clair, T., Colombo, L., Fölster, J., Jeffries, D., László, B., Majer, V., Monteith, D., Mosello, R., Rogora, M., Rzychon, D.,

Steingruber, S., Stivrina, S., Stoddard, J.L., Srybny, A., Talkop, R., Vesely, J., Vuorenmaa, J., Wieting, J., Worsztynowicz, A., 2007. Trends in surface water chemistry and biota; The importance of confounding factors: 2. Trends in surface water chemistry 1994-2004. NIVA Rep. 5385-2007, ICP Waters Report 87/2007 12–28.

Driscoll, C.T., Lawrence, G.B., Bulger, T.J., Cronan, C.S., Eagar, C., Lambert, K.F., Likens, G.E., Stoddard, J.L., Weathers, K.C., 2001. Acid Rain Revisited: Advances in Scientific Understanding Since the Passage of the 1970 and 1990 Clean Air Amendments 1.

Fanning, D.S., Fanning, M.C.B., 1989. Soil Morphology, Genesis, and Classification.

Ferry, J.M., 1991. Regional Metamorphism of the Waits River Formation, Eastern Vermont: Delineatoin of a New Type of Giant Metamorphic Hydrothermal System. J. Petrol. 33, 45–94.

Frisbee, M.D., Phillips, F.M., Campbell, A.R., Liu, F., Sanchez, S.A., 2011. Streamflow generation in a large, alpine watershed in the southern Rocky Mountains of Colorado: Is streamflow generation simply the aggregation of hillslope runoff responses? Water Resour. Res. 47.

Garmo, Ø.A., Skjelkvåle, B.L., de Wit, H.A., Colombo, L., Curtis, C., Fölster, J., Hoffmann, A., Hruška, J., Høgåsen, T., Jeffries, D.S., Keller, W.B., Krám, P., Majer, V., Monteith, D.T., Paterson, A.M., Rogora, M., Rzychon, D., Steingruber, S., Stoddard, J.L., Vuorenmaa, J., Worsztynowicz, A., 2014. Trends in Surface Water Chemistry in Acidified Areas in Europe and North America from 1990 to 2008. Water. Air. Soil Pollut. 225, 1880. https://doi.org/10.1007/s11270-014-1880-6

Hawkins, W.A., Graham, R.C., 2017. Soil Mineralogy of a Vernal Pool Catena in Southern California. Soil Mineral.

Hornbeck, J.., Bailey, S.., Buso, D.., Shanley, J.., 1997. Streamwater chemistry and nutrient budgets for forested watersheds in New England: variability and management implications. For. Ecol. Manag. 93, 73–89. https://doi.org/10.1016/S0378-1127(96)03937-0

Huang, Q.B., Qin, X.Q., Liu, P.Y., Zhang, L.K., Su, C.T., 2017. Impact of sulfuric and nitric acids on carbonate dissolution, and the associated deficit of CO2 uptake in the upper-middle reaches of the Wujiang River, China. J Contam Hydrol 203, 18–27. https://doi.org/10.1016/j.jconhyd.2017.05.006

Jenny, H., 1941. Factors of soil formation. McGraw-Hill, New York.

Jin, L., Ravella, R., Ketchum, B., Bierman, P.R., Heaney, P., White, T., Brantley, S.L., 2010. Mineral weathering and elemental transport during hillslope evolution at the Susquehanna/Shale Hills Critical Zone Observatory. Geochim. Cosmochim. Acta 74, 3669–3691. https://doi.org/10.1016/j.gca.2010.03.036

Johnson, C.E., Driscoll, C.T., Siccama, T.G., Likens, G.E., 2000. Element Fluxes and Landscape Position in a Northern Hardwood Forest Watershed Ecosystem. Ecosystems 3, 159–184. https://doi.org/10.1007/s100210000017

Johnson, N.M., Driscoll, C.T., Eaton, J.S., Likens, G.E., McDowell, W.H., 1981. "Acid rain", dissolved aluminum and chemical weathering at the Hubbard Brook Experimental Forest, New Hampshire. Geochim. Cosmochim. Acta 45, 1421–1437. https://doi.org/10.1016/0016-7037(81)90276-3

Kendall, K.., Shanley, J.., McDonnell, J.., 1999. A hydrometric and geochemical approach to test the transmissivity feedback hypothesis during snowmelt. J. Hydrol. 219, 188–205. https://doi.org/10.1016/S0022-1694(99)00059-1

Kim, K., 1999. Geochemical evolution of groundwater along a flowpath determined from oxygen isotope analysis in a carbonate free, silicate aquifer. Geosci. J. 3, 191–200. https://doi.org/10.1007/BF02910490

Kopáček, J., Hejzlar, J., Kaňa, J., Porcal, P., Turek, J., 2016. The Sensitivity of Water Chemistry to Climate Forested, Nitrogen-Saturated Catchment Recovering from Acidification. Ecol. Indic. 63, 196–208.

Lagaly, G., 1993. Reaktionen des Tonminerale, in: Jasmund K, Lagaly G (Eds.), Tonminerale Und Tone: Struktur, Eigenschaften Und Einsatz in Industrie Und Umwelt. Steinkopff Verlag, Darmstadt, pp. 89–167.

Lawrence, G.B., Hazlett, P.W., Fernandez, I.J., Ouimet, R., Bailey, S.W., Shortle, W.C., Smith, K.T., Antidormi, M.R., 2015. Declining Acidic Deposition Begins Reversal of Forest-Soil Acidification in the Northeastern U.S. and Eastern Canada. Environ. Sci. Technol. 49, 13103–13111. https://doi.org/10.1021/acs.est.5b02904

Lidman, F., Boily, A., Laudon, H., Köhler, S.J., 2017. From soil water to surface water – how the riparian zone controls element transport from a boreal forest to a stream. Biogeosciences 14, 3001–3014. https://doi.org/10.5194/bg-14-3001-2017

Likens, G.E., Bormann, F.H., Johnson, N.M., 1972. Acid Rain. Environ. Sci. Policy Sustain. Dev. 14, 33–40. https://doi.org/10.1080/00139157.1972.9933001

Likens, G.E., Driscoll, C.T., Buso, D.C., 1996. Long-term effects of acid rain: response and recovery of a forest ecosystem. Science 272, 244–246.

Lybrand, R.A., Rasmussen, C., 2015. Quantifying Climate and Landscape Position Controls on Soil Development in Semiarid Ecosystems. Soil Sci. Soc. Am. J. 79, 104–116. https://doi.org/10.2136/sssaj2014.06.0242

Maher, K., 2011. The role of fluid residence time and topographic scales in determining chemical fluxes from landscapes. Earth Planet. Sci. Lett. 312, 48–58. https://doi.org/http://dx.doi.org/10.1016/j.epsl.2011.09.040

Matzner, E., Murach, D., 1995. Soil changes induced by air pollutant deposition and their implication for forests in central Europe. Water. Air. Soil Pollut. 85, 63–76. https://doi.org/10.1007/BF00483689

Mayer, B., Shanley, J.B., Bailey, S.W., Mitchell, M.J., 2010. Identifying sources of stream water sulfate after a summer drought in the Sleepers River watershed (Vermont, USA) using hydrological, chemical, and isotopic techniques. Appl. Geochem. 25, 747–754. https://doi.org/10.1016/j.apgeochem.2010.02.007

McIntosh, J.C., Schaumberg, C., Perdrial, J., Harpold, A., Vázquez-Ortega, A., Rasmussen, C., Vinson, D., Zapata-Rios, X., Brooks, P.D., Meixner, T., Pelletier, J., Derry, L., Chorover, J., 2017. Geochemical evolution of the Critical Zone across variable time scales informs concentration-discharge relationships: Jemez River Basin Critical Zone Observatory. Water Resour. Res. n/a-n/a. https://doi.org/10.1002/2016WR019712

McLeod, A.I., 2011. Kendall: Kendall rank correlation and Mann-Kendall trend test.

Meybeck, M., 1993. Riverine transport of atmospheric carbon: Sources, global typology and budget. Water. Air. Soil Pollut. 70, 443–463. https://doi.org/10.1007/BF01105015

Moore, D.M., Reynolds, R.C., 1997. X-Ray Diffraction and the Identification and Analysis of Clay Minerals, 2nd ed. New York: Oxford University Press.

Mulholland, P.J., Hill, W.R., 1997. Seasonal patterns in streamwater nutrient and dissolved organic carbon concentrations: Separating catchment flow path and in-stream effects. Water Resour Res 33, 1297–1306. https://doi.org/10.1029/97wr00490

Newell, A.D., Skjelkvåle, B.L., 1997. Acidification Trends in Surface Waters in the International Program on Acidification of Rivers and Lakes. Water. Air. Soil Pollut. 93, 27–57. https://doi.org/10.1023/A:1022126704750

Nezat, C.A., Blum, J.D., Klaue, A., Johnson, C.E., Siccama, T.G., 2004. Influence of landscape position and vegetation on long-term weathering rates at the Hubbard Brook Experimental Forest, New Hampshire, USA11Associate editor: K. L. Nagy. Geochim. Cosmochim. Acta 68, 3065–3078. https://doi.org/10.1016/j.gca.2004.01.021

Olson, K.R., Jones, R.L., Gennadiyev, A.N., Chernyanskii, S., Woods, W.I., Lang, J.M., 2003. SOIL CATENA FORMATION AND EROSION OF TWO MISSISSIPPIAN MOUNDS AT CAHOKIA ARCHAEOLOGICAL SITE, ILLINOIS. Soil Sci. 168.

Pavich, M.J., Obermeier, L., Estabrook, J.R., 1989. Investigations of the characteristics, origin, and residence time of the Upland residual mantle of the Piedmont of Fairfax County, Virginia. (U.S. Geological Survey professional paper No. 1352).

Perdrial, J., Thompson, A., Chorover, J., 2015. Chapter 6 - Soil Geochemistry in the Critical Zone: Influence on Atmosphere, Surface- and Groundwater Composition, in: John R. Giardino and Chris Houser (Ed.), Developments in Earth Surface Processes. Elsevier, pp. 173–201. https://doi.org/10.1016/B978-0-444-63369-9.00006-9

Perdrial, J.N., Warr, L.N., Perdrial, N., Lett, M.-C., Elsass, F., 2009. Interaction between smectite and bacteria: Implications for bentonite as backfill material in the disposal of nuclear waste. Chem. Geol. 264, 281–294. https://doi.org/10.1016/j.chemgeo.2009.03.012

Peters, N., Aulenback, B., 2009. Flowpath Contributions of Weathering Products to Stream Fluxes at the Panola Mountain Research Watershed, Georgia.

Pohlert, T., 2018. trend: Non-Parametric Trend Tests and Change-Point Detection.

Poppe, L.J., Paskevich, V.F., Hathaway, J.C., Blackwood, D.S., 2001. A Laboratory manua for X-Ray Powder Diffraction (Open-File No. 1–41). USGS.

R Core Development Team, 2017. R: A language and environment for statistical computing. R Foundation for statistical computing, Vienna, Austria.

Raddum, G.G., Fjellheim, A., Erikson, L., Fott, J., Halvorsen, G.A., Heegaard, E., Kohout, L., Kifinger, B., Schaumberg, J., Maetze, A., Zahn, H., 2007. Trends in surface water chemistry and biota; The importance of confounding factors: 5. Biological recovery. NIVA Rep. 5385-2007, ICP Waters Report 87/2007 50–63.

Ratcliffe, N., Stanley, R., Gale, M., Thompson, P., Walsh, G., 2011. Bedrock Geologic Map of Vermont. USGS Scientific Investigations Series Map 3184.

Rice, K.C., Herman, J.S., 2012. Acidification of Earth: An assessment across mechanisms and scales. Appl. Geochem. 27, 1–14. https://doi.org/10.1016/j.apgeochem.2011.09.001

Rogora, M., Colombo, L., Lepori, F., Marchetto, A., Steingruber, S., Tornimbeni, O., 2013. Thirty Years of Chemical Changes in Alpine Acid-Sensitive Lakes in the Alps. Water. Air. Soil Pollut. 224, 1746. https://doi.org/10.1007/s11270-013-1746-3

Runkel, R.L., Crawford, C.G., Cohn, T.A., 2004. Load estimator (LOADEST): a FORTRAN program for estimating constituent loads in streams and rivers. USGS Techniques and Methods Book 4, Chapter A5., U.S. Geological Survey, Reston, Virginia, USA.

Schimel D., Stillwell M. A., Woodmansee R. G., 1985. Biogeochemistry of C, N, and P in a Soil Catena of the Shortgrass Steppe. Ecology 66, 276–282. https://doi.org/10.2307/1941328

Schuster, P.F., Shanley, J., Marvin-Dipasquale, M., Reddy, M.M., Aiken, G.R., Roth, D.A., Taylor, H.E., Krabbenhoft, D.P., DeWild, J.F., 2007. Mercury and Organic

Carbon Dynamics During Runoff Episodes from a Northeastern USA Watershed. Water. Air. Soil Pollut. 187, 89–108.

Sebestyen, S.D., Boyer, E.W., Shanley, J.B., Kendall, C., Doctor, D.H., Aiken, G.R., Ohte, N., 2008. Sources, transformations, and hydrological processes that control stream nitrate and dissolved organic matter concentrations during snowmelt in an upland forest. Water Resour. Res. 44, W12410. https://doi.org/10.1029/2008WR006983

Shanley James B., Chalmers Ann T., Mack Thomas J., Smith Thor E., Harte Philip T., 2016. Groundwater Level Trends and Drivers in Two Northern New England Glacial Aquifers. JAWRA J. Am. Water Resour. Assoc. 52, 1012–1030. https://doi.org/10.1111/1752-1688.12432

Shanley, J.B., 2000. Sleepers River Watershed -- A USGS WEBB Program Site: U.S. Geological Survey Fact Sheet.

Shanley, J.B., Kram, P., Hruska, J., Bullen, T.D., 2004. A biogeochemical comparison of two well-buffered catchments with contrasting histories of acid deposition. Water Air Soil Pollut. Focus 4, 325–342. https://doi.org/10.1023/B:WAFO.0000028363.48348.a4

Skjelkvåle, B.L., 2003. The 15-year report: Assessment and monitoring of surface waters in Europe and North America; acidification and recovery, dynamic modelling and heavy metals. NIVA Rep. 4716-2003, ICP Waters Report 73/2003.

Skjelkvåle, B.L., Stoddard, J.L., Andersen, T., 2001. Trends in Surface Water Acidification in Europe and North America (1989–1998). Water. Air. Soil Pollut. 130, 787–792. https://doi.org/10.1023/A:1013806223310

Skjelkvåle, B.L., Stoddard, J.L., Jeffries, D.S., Tørseth, K., Høgåsen, T., Bowman, J., Mannio, J., Monteith, D.T., Mosello, R., Rogora, M., Rzychon, D., Vesely, J., Wieting, J., Wilander, A., Worsztynowicz, A., 2005. Regional scale evidence for improvements in surface water chemistry 1990–2001. Recovery Acidif. UK Evid. 15 Years Acid Waters Monit. Acidif. UK Evid. 15 Years Acid Waters Monit. 137, 165–176. https://doi.org/10.1016/j.envpol.2004.12.023

Smith, S., Aardenne, J., Klimont, Z., Andres, R., Volke, A., Delgado Arias, S., 2010. Anthropogenic sulfur dioxide emissions: 1850–2005. https://doi.org/10.5194/acpd-10-16111-2010

Sommer, M., 2006. Influence of soil pattern on matter transport in and from terrestrial biogeosystems—A new concept for landscape pedology. Adv. Landsc.-Scale Soil Res. 133, 107–123. https://doi.org/10.1016/j.geoderma.2006.03.040

Spence, J., Telmer, K., 2002. The Significance of Sulphuric Acid Induced Chemical Weathering on Long Term Fluxes of CO2 Between the Atmosphere-Ocean and Rocks: Evidence From River Chemistry and Carbon Isotopes in the Canadian Cordillera. AGU Fall Meet. Abstr.

Stoddard, J.L., Jeffries, D.S., Lukewille, A., Clair, T.A., Dillon, P.J., Driscoll, C.T., Forsius, M., Johannessen, M., Kahl, J.S., Kellogg, J.H., Kemp, A., Mannio, J., Monteith, D.T., Murdoch, P.S., Patrick, S., Rebsdorf, A., Skjelkvale, B.L., Stainton, M.P., Traaen, T., van Dam, H., Webster, K.E., Wieting, J., Wilander, A., 1999. Regional trends in aquatic recovery from acidification in North America and Europe. Nature 401, 575–578. https://doi.org/10.1038/44114

Strawn, D.G., Hinrich, B.L., O'Connor, G.A., 2015. Soil Chemistry, Fourth. ed. John Wiley & Sons, Ltd.

Taylor, A.B., Velbel, M.A., 1991. Geochemical mass balances and weathering rates in forested watersheds of the southern Blue Ridge II. Effects of botanical uptake terms. Weather. Soils 51, 29–50. https://doi.org/10.1016/0016-7061(91)90065-2

Vebel, M.A., 1985. Geochemical mass balances and weathering rates in forested watersheds of the southern Blue Ridge. Am. J. Sci. 285.

Vidon Philippe, Allan Craig, Burns Douglas, Duval Tim P., Gurwick Noel, Inamdar Shreeram, Lowrance Richard, Okay Judy, Durelle Scott, Sebestyen Steve, 2010. Hot Spots and Hot Moments in Riparian Zones: Potential for Improved Water Quality Management1. JAWRA J. Am. Water Resour. Assoc. 46, 278–298. https://doi.org/10.1111/j.1752-1688.2010.00420.x

White, A.F., Bullen, T.D., Schulz, M.S., Blum, A.E., Huntington, T.G., Peters, N.E., 2001. Differential rates of feldspar weathering in granitic regoliths. Geochim. Cosmochim. Acta 65, 847–869. https://doi.org/10.1016/S0016-7037(00)00577-9

Wiekenkamp, I., Huisman, J., Bogena, H., Lin, H., Vereecken, H., 2016. Spatial and temporal occurence of preferential flow in a forested headwater catchment. J. Hydrol. 534, 139–149.

Winterdahl, M., Temnerud, J., Futter, M., Löfgren, S., Moldan, F., Bishop, K., 2011. Riparian Zone Influence on Stream Water Dissolved Organic Carbon Concentrations at the Swedish Integrated Monitoring Sites. AMBIO - J. Hum. Environ. 40, 920–930. https://doi.org/10.1007/s13280-011-0199-4

CHAPTER 2: Article Submitted to Frontiers in Earth Science (Under Review)

Does stream water composition at Sleepers River in Vermont reflect dynamic changes in soils during recovery from acidification?

Jesse R. Armfield[1], Julia N. Perdrial[1*], Alex Gagnon[1], Jack Ehrenkranz[1], Nicolas Perdrial[1], Malayika Cincotta[1], Donald Ross[2], James Shanley[3], Kristen L. Underwood[4], Peter Ryan[5]

[1]Environmental Biogeochemistry Lab, University of Vermont, Geology Department, Burlington, VT, USA

[2]US Geologic Survey, Montpelier, VT, USA

[3]University of Vermont, Civil & Environmental Engineering, Burlington, VT, USA

[4]University of Vermont, Civil & Environmental Engineering, Burlington, VT, USA

[5]Middlebury College, Geology Department, Middlebury, VT, USA

Keywords: weathering, recovery, acid impact, Sleepers River, carbonate.

Abstract

Stream water pH and composition are widely used to monitor ongoing recovery from the deposition of strong anthropogenic acids in many forested headwater catchments in the northeastern US. However, stream water composition is a function of highly complex and coupled processes, intersecting flowpaths, and variations in soil and bedrock composition. Spatial heterogeneity is especially pronounced in headwater catchments with steep topography, potentially limiting stream water composition as indicators for changes in critical zone (CZ) dynamics during system recovery. To investigate the link between catchment characteristics, landscape position, and stream water composition we used long-term data (1991-2015) from the Sleepers River Research Watershed (SRRW) in northeastern Vermont. We investigated trends with time in stream water and trends with time, depth, and landscape position (hilltop, hillslope, and riparian zone) in ground water (GW) and soil solution. We further determined soil elemental composition and mineralogy on archived (1996) and modern (2017) soil samples to assess changes in composition with time. Our results show that SRRW is indeed recovering from acidification and that solutes typically derived from carbonate (not silicate) weathering decrease progressively with time in GW. A mixture of lateral transfer of weathering-derived materials and upwelling of solute rich GW is responsible for enrichments seen in riparian soils, especially in Ca. Despite the decrease in the Ca concentration of GW, stream water Ca fluxes showed a slight increase over the past two decades, likely from leaching of riparian soil stores. At

SRRW the stream integrates signals from weathering and base cation leaching, flowpaths, and Ca storage in riparian zones.

2.1 Introduction

Streams indicate critical zone (CZ) function, because they represent an integrated signal of watershed processes (Frisbee et al., 2011) including internal stream processes (Dawson et al., 2001; Mulholland and Hill, 1997) and processes occurring at the interfaces (i.e. riparian or hyporheic zones) (Bishop et al., 2004; Winterdahl et al., 2011). For example, the effects of acid deposition, especially prevalent in the northeastern US (Likens et al., 1972), have been monitored using stream water observations (Amiotte-Suchet et al., 1999; Huang et al., 2017; Newell and Skjelkvåle, 1997).

Acid deposition forms when emission-derived sulfur dioxide and nitrogen oxides interact with precipitation, which impacts the entire CZ through a multitude of complex and coupled processes including declining tree and soil quality due to low pH and base cation leaching (Driscoll et al., 2001; Matzner and Murach, 1995; Raddum et al., 2007). The ensuing stream water signals were typically sensitive to these effects and showed low pH, increased concentrations of acid anions (sulfate and nitrate), and increased effluxes of base cations (e.g. Ca, Na) from many acid impacted systems (Driscoll et al., 2001; Garmo et al., 2014; Newell and Skjelkvåle, 1997). In the U.S., legislation passed in 1970 and 1990 led to reductions in emissions that caused a slow increase in precipitation pH as well as a decrease in the acid anion content across affected regions, and stream water composition has since been monitored closely for signs of recovery (Driscoll et al., 2001; Garmo et al., 2014; Kopáček et al., 2016; Newell and Skjelkvåle, 1997; Rogora et al., 2013; Skjelkvåle, 2003).

However, because streams merge water and solutes from various sources, the attribution of changes in stream water chemistry to specific process locations without detailed investigations of the CZ is difficult. For example, one CZ process strongly affected by the presence of strong acids (mostly H_2SO_4 and HNO_3) is weathering, i.e. the breakdown of bedrock and regolith through physical and chemical processes (Jin et al., 2010). Chemical weathering includes simple dissolution reactions (typical for carbonates) and hydrolysis (typical for silicates). Both processes are driven by proton availability and in the case of most silicate minerals weathering reactions are incongruent i.e. they lead to the production of dissolved weathering products as well as the formation of secondary minerals (Strawn et al., 2015). As such, weathering and soil development continuously change the composition of the solid CZ and the composition of percolating waters (e.g. soil solution and ground water (GW)). Another important process is the leaching of base cations from acid impacted soils that cause an overall decline in soil health. These changes can be clear in headwater catchments with pronounced topography, even within just a few decades of changes in precipitation chemistry due to the transfer of soluble materials to deeper soil layers, GW (vertical transfer), and/or via lateral transfer to low-lying landscape positions

(Bailey et al., 2014; Brantley et al., 2007; Johnson et al., 2000; Lawrence et al., 2015; Lybrand and Rasmussen, 2015; Nezat et al., 2004).

Stream water composition is therefore strongly affected by flowpaths. Sampling different layers of a heterogeneous CZ and backtracking to specific processes requires information on soils as well as subsurface waters. We attempt this backtracking to identify signals of recovery in streams and soils using the well-studied Sleepers River Research Watershed (SRRW) in northeastern Vermont as a testbed. SRRW received strong acids through wet and dry deposition but, unlike many other watersheds in the NE, contains carbonate-bearing parent material that buffers the pH of percolating water. The impact of acid deposition on the CZ is therefore less dramatic but potentially visible due to the sensitivity of carbonates to only small changes in acid inputs (Huang et al., 2017).

In order to investigate how the CZ at SRRW responds to changes in precipitation chemistry in the stream signal and how compositional differences by landscape position influence this signal, we analyzed long-term stream water (1991-present), soil solution (2004-2013), and GW composition (2004-2013) at various landscape positions. Data analyzed includes: pH, anthropogenic acid anions (nitrate and sulfate), base cations (Na, Ca) and Si. To test for changes in soil composition with time we investigated soil elemental composition (Si, Al, Na, Ca) and mineralogy data from archived (1996) and modern (2017) soil samples of varying landscape position.

Because silicate weathering at the watershed scale is a slow process, we hypothesize that changes in acid deposition are not recorded as significant trends of silicate weathering products in the stream over our 24-year study period. However, we hypothesize that carbonate weathering and base cation leaching slowed, leading to decreases in Ca flux in the stream since 1991. We further hypothesize that topographically induced transfer of base cations led to depletions in shallow horizons at hilltop and hillslope locations while near stream soils accumulate base cations, especially Ca.

2.2 Materials and Methods

2.2.1 Field Site

The SRRW comprises a series of nested catchments with varying land use in northeastern VT (Fig. 2-1). The forested headwater watershed, W-9, is the focus of this study and is underlain by the Waits River Formation, which includes a quartz-mica phyllite member interbedded with calcareous granulite (Ferry, 1991; Ratcliffe et al., 2011). This formation is covered by several meters of dense silty basal till from the last glaciation (Shanley, 2000) which itself is sourced from the underlying Waits River Formation (53%) and the nearby Gile Mountain Formation (25%; Hornbeck et al., 1997). The presence of carbonates in bedrock and till contributes to the high buffering capacity and high pH in stream waters, despite historic acid deposition (Hornbeck et al., 1997; Shanley, 2000).

Landscape position strongly influences soils in W-9: Inceptisols (most prevalent) and Spodosols are typical for well-drained upland areas such as hilltop and hillslope areas (Shanley et al., 2004). Histosols are mostly found in poorly-drained riparian areas and are often located where GW upwelling occurs (Shanley et al., 2004). Vegetation is dominated by northern hardwoods species sugar maple, yellow birch, white ash and American beech, but softwood species (balsam fir and red spruce) are also present (Shanley et al., 2004). Like other catchments in the Northeastern US, SRRW has been impacted by acid deposition which caused forest decline (branch dieback, some declining crown vigor) and low soil pH (Shanley et al., 2004). However, due to emissions regulations, SRRW is experiencing reduced acid inputs (Burns et al., 2005; Stoddard et al., 1999).

2.2.2 Sampling Methods

In order to assess trends in soil-, ground- and stream water composition, we used existing data on pH, sulfate, nitrate, Si, Ca, and Na that have been collected weekly and during events at SRRW over 24 years. For soil solution, we used data from 3 sets of nested zero-tension lysimeters that occupy three main landscape positions (hilltop, hillslope, and base of the hill) and sample at 15cm (shallow), and 50cm (deep). Data from wells, which occupy the same landscape positions as lysimeters and are screened at various depths (Table 2-1), were used to monitor changes in GW composition. Both soil solution and GW data were generated from approximately weekly collection between 2004 and 2013 but due to intermittently dry conditions, soil solution samples were obtained less frequently. Data on stream water composition for the same solutes were generated from approximately weekly grab sample collection between 1991 and 2015 at the stream gauge at the base of the watershed (Fig. 2-1).

In addition to existing data, we collected samples from lysimeters, wells and the stream in the fall of 2017 for dissolved inorganic carbon (DIC) isotope analysis to test for carbonate weathering signals. Lysimeters and wells were pumped and allowed to recharge prior to sampling and all samples were capped immediately with no headspace, placed in a cooler, and shipped to the UC Davis Stable Isotope Facility within 24 hours of collection.

To investigate landscape position controls on soil composition, we took soil samples every 1-3 meters in three transects that spanned from hilltop to hillslopes to near-stream areas (Fig. 2-1). Two transects cut across the two main tributaries to stream B, and one transect cut across a few meters below the confluence of the tributaries (Fig. 2-1). These transect samples were taken using a bucket auger in 15-cm depth increments until 90 cm or depth of refusal.

To increase the statistical power of results and to allow for an in-depth analysis of compositional changes in soil with depth and landscape position, we additionally sampled each of the three soil orders from soil pits by taxonomic horizon in various locations throughout the W-9 in 2017 (Fig. 2-1). In order to allow for comparison with soils prior to recovery, we also analyzed archived samples (stored at room temperature in the dark in sealed glass vials) collected as part of a soil survey in 1996 (n=156). We use average values

of soil composition in archived (1996) and modern (2017) samples, some of which were re-sampled in the same approximate location (Fig. 2-1c).

2.2.3 Sample Processing and Analyses

Soil samples prepared for XRF and powder XRD were air dried (4-5 days), sieved (<2mm), ground and homogenized in a ball mill, and stored dry prior to analysis. Soil elemental composition was determined on both archived samples (n=156) and modern transect samples (n=121) as well as samples from representative landscape positions of modern (n=43) and archived soils (n=78) using a Thermo Scientific Niton XL3t X-Ray Fluorescence Analyzer and a Thermo Scientific ARL QUANT'X X-Ray Fluorescence Spectrometer at in the Geology Department at the University of Vermont and Middlebury College, respectively. From these data we calculated tau values (eq. 1) to determine the pedogenetic behavior of selected elements (Si, Al, Na, Ca; Brantley et al., 2007; Brimhall and Dietrich, 1987). As parent material we used the deepest sampled horizon (i.e. partially weathered till) because parent material composition in this area varies greatly across the watershed and cores were only drilled in a few, potentially not representative, locations. Tau values therefore only show depletion vs. enrichment relative to the deepest accessible horizon. We used Ti as an immobile element because of its normal distribution in the parent material. All data from each soil order of the 1996 survey as well as the representative data from 2017 were averaged by horizon to assess the variability of each horizon of each soil order.

[eq. 1]: $\tau_{I,M} = \frac{C_{W,M}}{C_{P,M}} * \frac{C_{P,I}}{C_{W,I}}$

Where τ (dimensionless) is the ratio of the concentration (C) of an element of interest (subscript M) relative to an immobile element (subscript I) in the weathered soil (subscript W) and the parent material (subscript P). Soil mineralogy was identified using X-ray diffraction (XRD) on random powder mounts from modern soil samples from each resampled pit. In order to identify secondary clay minerals, samples from the lowest horizon (till) were also analyzed using oriented texture preparations of the <2µm fraction that was separated by decantation (Poppe et al., 2001). Suspensions were pipetted on glass slides preparations and allowed to air-dry. This approach allows for an orientation of crystallites that restricts diffraction the crystallographic c-direction and hence only the (00l) intervals are visible (Lagaly, 1993; Moore and Reynolds, 1997). The clay fraction was analysed air-dried (AD), treated with ethylene Glycol (EG, to test for presence of swelling clay), and heat-treated (HT, 400˚C, 550˚C) to collapse the chlorite peaks to test for overlap with the kaolinite reflections (Moore and Reynolds, 1997). XRD analysis of all samples was conducted on a Rigaku MiniflexII Powder Diffractometer with CuKα radiation, operated at 30kV and 15 mA. Scanning parameters were set at 0.02 step width and a count time of 10 seconds per step between 3 and 5-65 °2θ.

2.2.4 Statistical Methods

All statistical analyses were completed in R (R Core Development Team, 2017). Stream flux was calculated to evaluate trends in recovery (sulfate, nitrate) and weathering (Si, Na, Ca). All stream flux calculations were completed using the USGS LoadEst functions (Runkel et al., 2004) implemented within the LoadFlex package and trend analyses were conducted using the Kendall and trend packages (Appling et al., 2015; McLeod, 2011; Pohlert, 2018; R Core Development Team, 2017). Autocorrelation was reduced by averaging the concentration and discharge measurements made during highly sampled storm events. The best of the predefined USGS models was then selected based on how accurately it predicted measured values and was applied to a more complete discharge record for annual flux calculation.

Flow-adjusted residuals of the concentration-discharge relationship were then evaluated and, if they were not normally distributed, a Mann-Kendall trend analysis was conducted and the sen-slope was calculated. Baseflow composition was determined by calculating the mean stream composition during discharge conditions lower than the 20^{th} percentile and storm flow composition was determined by calculating the mean stream composition during discharge conditions greater than the 80^{th} percentile. Data on baseflow and stormflow composition computed at less than the 5^{th} percentile and greater than 95^{th} percentile are also provided.

The significance of trends in soil solution and GW composition with time and space were evaluated using several methods. For temporal trends in GW, linear regressions on raw data were used first as this method is powerful and if significance is established no more statistical analyses are needed to draw conclusions. Temporal trends in GW concentration were evaluated and exemplified using data from the well with the most complete record (i.e. the well at the hilltop). In the case of highly variable seasonal compositions regressions on annual averages were implemented. When large parts of the datasets (>1/3 of the record) were missing or other tests failed to establish a trend, Welch's 2 sample t tests were used to elucidate any differences in composition. Trends in space were evaluated by calculating the average and standard error at each depth and landscape position. If averages were within error of one another Welch's 2 sample t test was used to determine whether the data sets were significantly different.

2.3 Results

2.3.1 Trends in Stream Water Composition and Flux

Stream water pH values showed large, mostly seasonal, variations between 1991 and 2004 with values ranging from 6.7 up to 8.6 with less variability thereafter (Fig. 2-2a). Annual stream water sulfate flux decreased by over 30% since 1991 (from 870 to 580 kg yr^{-1}, Fig. 2-2b) and Mann Kendall trend analysis on flow adjusted model residuals indicated a significant negative trend in sulfate concentration (τ = -0.442, Sen's Slope = -0.007, $p < 0.05$). The annual nitrate flux showed large interannual variability (between 60 and 105 kg yr^{-1}) but no significant increase or decrease over time (Fig. 2-2c).

Both Si and Na stream water flux showed large interannual variability (ranging from 750 to 1400 kg yr^{-1} for Si and from 180 to 330 kg yr^{-1} for Na, Fig. 2-2d & e). Mann Kendall trend analyses revealed a slight decrease in the stream water Si concentration (τ = -0.066, Sens Slope = -0.0003, $p < 0.05$) while no significant trend in Na concentration was found (τ = -0.0135, Sens Slope = $-1.02*10^{-5}$, $p > 0.05$). The flux of Ca showed similarly large variations (ranging from 3450 and 6450 kg yr^{-1}) and a slight increase in concentration that was significant (τ = 0.078, Sens Slope = 0.002, $p < 0.05$).

2.3.2 Temporal and Spatial Tends in Ground and Soil Water Composition

We also investigated groundwater and soil water composition for trends with time, depth, and landscape position (hilltop vs. hillslope vs. base of the hill). Temporal trends are represented as annual averages for selected years (2004, 2008, 2012) with typical annual precipitation. Significance was established using step trends between sets of annual fluxes (see supplementary materials for complete time series of GW composition).

Soil solution pH increased over time especially in deep and some shallow soil solution and was generally greater at depth and with proximity to the stream (Fig. 2-3a). GW pH in the hilltop well increased from an annual average of 7.9±0.3 in 2004 to an annual average of 8.1±0.2 in 2012, which is higher than the average stream water pH at base flow (7.8±0.2, Table 2-2).

Sulfate concentrations generally decreased with time but were greater at depth and with proximity to the stream (Fig. 2-4b). For example, the average sulfate concentration in all shallow soil water decreased from 3.2±1.5 mg L^{-1} in 2004 to 1.6±1.1 mg L^{-1} in 2008. GW sulfate decreased from an average of 5.3±0.7 mg L^{-1} in 2004 to 4.4±0.3 mg L^{-1} in 2012. The trend of increasing sulfate concentrations with depth was best observed at the hilltop position where the sulfate concentration in GW was four times higher than in soil water. The average stream water sulfate concentration at baseflow (8.1±2.3 mg L^{-1}) was the highest mean sulfate concentration of any water source (Table 2-2).

Nitrate concentrations did not change significantly over time and were lower at depth and closer to the stream (Fig. 2-3c). Annual average nitrate concentrations in shallow soil solution ranged from 0.02±0.01 to 0.26±0.12 mgL^{-1} in 2004 and 2008, respectively (Fig. 2-3c). Compared to hilltop, nitrate concentrations at the base of the hill were slightly lower and similar to base flow stream water concentrations (Table 2-2).

Average annual soil and ground water Si concentrations did not show significant changes with time but, like pH and sulfate, concentrations were generally greater with depth and proximity to the stream (Fig. 2-3d). For example, Si in GW at the hilltop remained relatively constant since 2004 at an average value of 12±0.2 mg L^{-1} (Figure 2-3d). Soil water Si concentrations were generally greater (6.7±0.8 mgL^{-1} at the base of the hill). In contrast, near stream GW Si concentrations (8.4±1.2 mg L^{-1}) were almost 30% lower than

hilltop GW concentrations (12.0±0.8 mg L^{-1}) which is still almost 3 times higher than stream water base flow concentrations (Table 2-2).

Annual average Na concentrations decreased with time in deep soil solution at the hilltop and hillslope positions and were generally lowest in hilltop soil waters (as low as 0.6±0.1 mg L^{-1}) and largest in GW, which was similar to stream water composition at base flow (Table 2-2).

Ca concentrations generally decreased through the study period but were greater at depth and proximal to the stream (Fig. 2-3f). Hilltop GW Ca concentrations decreased significantly from 18.8±1.3 mgL^{-1} in 2004 to 16.0±0.8 mgL^{-1} in 2012 (Fig. 2-3f) and were generally greater at depth (1.0±0.7 mgL^{-1} in shallow soil water vs. 16.4±2.4 mgL^{-1} in GW). Stream water Ca concentrations at base flow were similar to GW concentrations (Table 2-2).

The isotopic composition of DIC was determined for soil solution and GW. The mean δ^{13}C-DIC of soil solution was significantly lower than that of GW (-20.8±1.2 and -14.5±1.5, respectively) indicating a carbonate weathering signal in GW. δ^{13}C-DIC values also generally increased with proximity to the stream (Table 2-3).

2.3.3 Spatial and Temporal Trends of Selected Elements in Soil

Spatial trends on transect samples generally showed depletions at hilltop and hillslope locations and accumulations in riparian areas (Fig. 2-4, supplementary materials Figs. 2-2-3). The exception was Si that was, relative to the parent material, variably enriched or depleted in hilltop and hillslope positions (tau values ranging from -0.51 to 0.64). Al was mildly depleted from hilltop soils (-0.10 to -0.39) and accumulated in the top 45cm of the profile closest to the stream. The base cations Na and Ca were typically depleted from the hilltop soils (e.g. tau values ranging from -0.86 to -0.08 for Ca) and accumulated in near stream soils, especially in the top 30cm (up to 31.2 for Ca, Fig. 2-4).

Temporal trends in soil elemental composition were investigated by comparing tau values from archived and modern samples (Figs. 2-5-7). The variability in typical hilltop soils (mostly Spodosols) was great, as indicated by the broad shaded areas (Fig. 2-5), but generally showed a combined accumulation-depletion pattern (Fig. 2-5). For example, tau values for Si indicated mild enrichments (e.g. archived mean=0.12±0.36 in the O horizon) in the upper horizons (O, A, E) and depletions in lower horizons (e.g. archived mean=-0.28±0.11 for the BC horizon). Al also showed an addition-depletion profile where tau values were negative at the surface and positive in the spodic horizon. Base cations were generally enriched and highly variable in the O horizon but depleted in underlying mineral soil (e.g. archived mean up to -0.58±0.19 for Na). The differences between archived and modern samples were not significant for any of the investigated elements except Ca, which was generally more enriched in the top horizons of archived soils.

Hillslope Inceptisol composition in the study area was less variable compared to Spodosols (shaded areas are less broad, Fig. 2-6). Overall, Si was depleted throughout the profile (archived means between -0.04±0.25 and -0.16±0.17, Fig. 2-6), while Al in archived samples was somewhat depleted in upper horizons and in modern samples was depleted in lower horizons. Tau values for base cations, especially Ca were highly variable in the O horizon (e.g. archived mean = 3.65±4.18 for Ca). As for the Spodosol, differences between archived and modern samples was only significant for Ca in the top horizons, where Ca tau values were significantly higher in archived soils.

The variability of riparian soil composition in the study area was high for most elements, especially in archived samples. For example, tau values were generally positive for Si, negative for Al (especially in modern samples; Fig. 2-7). Base cation tau values were generally positive, especially for Ca, in the two upper-most organic horizons (32.06±33.55 and 19.87±29.71). Again, the differences between archived and modern samples was significant for Ca in the top horizons, where Ca tau values were significantly higher in archived soils.

2.3.4 Mineralogy of Till and Soils

The deepest horizons (weathered till) contained primary minerals of the Waits River and Gile Mountain Formations including micas (with a prominent peak at 10.0Å), chlorite (14.2/7.1/3.5Å), pyroxenes (e.g. at 3.0Å), feldspars (e.g. at 3.1Å), quartz (at 3.3Å), amphibole (at 8.5Å), oxides (rutile or spinel at 2.5Å), and apatite (2.8Å, see supplementary materials for diffractograms). Representative soils for all landscape positions (Spodosol for hilltops, Inceptisols for most hillslopes and Histosols for riparian zones) showed most peaks for the primary minerals associated with contributing bedrock formations, but several of these peaks changed or disappeared towards upper horizons (supplementary materials Fig. 2-4-6). For example, quartz peaks decreased in intensity towards shallower horizons, whereas feldspar, muscovite, amphibole and pyroxene peaks varied but became difficult to resolve in the organic horizon of all soils. Primary chlorite is present in all soils (intense peak at 14.2Å in powder samples). The secondary swelling clay mineral smectite (confirmed by EG treatment, supplementary materials Fig. 2-4-6) and illite were found in deeper horizons of most soils. Smectite was most prominent in Spodosols and not well resolved in the riparian Histosol. Calcite in contrast was only identified in the riparian Histosol (in the lowest horizons).

2.4 Discussion

2.4.1 Streams as Indicators of Recovery from Acidification?

Changes in stream water composition can indicate changes in CZ dynamics (Maher, 2011; McIntosh et al., 2017; Meybeck, 1993), however, a multitude of complex and coupled processes in the watershed and the stream itself can make the identification of specific processes or source locations difficult. Using the acid-impacted SRRW as a testbed, we investigated the potential and limitations of stream water composition as an indicator of

watershed recovery from acidification and explored whether changes in soil composition contributed to this signal.

Generally, decreasing stream water nitrate and sulfate fluxes and overall increases in stream water pH are typical indicators of chemical recovery at the watershed scale (Driscoll et al., 2001; Garmo et al., 2014; Newell and Skjelkvåle, 1997; Rogora et al., 2013; Skjelkvåle et al., 2001, 2005). At SRRW, sulfate fluxes in the stream indeed declined significantly (Fig. 2-2) despite the fact that GW sulfate concentrations are high due to pyrite weathering at greater depth (Mayer et al., 2010) and despite the fact that precipitation increased (by about 14 mm/yr, over the past decade; Shanley et al., 2016). If sulfate was still sourced from the deposition of sulfuric acid, increases in annual precipitation would have led to stream water flux increases, not decreases and overall these results indicate a substantial reduction in acid inputs. In contrast, stream water nitrate flux did not change significantly despite reductions in NO_x emissions and deposition. Stream water pH never dropped below 6.7, due to the high buffering capacity of the bicarbonate-rich waters (Shanley, 2000; Shanley et al., 2004) but the magnitude of pH fluctuations decreased, especially after 2004 (Fig. 2-1a). These early fluctuations were likely the result of episodic acidification events (e.g., re-wetting after drought) that temporarily led to low pH values in the stream (Mayer et al., 2010).

Because the reduction of acid deposition reduces proton availability for weathering, we had hypothesized that stream water fluxes of Ca from carbonate weathering and base cation leaching would decrease significantly. Indeed, many recovering watersheds in the region also show a substantial reduction in base cation fluxes including Ca and Na (Burns et al., 2005; Garmo et al., 2014; Newell and Skjelkvåle, 1997; Stoddard et al., 1999). However, SRRW Na (and Si) fluxes remained unchanged, whereas Ca fluxes increased (Figure 2-1d-e).

Because GW can indicate subsurface processes more directly than stream water (Peters and Aulenbach, 2009), we investigated temporal trends in GW Ca, Na and Si concentrations and found that the concentrations of Si remained stable, Na decreased slightly and that Ca decreased by over 30% since 2004 (Fig. 2-3f). The relatively high δ^{13}C-DIC values measured in GW are typical for a mixture of pedogenic DIC and carbonate weathering, confirming that carbonate is still actively weathering (Amiotte-Suchet et al., 1999; Cerling, 1984). Coupled with the decreases in GW Ca concentrations on the hilltop and hillslope, the isotopic patterns are consistent with either decreased carbonate weathering or increased plant Ca uptake during recovery, but they do not explain the increased Ca flux in stream water. We will discuss the potential role of Ca accumulation in the riparian zone as a mechanism to explain this pattern (section 2.4.3).

2.4.2 From Subsurface to Stream: Changes in Soil and Water Composition by Landscape position

We had hypothesized that long-term lateral transfer of leached base cations would lead to depleted shallow horizons, especially at hilltop or hillslope locations, while the

accumulation of base cations, especially Ca, would be largest in near stream locations. Indeed, base cation and Si concentrations in soil water generally increased with depth and also increased towards low-lying landscape positions, which might reflect a combination of vertical and lateral transfer through shallow flowpaths and supply from GW when water tables rise (Sommer, 2006). Highly variable Si tau values at all landscape positions and in all soil horizons (Fig. 2-4) might reflect a combination of unweathered quartz high in the profile as well as transfer of Si from the weathering of less stable aluminosilicates (Fig. 2-4). Aluminum, at hilltop locations, showed a typical Spodosol depletion-enrichment pattern due to pH driven changes in Al solubility (Cronan and Schofield, 1979) but had significant enrichments in riparian soil horizons. XRD analyses indicate the weathering of aluminosilicate phases (especially amphiboles and pyroxenes) in most horizons and many of these minerals were still present in mineral soil horizons (supplementary materials Figs. 2-4-6). Together with the high soil solution concentrations of Si (and partially for Na as well) these results indicate active silicate weathering in these soils.

Solid phase analyses of Na and Ca revealed negative tau values for these elements in hilltop and hillslope soils but showed, again, substantial enrichments in riparian soils (Figs. 2-5-7), a pattern that was also visible in soils taken in transect associated with these landscape positions (Fig. 2-4). E.g. Ca and Na were generally depleted in hilltop-Spodosols (except for top horizons), relatively stable in the hillslope-Inceptisols and enriched in riparian-Histosols, especially in top layers (Fig. 2-4). Organic rich horizons tend to have less Ti, and hence the normalization to this otherwise immobile element to calculate tau values can overestimate enrichments. However, riparian Histosol Ca content reaches up to 72,000 mg kg^{-1}, compared to a mean of 26000±13000 for hillslope samples. XRD analyses of these soils explain most of these patterns through weathering and disappearance of amphiboles, chlorite, apatite, and pyroxenes. The lack of calcite in the till at hilltop and hillslope locations indicates that the carbonate weathering front is much lower than the silicate weathering front (i.e. in the deep till). The lack of significant amounts of secondary Ca-bearing minerals in near-stream locations further suggests that the large amounts of Ca are not accommodated in crystalline phases.

2.4.3 The Riparian Zone: Integrator of Flowpaths and Soil Processes

At SRRW, the riparian zones are areas of confluence where shallow and deep flowpaths meet, GW discharges and base cations accumulate, hence the riparian zone has a high potential for impacting stream water composition for these solutes.

Si and Na concentrations were similarly high in GW at hilltop and hillslope locations, however, concentrations were significantly lower in riparian zone waters and even lower in stream water (e.g. base flow stream water Si concentrations were almost 6 mg L^{-1} lower than riparian GW (Fig. 2-3, Table 2-2), an observation consistent with previous research (Kendall et al., 1999). The missing Si and Na might be stored in secondary minerals, such as smectites that were identified in weathered till (supplementary materials Figs. 2-4-6). However, as mentioned above, we cannot explain the high riparian soil Ca content through only the accumulation of secondary minerals.

Cincotta et al. (2018, this issue) found riparian soils at SRRW were rich in both Ca and organic carbon. Ca is common in biofilms and, as a divalent cation, can help bridge charges between negative soil particles, effectively stabilizing soil aggregates (Perdrial et al., 2009). Furthermore, organic matter readily forms complexes with free Ca^{2+} ions, and Ca is the dominant exchangeable cation in organic soils with high pH and cation exchange capacity. Therefore, Ca in riparian soils is likely associated with and stabilized by organic materials. Cincotta et al. (2018) also showed that recovery from acidification can lead to the breakup of soil aggregates and the release of associated organic matter into soil solution. Their study did not investigate Ca release, but if Ca is associated with organic matter it would be liberated in the same process. Indeed, stream water DOC flux has been increasing at SRRW since 1992 (Schuster et al., 2007; Sebestyen et al., 2008; Cincotta et al., 2018). Thus, the slight but significant increase in stream water Ca flux and discharge-adjusted concentration (Fig. 2-2f) could have the same origin as the stream DOC increase, i.e. release from soil aggregates. Both indicate riparian processes driven by changes in aggregate stability and solubility instead of increased carbonate weathering.

Furthermore, our results on modern vs. archived soil samples are in agreement with a gradual, recovery-induced, leaching of Ca from riparian organic matter. The Ca concentration of the riparian soils decreased measurably between archived (1996) and modern samples (2017) throughout the study area as well (Fig. 2-7). We illustrate the strong impact of riparian soils and near stream waters vs. hillslopes on stream water in a mixing diagram of Na-normalized mole ratios (Fig. 2-8). Here, composition of hilltop and hillslope soils have overall lower Ca/Na ratios than the riparian soils, which again have lower ratios than GW or stream water. These results confirm that riparian zones are highly reactive parts of the CZ and exert a strong control on stream composition (Lidman et al., 2017; Peters and Aulenbach, 2009; Vidon et al., 2010). In the case of SRRW, the complex interactions among weathering, intersecting flowpaths, GW upwelling (providing changes in pH and further accumulation of more reactants), temporal solute storage, and interaction with organics, produce a highly reactive zone that responds to the same driver (decrease of acid inputs) in fundamentally different ways than the hillslopes.

2.4.4 Limitations of Streams as Indicators

Streams are integrators of watershed scale processes and many acid deposition studies have interpreted shifts in stream water composition to assess watershed response to changing CZ inputs (Garmo et al., 2014; Newell and Skjelkvåle, 1997; Skjelkvåle et al., 2001; Skjelkvåle, 2003; Skjelkvåle et al., 2005). Using data on soil composition, GW and soil solution we showed that stream water flux was not representative of conditions throughout the watershed but was representative of low lying landscape positions. Especially Ca decreases in riparian soils are in agreement with the slow leaching of Ca into the stream and underlines the impact of riparian zones on stream water composition.

2.5 Tables and Figures

Installation	Top (cm)	Bottom (cm)
Near Stream GW (NSGW)	170	245
Near Stream GW (NSGW)	90	170
Near Stream GW (NSGW)	25	100
Hilltop GW (HTWG)	160	310
Hillslope GW (HSGW)	70	220
Shallow Lysimeters (HT-, HS-, BH-SS)	15	
Deep Lysimeters (HT-, HS-, BH-SS)	50	

Table 2-1: *sample depth of the wells and lysimeters. Abbreviations: HS – hillslope, BH – base of hill, NS – near stream, GW – GW, SS – soil solution*

	Baseflow (<20%)	Error	Baseflow (<5%)	Error	Stormflow (>80%)	Error	Stormflow (>95%)	Error
pH	7.74	0.15	7.77	0.14	7.53	0.22	7.34	0.17
Sulfate	8.07	2.28	8.73	2.69	4.64	1.3	3.77	1.4
Nitrate	0.14	0.08	0.11	0.05	0.25	0.16	0.3	0.19
Silicon	3.21	0.42	3.56	0.28	2	0.29	1.74	0.25
Calcium	27.83	3.88	31.24	3.19	15.02	2.97	12.32	1.99
Sodium	0.84	0.14	0.98	0.14	0.46	0.09	0.38	0.07

Table 2-2: *stream water pH and concentration of selected solutes (mg/L) during baseflow and stormflow conditions from 1991-2015.*

Landscape Position	Depth (cm)	$d^{13}C_{VPDB}$	mg C/L
Hilltop	50	-22.07	4.7
Hilltop	15	-21.06	6.6
Hilltop	160-310	-14.75	13.4
Base of Hill	70-220	-17.24	17.9
Near Stream	40	-19.18	13.7
Near Stream	25-100	-14.06	19.8
Near Stream	90-170	-13.33	17.0
Near Stream	170-245	-13.12	14.3

Table 2-3: *δC^{13} of dissolved organic carbon (DIC) and concentrations in soil solution and GW at different landscape positions and depths*

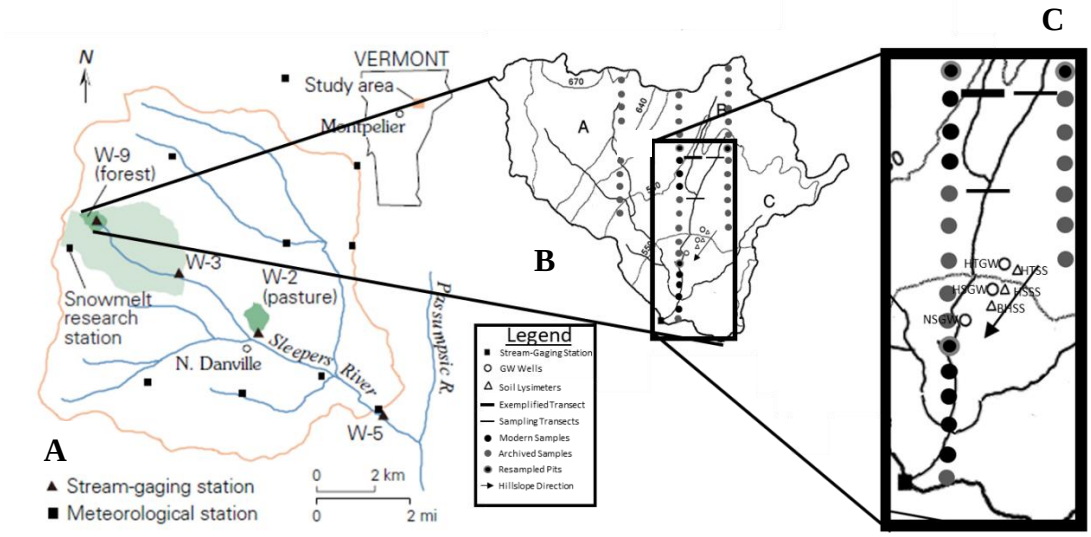

Figure 2-1. *A: location of the Sleeper River watershed and nested sub watersheds in Vermont (Modified from Shanley, 2000 with permission). B: the W-9 sub watershed with streams A, B and C (Modified from Kendall et al., 1999 with permission). C: location of wells, soil samples and soil pits as well as augered transects in proximity to stream B.*

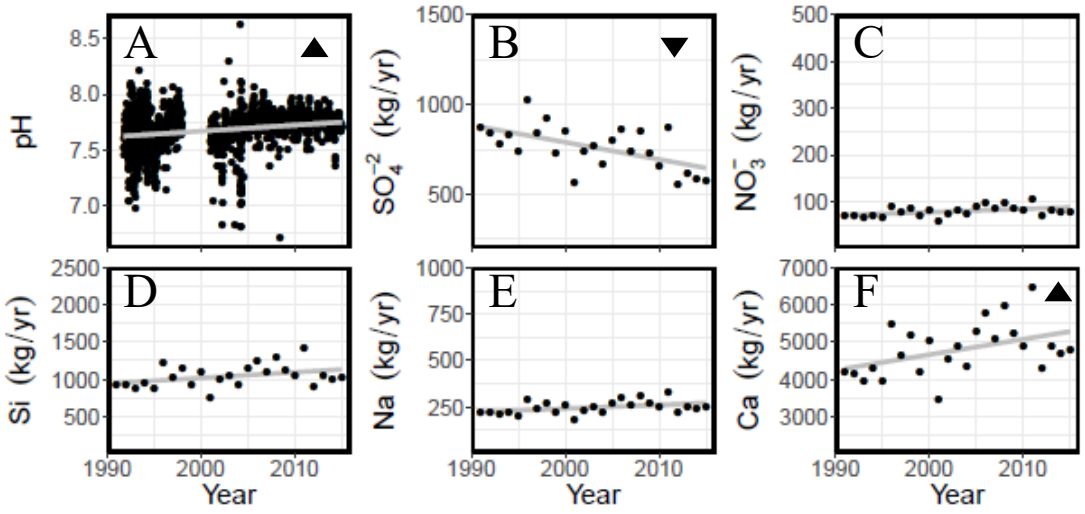

Figure 2-2. *complete time series for pH measurements and modeled annual flux of selected solutes. Triangles in the top right corner of each subset indicate the directionality of statistically significant trends. Grey lines indicate best fit (linear).*

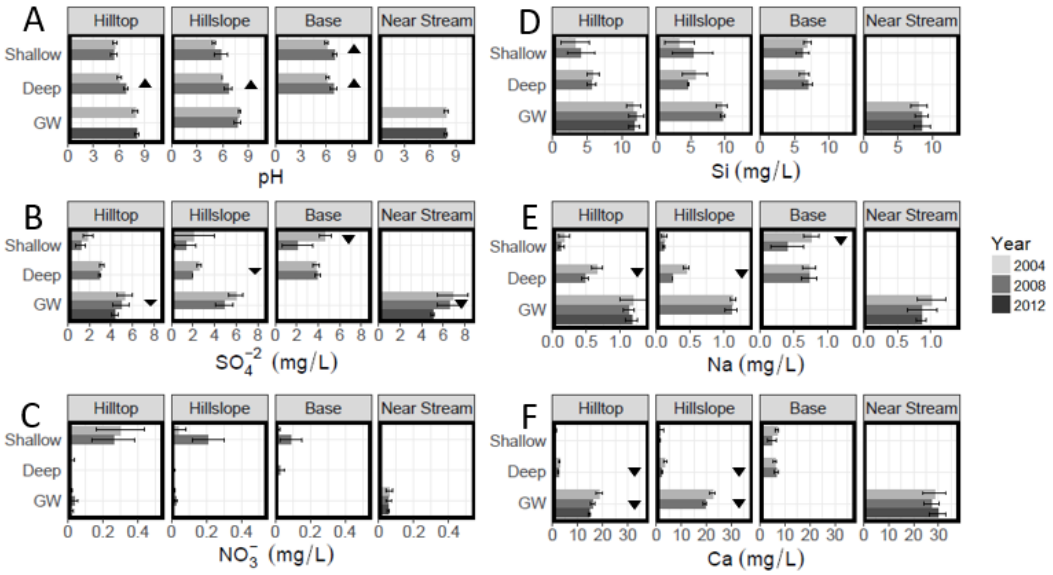

Figure 2-3. *pH and concentrations of selected solutes in soil water (shallow= 15cm and deep= 50cm) and GW at four landscape positions (hilltop, slope, base and near stream) between 2004 and 2012. Base of the hill (soil solution samples) and near stream (GW well) are in proximity to each other. Triangles indicate the directionality of statistically significant trends on the complete time series of data for each depth and landscape position.*

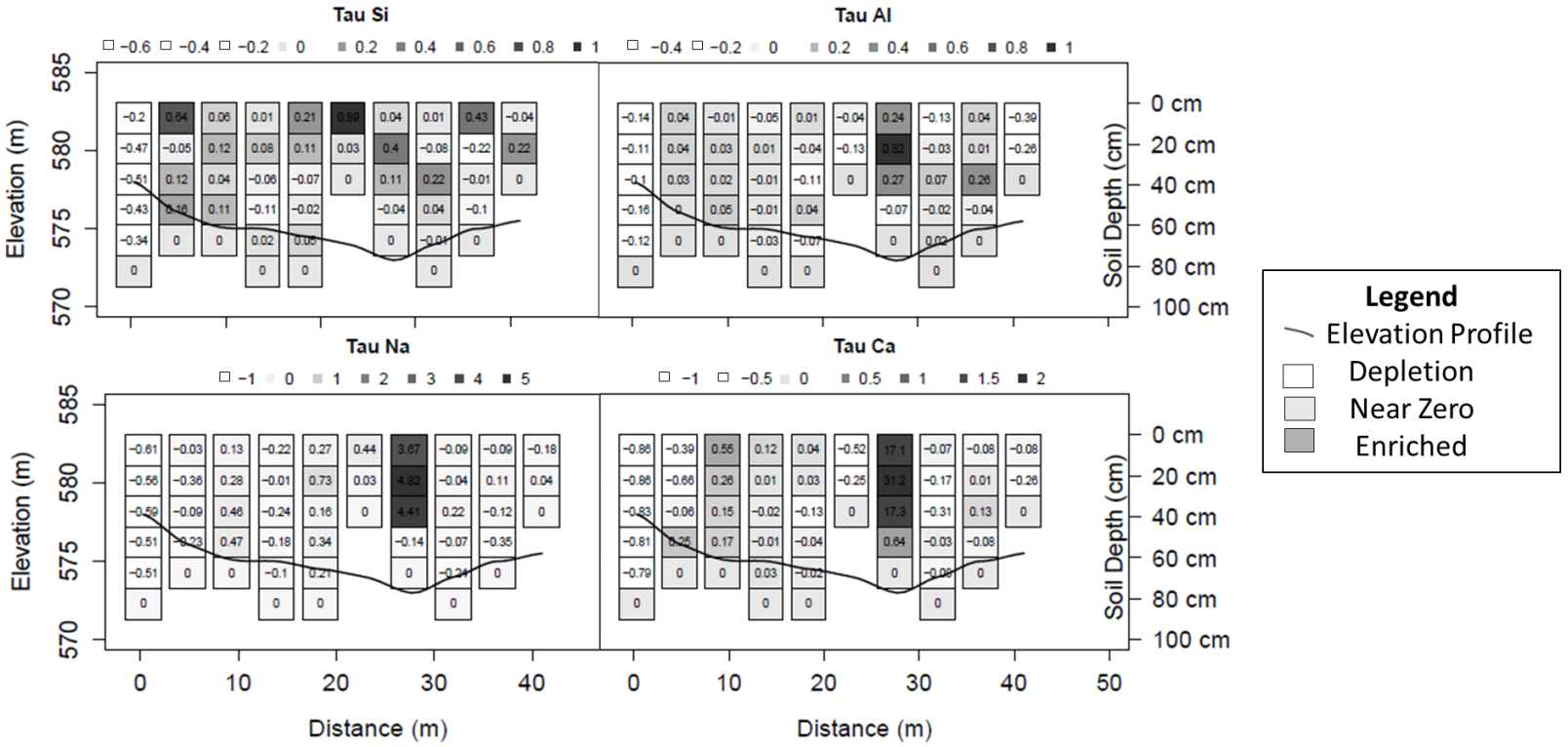

Figure 2-4. *tau values for selected elements on the exemplified transect with the greatest relief. Hilltop soils are located on each end of the elevation contour, near stream soils are located in the at the lowest elevation, and all other soils are defined as hillslope soils. The color ramp ranges from white to black indicating depletions (white), near zero values (grey), and enrichments (black).*

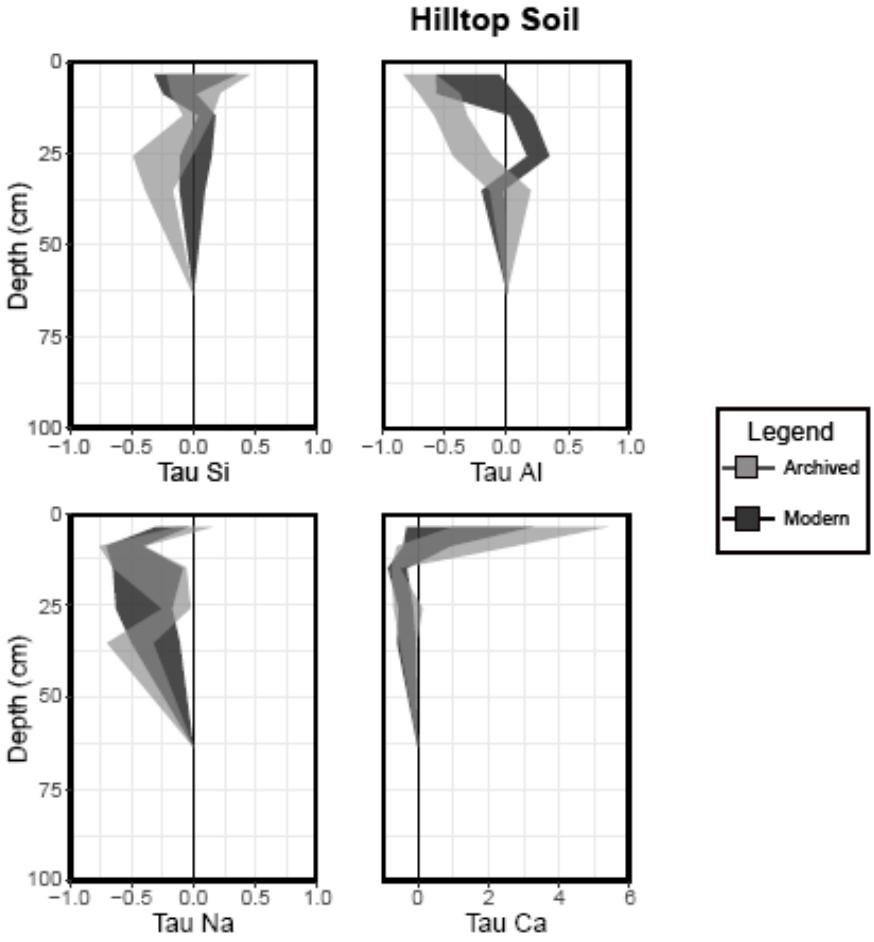

Figure 2-5. *tau values of selected elements for a typical hilltop soil (Spodosol). Light grey shaded areas indicate standard deviations of means for each element measured in archived samples (1996, 8 pits), dark grey shaded areas indicate standard deviations of means for each element of modern samples (2017, 3 pits).*

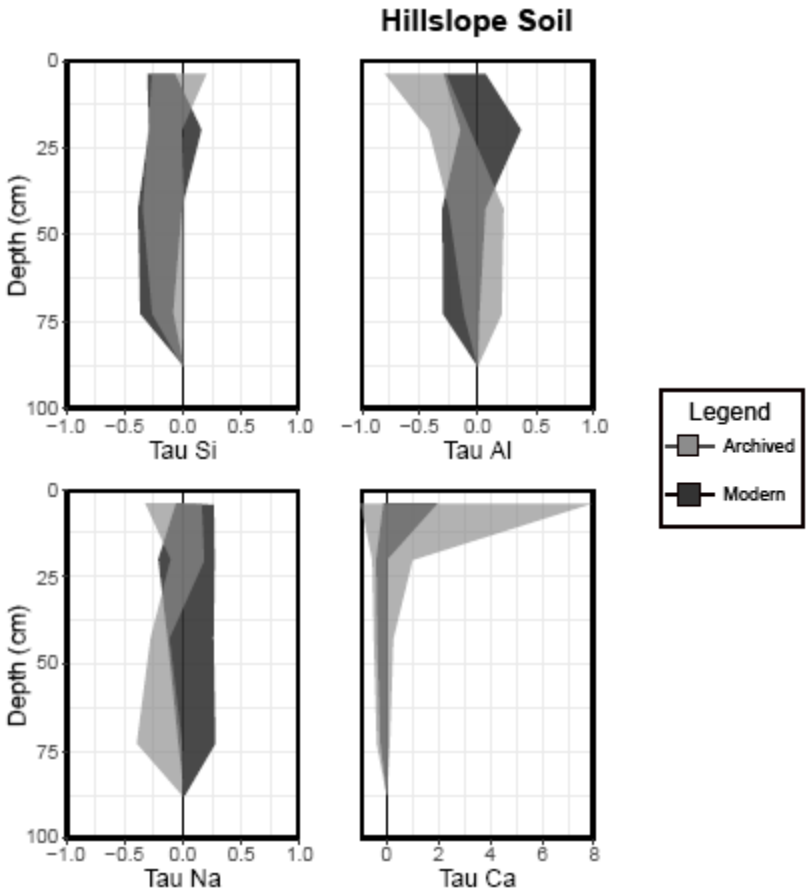

Figure 2-6. *tau values of selected elements for a typical hillslope soil (Inceptisol). Light grey shaded areas indicate standard deviations of means for each element measured in archived samples (1996, 18 pits), dark grey shaded areas indicate standard deviations of means for each element of modern samples (2017, 4 pits).*

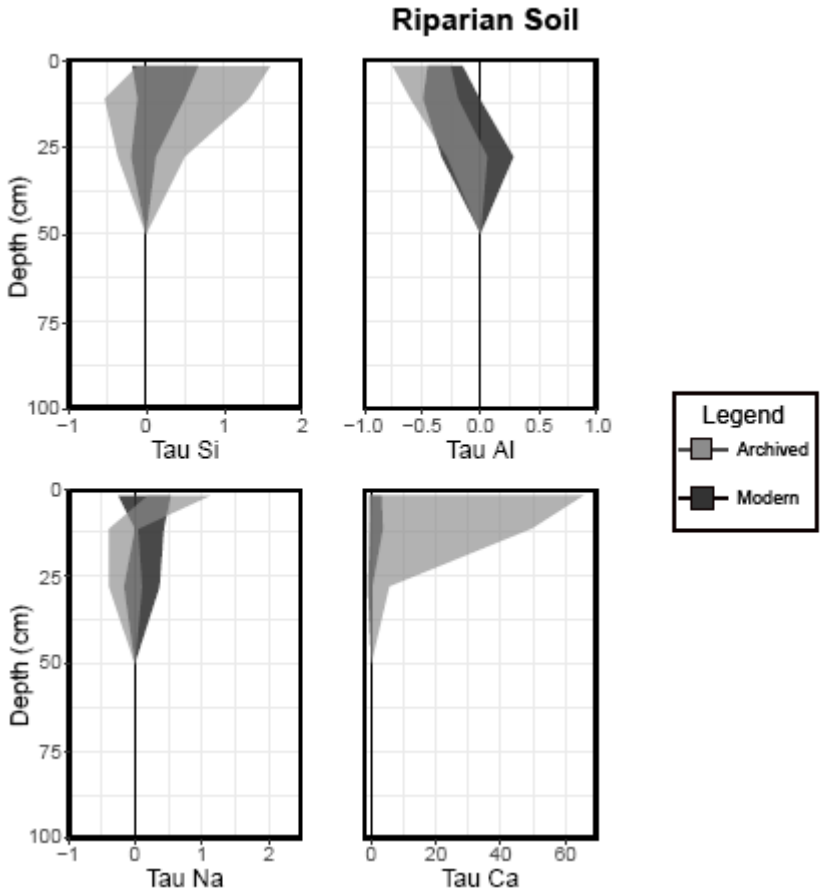

Figure 2-7. *tau values of selected elements for a typical riparian soil (Histosol). Light grey shaded areas indicate standard deviations of means for each element measured in archived samples (1996, 11 pits), dark grey shaded areas indicate standard deviations of means for each element of modern samples (2017, 3 pits).*

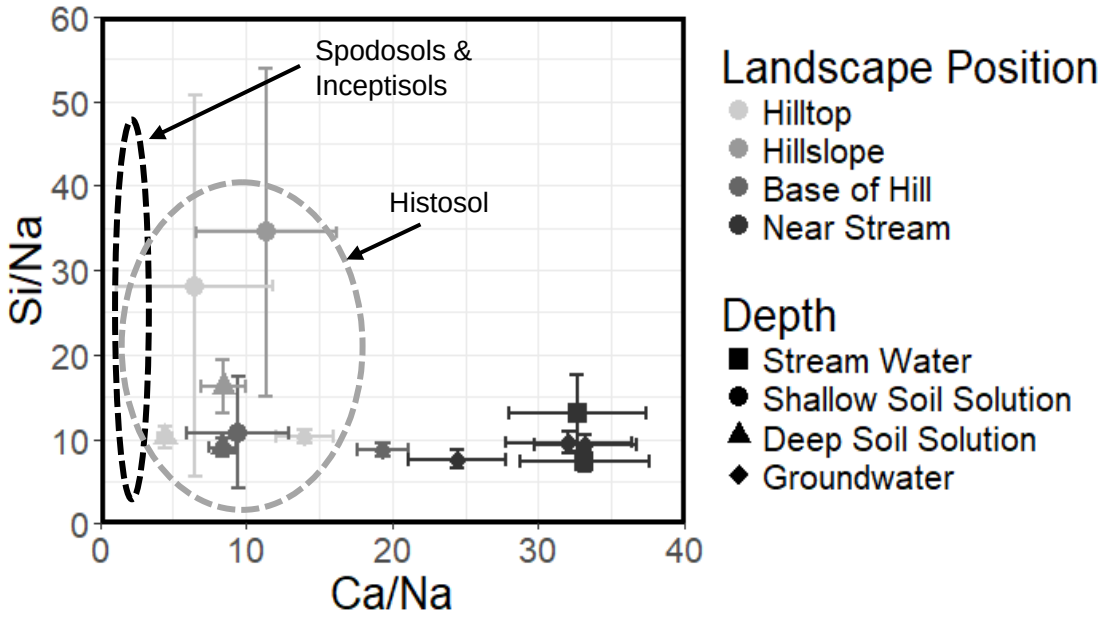

Figure 2-8. *mixing diagram of Na-normalized mean molar ratios mean ratios and standard error for water composition by source (symbols) and landscape position (gray shades). Black dashed lines indicate the range of molar ratios in Spodosols and Inceptisols while grey dashed line represents this range in Histosols.*

2.6 Supplementary Materials

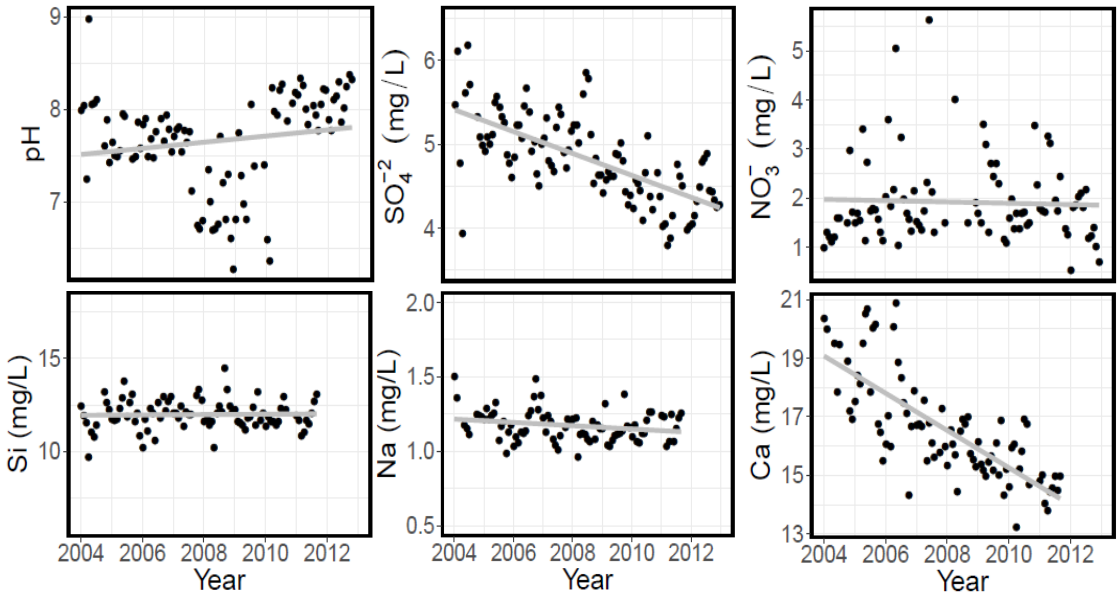

Supplementary Figure 2-1. *complete time series of selected ground water pH and selected solutes from 2004 through 2012 at the hilltop well. The presence of a triangle in the top right corner of a subset plot indicates the directionality of a significant trend.*

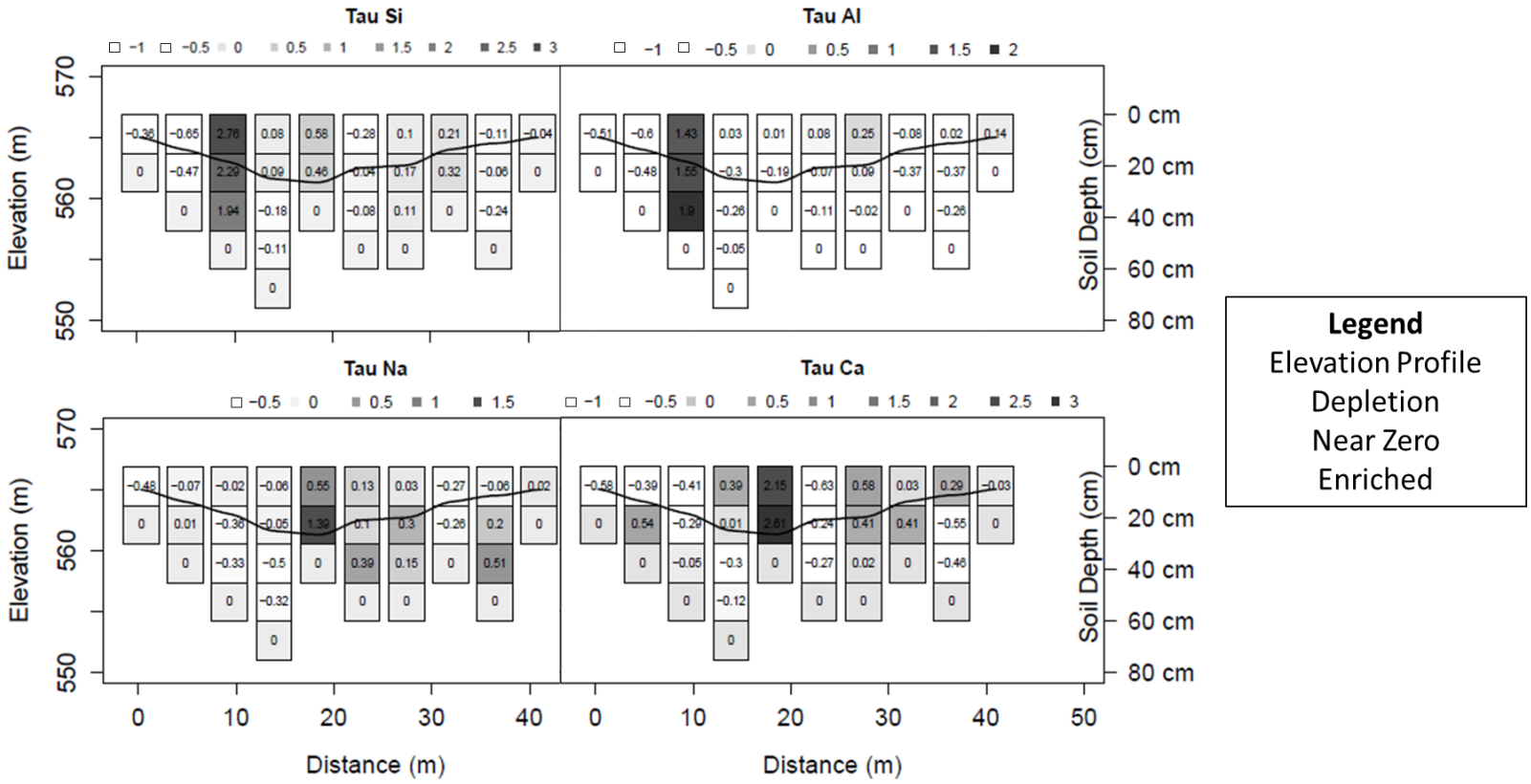

Supplementary Figure 2-2. *tau values for selected elements on the transect with the least relief. Hilltop soils are located on each end of the elevation contour, near stream soils are located in the at the lowest elevation, and all other soils are defined as hillslope soils.*

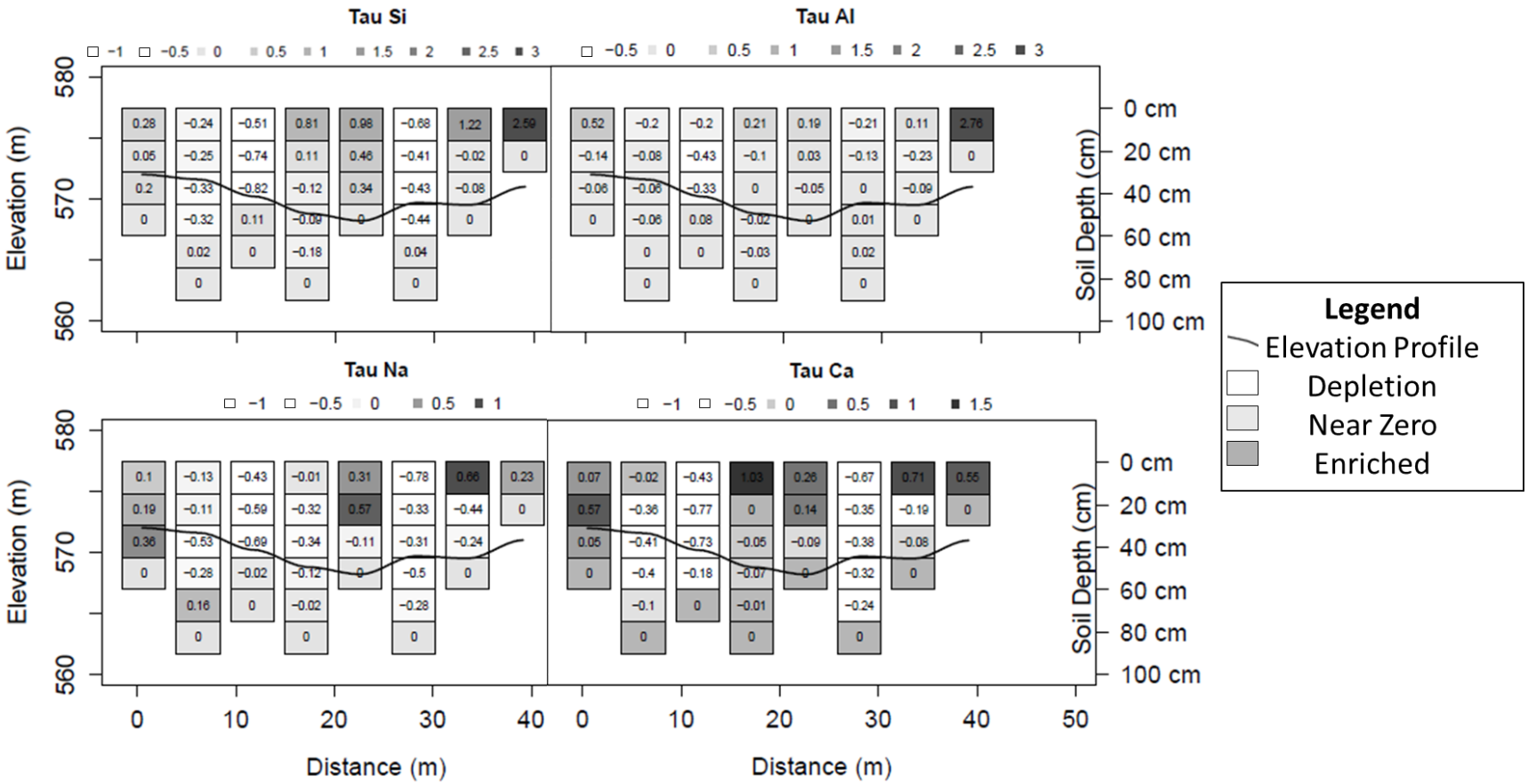

Supplementary Figure 2-3. *tau values for selected elements on the transect with intermediate relief. Hilltop soils are located on each end of the elevation contour, near stream soils are located at the lowest elevation, and all other soils are defined as hillslope soils.*

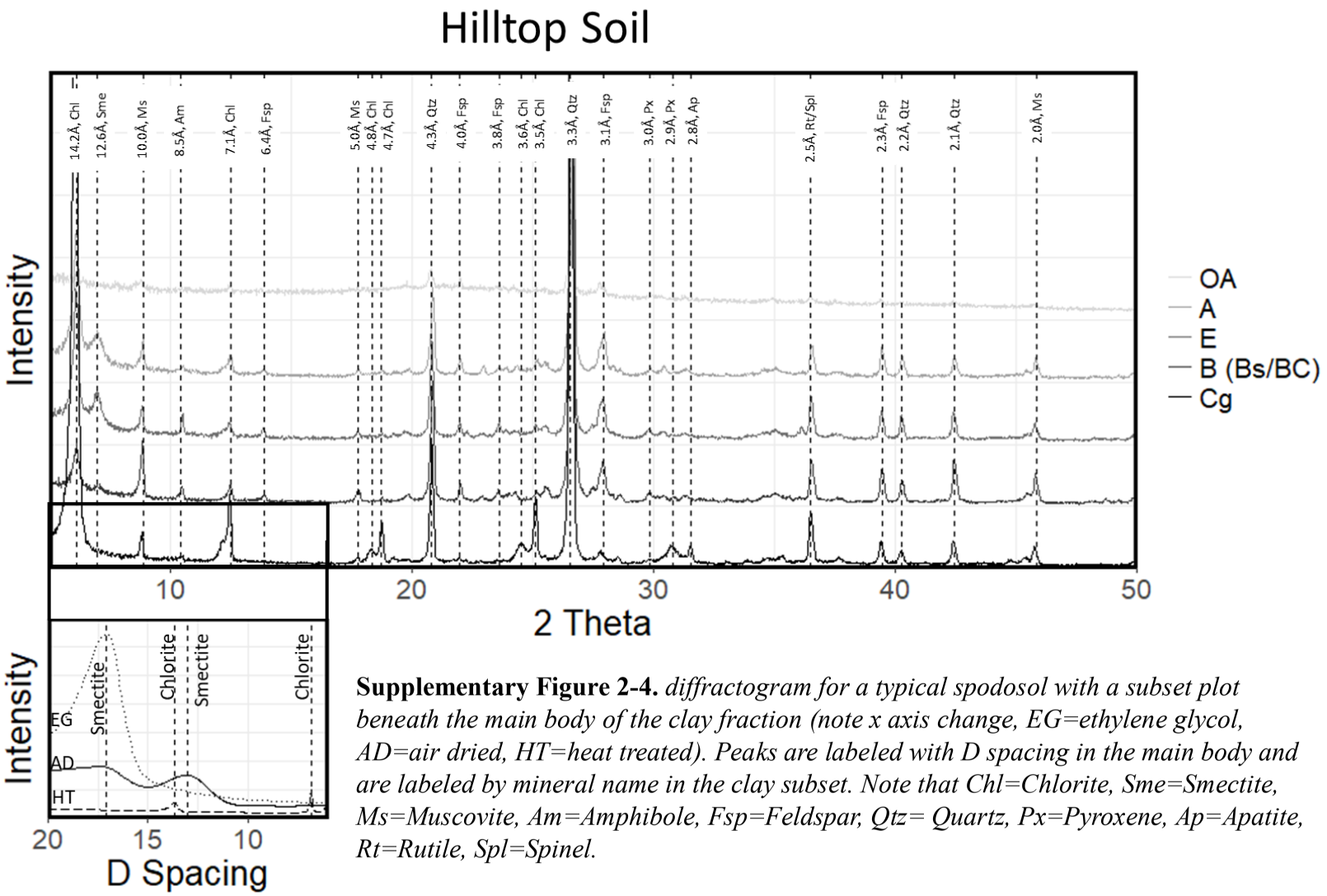

Supplementary Figure 2-4. *diffractogram for a typical spodosol with a subset plot beneath the main body of the clay fraction (note x axis change, EG=ethylene glycol, AD=air dried, HT=heat treated). Peaks are labeled with D spacing in the main body and are labeled by mineral name in the clay subset. Note that Chl=Chlorite, Sme=Smectite, Ms=Muscovite, Am=Amphibole, Fsp=Feldspar, Qtz= Quartz, Px=Pyroxene, Ap=Apatite, Rt=Rutile, Spl=Spinel.*

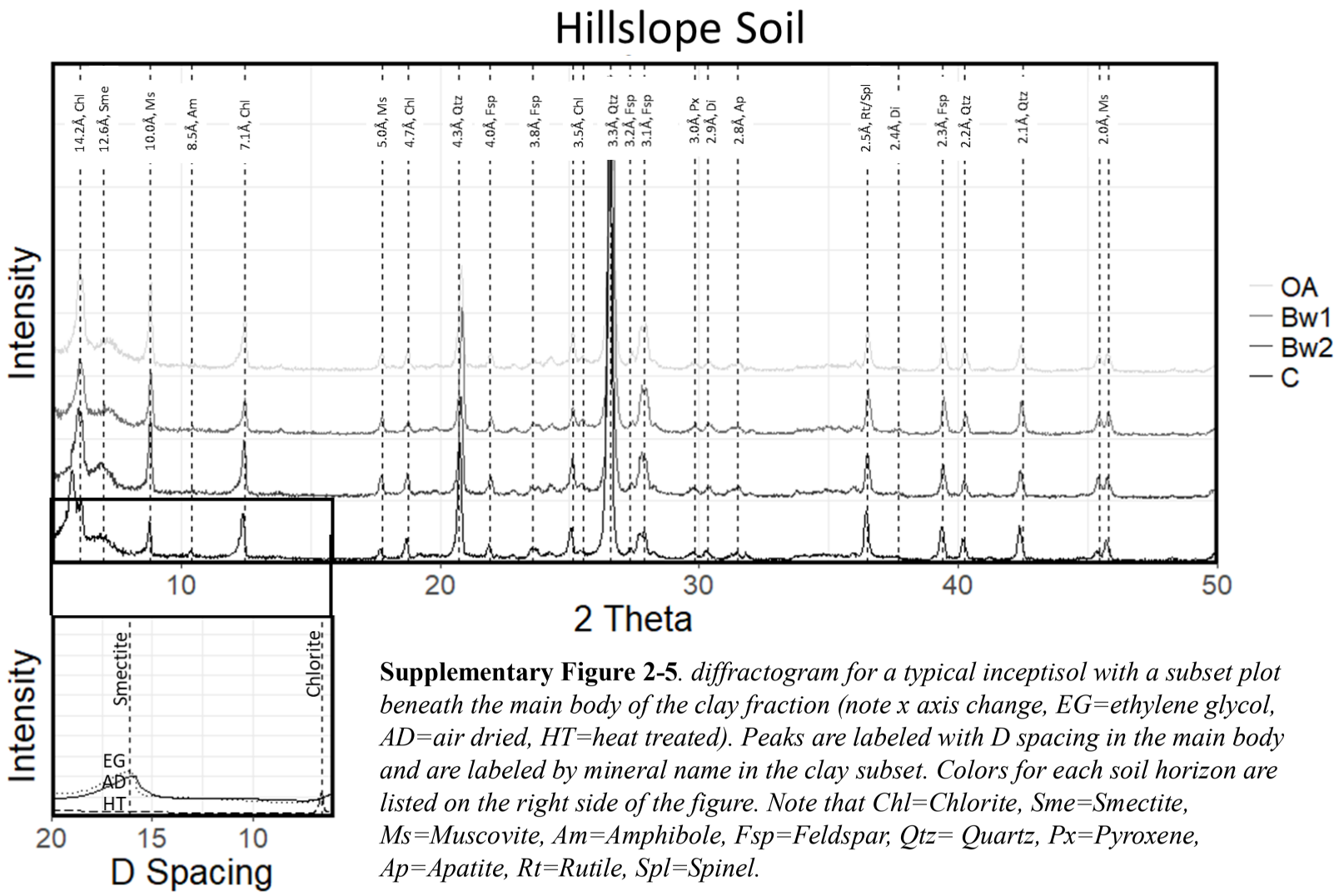

Supplementary Figure 2-5. *diffractogram for a typical inceptisol with a subset plot beneath the main body of the clay fraction (note x axis change, EG=ethylene glycol, AD=air dried, HT=heat treated). Peaks are labeled with D spacing in the main body and are labeled by mineral name in the clay subset. Colors for each soil horizon are listed on the right side of the figure. Note that Chl=Chlorite, Sme=Smectite, Ms=Muscovite, Am=Amphibole, Fsp=Feldspar, Qtz= Quartz, Px=Pyroxene, Ap=Apatite, Rt=Rutile, Spl=Spinel.*

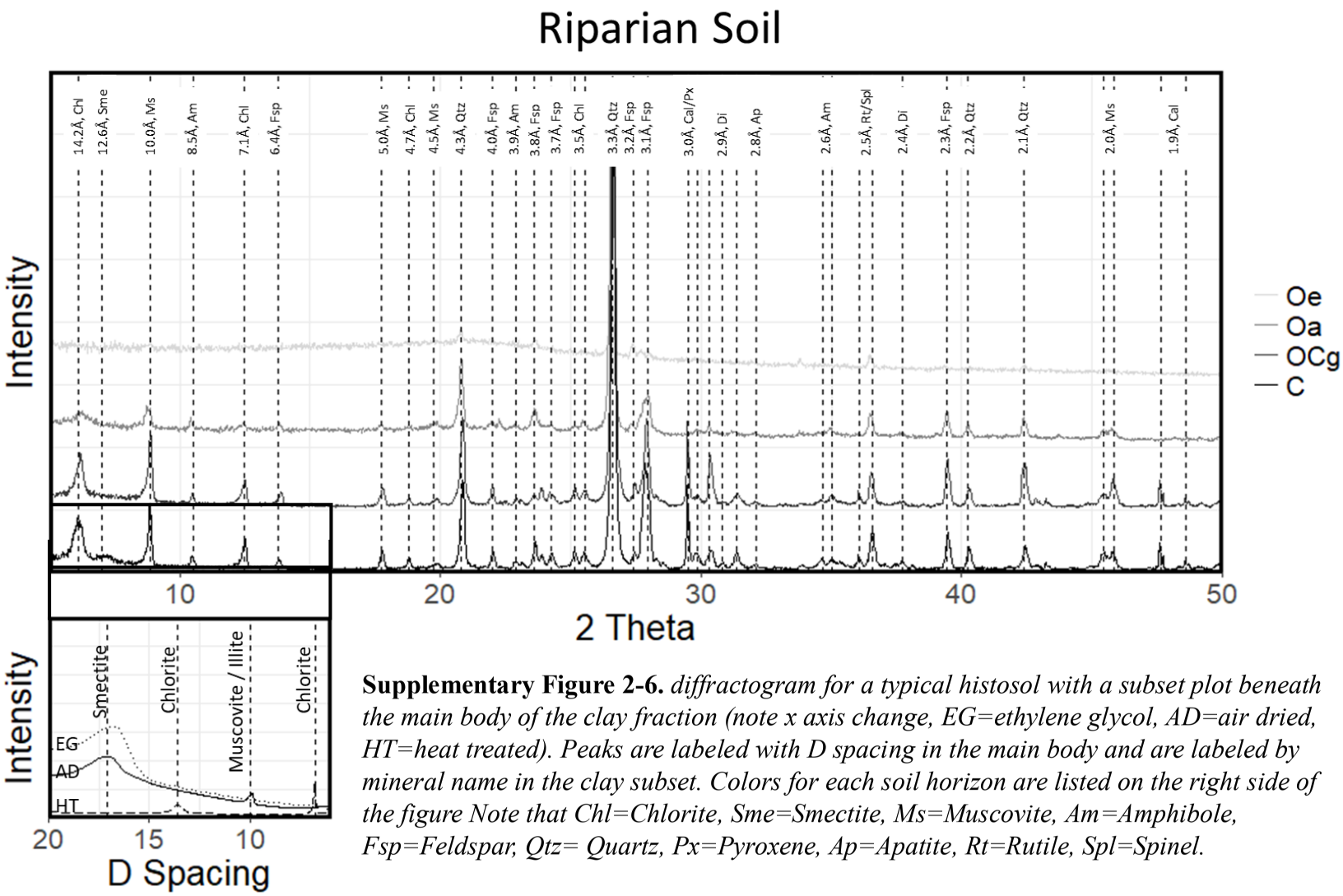

Supplementary Figure 2-6. *diffractogram for a typical histosol with a subset plot beneath the main body of the clay fraction (note x axis change, EG=ethylene glycol, AD=air dried, HT=heat treated). Peaks are labeled with D spacing in the main body and are labeled by mineral name in the clay subset. Colors for each soil horizon are listed on the right side of the figure Note that Chl=Chlorite, Sme=Smectite, Ms=Muscovite, Am=Amphibole, Fsp=Feldspar, Qtz= Quartz, Px=Pyroxene, Ap=Apatite, Rt=Rutile, Spl=Spinel.*

2.7 References:

Amiotte-Suchet, P., Aubert, D., Probst, J.L., Gauthier-Lafaye, F., Probst, A., Andreux, F., Viville, D., 1999. δ13C pattern of dissolved inorganic carbon in a small granitic catchment: the Strengbach case study (Vosges mountains, France). Chem. Geol. 159, 129–145. https://doi.org/10.1016/S0009-2541(99)00037-6

Appling, A.P., Leon, M.C., McDowell, W.H., 2015. Reducing bias and quantifying uncertainty in watershed flux estimates: the R package loadflex., Ecosphere 6(12):269.

Bailey, S.W., Brousseau, P.A., McGuire, K.J., Ross, D.S., 2014. Influence of landscape position and transient water table on soil development and carbon distribution in a steep, headwater catchment. Geoderma 226–227, 279–289. https://doi.org/10.1016/j.geoderma.2014.02.017

Berner, E.K., Berner, R.A., 2012. Chemical Weathering: Minerals, Plants, and Water Chemistry, in: Global Environment: Water, Air, and Geochemical Cycles. Princeton University Press, pp. 151–184.

Bishop, K., Seibert, J., Köhler, S., Laudon, H., 2004. Resolving the Double Paradox of rapidly mobilized old water highly variable responses in runoff chemistry. Hydrol. Process. 18, 185–189. https://doi.org/10.1002/hyp.5209

Bonifacio, E., Zanini, E., Boero, V., Franchini-Angela, M., 1997. Pedogenesis in a soil catena on serpentinite in north-western Italy. Geoderma 75, 33–51. https://doi.org/10.1016/S0016-7061(96)00076-6

Brantley, S.L., Goldhaber, M.B., Ragnarsdottir, K.V., 2007. Crossing Disciplines and Scales to Understand the Critical Zone. Elements 3, 307–314.

Brimhall, G.H., Dietrich, W.E., 1987. Constitutive mass balance relations between chemical composition, volume, density, porosity, and strain in metasomatic hydrochemical systems: Results on weathering and pedogenesis. Geochim. Cosmochim. Acta 51, 567–587. https://doi.org/10.1016/0016-7037(87)90070-6

Burns, D.A., McHale, M.R., Driscoll, C.T., Roy, K.M., 2005. Response of Surface Water Chemistry to Reduced Levels of Acid Precipitation: Comparison of Trends in Two regions of New York, USA. Hydrol. Process. 20, 1611–1627.

Cerling, T.E., 1984. The stable isotopic composition of modern soil carbonateand its relationship to climate. Earth Planet. Sci. Lett. 71, 229–240.

Cronan, C.S., Schofield, C.L., 1979. Aluminum leaching response to Acid precipitation: effects on high-elevation watersheds in the northeast. Science 204, 304–306.

Dawson, J.J., Bakewell, C., Billett, M.F., 2001. Is in-stream processing an important control on spatial changes in carbon fluxes in headwater catchments? Sci Total Env. 265, 153–67.

de Wit, H., Skjelkvåle, B.L., Høgåsen, T., Clair, T., Colombo, L., Fölster, J., Jeffries, D., László, B., Majer, V., Monteith, D., Mosello, R., Rogora, M., Rzychon, D.,

Steingruber, S., Stivrina, S., Stoddard, J.L., Srybny, A., Talkop, R., Vesely, J., Vuorenmaa, J., Wieting, J., Worsztynowicz, A., 2007. Trends in surface water chemistry and biota; The importance of confounding factors: 2. Trends in surface water chemistry 1994-2004. NIVA Rep. 5385-2007, ICP Waters Report 87/2007 12–28.

Driscoll, C.T., Lawrence, G.B., Bulger, T.J., Cronan, C.S., Eagar, C., Lambert, K.F., Likens, G.E., Stoddard, J.L., Weathers, K.C., 2001. Acid Rain Revisited: Advances in Scientific Understanding Since the Passage of the 1970 and 1990 Clean Air Amendments 1.

Fanning, D.S., Fanning, M.C.B., 1989. Soil Morphology, Genesis, and Classification.

Ferry, J.M., 1991. Regional Metamorphism of the Waits River Formation, Eastern Vermont: Delineatoin of a New Type of Giant Metamorphic Hydrothermal System. J. Petrol. 33, 45–94.

Frisbee, M.D., Phillips, F.M., Campbell, A.R., Liu, F., Sanchez, S.A., 2011. Streamflow generation in a large, alpine watershed in the southern Rocky Mountains of Colorado: Is streamflow generation simply the aggregation of hillslope runoff responses? Water Resour. Res. 47.

Garmo, Ø.A., Skjelkvåle, B.L., de Wit, H.A., Colombo, L., Curtis, C., Fölster, J., Hoffmann, A., Hruška, J., Høgåsen, T., Jeffries, D.S., Keller, W.B., Krám, P., Majer, V., Monteith, D.T., Paterson, A.M., Rogora, M., Rzychon, D., Steingruber, S., Stoddard, J.L., Vuorenmaa, J., Worsztynowicz, A., 2014. Trends in Surface Water Chemistry in Acidified Areas in Europe and North America from 1990 to 2008. Water. Air. Soil Pollut. 225, 1880. https://doi.org/10.1007/s11270-014-1880-6

Hawkins, W.A., Graham, R.C., 2017. Soil Mineralogy of a Vernal Pool Catena in Southern California. Soil Mineral.

Hornbeck, J.., Bailey, S.., Buso, D.., Shanley, J.., 1997. Streamwater chemistry and nutrient budgets for forested watersheds in New England: variability and management implications. For. Ecol. Manag. 93, 73–89. https://doi.org/10.1016/S0378-1127(96)03937-0

Huang, Q.B., Qin, X.Q., Liu, P.Y., Zhang, L.K., Su, C.T., 2017. Impact of sulfuric and nitric acids on carbonate dissolution, and the associated deficit of CO2 uptake in the upper-middle reaches of the Wujiang River, China. J Contam Hydrol 203, 18–27. https://doi.org/10.1016/j.jconhyd.2017.05.006

Jenny, H., 1941. Factors of soil formation. McGraw-Hill, New York.

Jin, L., Ravella, R., Ketchum, B., Bierman, P.R., Heaney, P., White, T., Brantley, S.L., 2010. Mineral weathering and elemental transport during hillslope evolution at the Susquehanna/Shale Hills Critical Zone Observatory. Geochim. Cosmochim. Acta 74, 3669–3691. https://doi.org/10.1016/j.gca.2010.03.036

Johnson, C.E., Driscoll, C.T., Siccama, T.G., Likens, G.E., 2000. Element Fluxes and Landscape Position in a Northern Hardwood Forest Watershed Ecosystem. Ecosystems 3, 159–184. https://doi.org/10.1007/s100210000017

Johnson, N.M., Driscoll, C.T., Eaton, J.S., Likens, G.E., McDowell, W.H., 1981. "Acid rain", dissolved aluminum and chemical weathering at the Hubbard Brook Experimental Forest, New Hampshire. Geochim. Cosmochim. Acta 45, 1421–1437. https://doi.org/10.1016/0016-7037(81)90276-3

Kendall, K.., Shanley, J.., McDonnell, J.., 1999. A hydrometric and geochemical approach to test the transmissivity feedback hypothesis during snowmelt. J. Hydrol. 219, 188–205. https://doi.org/10.1016/S0022-1694(99)00059-1

Kim, K., 1999. Geochemical evolution of groundwater along a flowpath determined from oxygen isotope analysis in a carbonate free, silicate aquifer. Geosci. J. 3, 191–200. https://doi.org/10.1007/BF02910490

Kopáček, J., Hejzlar, J., Kaňa, J., Porcal, P., Turek, J., 2016. The Sensitivity of Water Chemistry to Climate Forested, Nitrogen-Saturated Catchment Recovering from Acidification. Ecol. Indic. 63, 196–208.

Lagaly, G., 1993. Reaktionen des Tonminerale, in: Jasmund K, Lagaly G (Eds.), Tonminerale Und Tone: Struktur, Eigenschaften Und Einsatz in Industrie Und Umwelt. Steinkopff Verlag, Darmstadt, pp. 89–167.

Lawrence, G.B., Hazlett, P.W., Fernandez, I.J., Ouimet, R., Bailey, S.W., Shortle, W.C., Smith, K.T., Antidormi, M.R., 2015. Declining Acidic Deposition Begins Reversal of Forest-Soil Acidification in the Northeastern U.S. and Eastern Canada. Environ. Sci. Technol. 49, 13103–13111. https://doi.org/10.1021/acs.est.5b02904

Lidman, F., Boily, A., Laudon, H., Köhler, S.J., 2017. From soil water to surface water – how the riparian zone controls element transport from a boreal forest to a stream. Biogeosciences 14, 3001–3014. https://doi.org/10.5194/bg-14-3001-2017

Likens, G.E., Bormann, F.H., Johnson, N.M., 1972. Acid Rain. Environ. Sci. Policy Sustain. Dev. 14, 33–40. https://doi.org/10.1080/00139157.1972.9933001

Likens, G.E., Driscoll, C.T., Buso, D.C., 1996. Long-term effects of acid rain: response and recovery of a forest ecosystem. Science 272, 244–246.

Lybrand, R.A., Rasmussen, C., 2015. Quantifying Climate and Landscape Position Controls on Soil Development in Semiarid Ecosystems. Soil Sci. Soc. Am. J. 79, 104–116. https://doi.org/10.2136/sssaj2014.06.0242

Maher, K., 2011. The role of fluid residence time and topographic scales in determining chemical fluxes from landscapes. Earth Planet. Sci. Lett. 312, 48–58. https://doi.org/http://dx.doi.org/10.1016/j.epsl.2011.09.040

Matzner, E., Murach, D., 1995. Soil changes induced by air pollutant deposition and their implication for forests in central Europe. Water. Air. Soil Pollut. 85, 63–76. https://doi.org/10.1007/BF00483689

Mayer, B., Shanley, J.B., Bailey, S.W., Mitchell, M.J., 2010. Identifying sources of stream water sulfate after a summer drought in the Sleepers River watershed (Vermont, USA) using hydrological, chemical, and isotopic techniques. Appl. Geochem. 25, 747–754. https://doi.org/10.1016/j.apgeochem.2010.02.007

McIntosh, J.C., Schaumberg, C., Perdrial, J., Harpold, A., Vázquez-Ortega, A., Rasmussen, C., Vinson, D., Zapata-Rios, X., Brooks, P.D., Meixner, T., Pelletier, J., Derry, L., Chorover, J., 2017. Geochemical evolution of the Critical Zone across variable time scales informs concentration-discharge relationships: Jemez River Basin Critical Zone Observatory. Water Resour. Res. n/a-n/a. https://doi.org/10.1002/2016WR019712

McLeod, A.I., 2011. Kendall: Kendall rank correlation and Mann-Kendall trend test.

Meybeck, M., 1993. Riverine transport of atmospheric carbon: Sources, global typology and budget. Water. Air. Soil Pollut. 70, 443–463. https://doi.org/10.1007/BF01105015

Moore, D.M., Reynolds, R.C., 1997. X-Ray Diffraction and the Identification and Analysis of Clay Minerals, 2nd ed. New York: Oxford University Press.

Mulholland, P.J., Hill, W.R., 1997. Seasonal patterns in streamwater nutrient and dissolved organic carbon concentrations: Separating catchment flow path and in-stream effects. Water Resour Res 33, 1297–1306. https://doi.org/10.1029/97wr00490

Newell, A.D., Skjelkvåle, B.L., 1997. Acidification Trends in Surface Waters in the International Program on Acidification of Rivers and Lakes. Water. Air. Soil Pollut. 93, 27–57. https://doi.org/10.1023/A:1022126704750

Nezat, C.A., Blum, J.D., Klaue, A., Johnson, C.E., Siccama, T.G., 2004. Influence of landscape position and vegetation on long-term weathering rates at the Hubbard Brook Experimental Forest, New Hampshire, USA11Associate editor: K. L. Nagy. Geochim. Cosmochim. Acta 68, 3065–3078. https://doi.org/10.1016/j.gca.2004.01.021

Olson, K.R., Jones, R.L., Gennadiyev, A.N., Chernyanskii, S., Woods, W.I., Lang, J.M., 2003. SOIL CATENA FORMATION AND EROSION OF TWO MISSISSIPPIAN MOUNDS AT CAHOKIA ARCHAEOLOGICAL SITE, ILLINOIS. Soil Sci. 168.

Pavich, M.J., Obermeier, L., Estabrook, J.R., 1989. Investigations of the characteristics, origin, and residence time of the Upland residual mantle of the Piedmont of Fairfax County, Virginia. (U.S. Geological Survey professional paper No. 1352).

Perdrial, J., Thompson, A., Chorover, J., 2015. Chapter 6 - Soil Geochemistry in the Critical Zone: Influence on Atmosphere, Surface- and Groundwater Composition, in: John R. Giardino and Chris Houser (Ed.), Developments in Earth Surface Processes. Elsevier, pp. 173–201. https://doi.org/10.1016/B978-0-444-63369-9.00006-9

Perdrial, J.N., Warr, L.N., Perdrial, N., Lett, M.-C., Elsass, F., 2009. Interaction between smectite and bacteria: Implications for bentonite as backfill material in the disposal of nuclear waste. Chem. Geol. 264, 281–294. https://doi.org/10.1016/j.chemgeo.2009.03.012

Peters, N., Aulenback, B., 2009. Flowpath Contributions of Weathering Products to Stream Fluxes at the Panola Mountain Research Watershed, Georgia.

Pohlert, T., 2018. trend: Non-Parametric Trend Tests and Change-Point Detection.

Poppe, L.J., Paskevich, V.F., Hathaway, J.C., Blackwood, D.S., 2001. A Laboratory manua for X-Ray Powder Diffraction (Open-File No. 1–41). USGS.

R Core Development Team, 2017. R: A language and environment for statistical computing. R Foundation for statistical computing, Vienna, Austria.

Raddum, G.G., Fjellheim, A., Erikson, L., Fott, J., Halvorsen, G.A., Heegaard, E., Kohout, L., Kifinger, B., Schaumberg, J., Maetze, A., Zahn, H., 2007. Trends in surface water chemistry and biota; The importance of confounding factors: 5. Biological recovery. NIVA Rep. 5385-2007, ICP Waters Report 87/2007 50–63.

Ratcliffe, N., Stanley, R., Gale, M., Thompson, P., Walsh, G., 2011. Bedrock Geologic Map of Vermont. USGS Scientific Investigations Series Map 3184.

Rice, K.C., Herman, J.S., 2012. Acidification of Earth: An assessment across mechanisms and scales. Appl. Geochem. 27, 1–14. https://doi.org/10.1016/j.apgeochem.2011.09.001

Rogora, M., Colombo, L., Lepori, F., Marchetto, A., Steingruber, S., Tornimbeni, O., 2013. Thirty Years of Chemical Changes in Alpine Acid-Sensitive Lakes in the Alps. Water. Air. Soil Pollut. 224, 1746. https://doi.org/10.1007/s11270-013-1746-3

Runkel, R.L., Crawford, C.G., Cohn, T.A., 2004. Load estimator (LOADEST): a FORTRAN program for estimating constituent loads in streams and rivers. USGS Techniques and Methods Book 4, Chapter A5., U.S. Geological Survey, Reston, Virginia, USA.

Schimel D., Stillwell M. A., Woodmansee R. G., 1985. Biogeochemistry of C, N, and P in a Soil Catena of the Shortgrass Steppe. Ecology 66, 276–282. https://doi.org/10.2307/1941328

Schuster, P.F., Shanley, J., Marvin-Dipasquale, M., Reddy, M.M., Aiken, G.R., Roth, D.A., Taylor, H.E., Krabbenhoft, D.P., DeWild, J.F., 2007. Mercury and Organic

Carbon Dynamics During Runoff Episodes from a Northeastern USA Watershed. Water. Air. Soil Pollut. 187, 89–108.

Sebestyen, S.D., Boyer, E.W., Shanley, J.B., Kendall, C., Doctor, D.H., Aiken, G.R., Ohte, N., 2008. Sources, transformations, and hydrological processes that control stream nitrate and dissolved organic matter concentrations during snowmelt in an upland forest. Water Resour. Res. 44, W12410. https://doi.org/10.1029/2008WR006983

Shanley James B., Chalmers Ann T., Mack Thomas J., Smith Thor E., Harte Philip T., 2016. Groundwater Level Trends and Drivers in Two Northern New England Glacial Aquifers. JAWRA J. Am. Water Resour. Assoc. 52, 1012–1030. https://doi.org/10.1111/1752-1688.12432

Shanley, J.B., 2000. Sleepers River Watershed -- A USGS WEBB Program Site: U.S. Geological Survey Fact Sheet.

Shanley, J.B., Kram, P., Hruska, J., Bullen, T.D., 2004. A biogeochemical comparison of two well-buffered catchments with contrasting histories of acid deposition. Water Air Soil Pollut. Focus 4, 325–342. https://doi.org/10.1023/B:WAFO.0000028363.48348.a4

Skjelkvåle, B.L., 2003. The 15-year report: Assessment and monitoring of surface waters in Europe and North America; acidification and recovery, dynamic modelling and heavy metals. NIVA Rep. 4716-2003, ICP Waters Report 73/2003.

Skjelkvåle, B.L., Stoddard, J.L., Andersen, T., 2001. Trends in Surface Water Acidification in Europe and North America (1989–1998). Water. Air. Soil Pollut. 130, 787–792. https://doi.org/10.1023/A:1013806223310

Skjelkvåle, B.L., Stoddard, J.L., Jeffries, D.S., Tørseth, K., Høgåsen, T., Bowman, J., Mannio, J., Monteith, D.T., Mosello, R., Rogora, M., Rzychon, D., Vesely, J., Wieting, J., Wilander, A., Worsztynowicz, A., 2005. Regional scale evidence for improvements in surface water chemistry 1990–2001. Recovery Acidif. UK Evid. 15 Years Acid Waters Monit. Acidif. UK Evid. 15 Years Acid Waters Monit. 137, 165–176. https://doi.org/10.1016/j.envpol.2004.12.023

Smith, S., Aardenne, J., Klimont, Z., Andres, R., Volke, A., Delgado Arias, S., 2010. Anthropogenic sulfur dioxide emissions: 1850–2005. https://doi.org/10.5194/acpd-10-16111-2010

Sommer, M., 2006. Influence of soil pattern on matter transport in and from terrestrial biogeosystems—A new concept for landscape pedology. Adv. Landsc.-Scale Soil Res. 133, 107–123. https://doi.org/10.1016/j.geoderma.2006.03.040

Spence, J., Telmer, K., 2002. The Significance of Sulphuric Acid Induced Chemical Weathering on Long Term Fluxes of CO2 Between the Atmosphere-Ocean and Rocks: Evidence From River Chemistry and Carbon Isotopes in the Canadian Cordillera. AGU Fall Meet. Abstr.

Stoddard, J.L., Jeffries, D.S., Lukewille, A., Clair, T.A., Dillon, P.J., Driscoll, C.T., Forsius, M., Johannessen, M., Kahl, J.S., Kellogg, J.H., Kemp, A., Mannio, J., Monteith, D.T., Murdoch, P.S., Patrick, S., Rebsdorf, A., Skjelkvale, B.L., Stainton, M.P., Traaen, T., van Dam, H., Webster, K.E., Wieting, J., Wilander, A., 1999. Regional trends in aquatic recovery from acidification in North America and Europe. Nature 401, 575–578. https://doi.org/10.1038/44114

Strawn, D.G., Hinrich, B.L., O'Connor, G.A., 2015. Soil Chemistry, Fourth. ed. John Wiley & Sons, Ltd.

Taylor, A.B., Velbel, M.A., 1991. Geochemical mass balances and weathering rates in forested watersheds of the southern Blue Ridge II. Effects of botanical uptake terms. Weather. Soils 51, 29–50. https://doi.org/10.1016/0016-7061(91)90065-2

Vebel, M.A., 1985. Geochemical mass balances and weathering rates in forested watersheds of the southern Blue Ridge. Am. J. Sci. 285.

Vidon Philippe, Allan Craig, Burns Douglas, Duval Tim P., Gurwick Noel, Inamdar Shreeram, Lowrance Richard, Okay Judy, Durelle Scott, Sebestyen Steve, 2010. Hot Spots and Hot Moments in Riparian Zones: Potential for Improved Water Quality Management1. JAWRA J. Am. Water Resour. Assoc. 46, 278–298. https://doi.org/10.1111/j.1752-1688.2010.00420.x

White, A.F., Bullen, T.D., Schulz, M.S., Blum, A.E., Huntington, T.G., Peters, N.E., 2001. Differential rates of feldspar weathering in granitic regoliths. Geochim. Cosmochim. Acta 65, 847–869. https://doi.org/10.1016/S0016-7037(00)00577-9

Wiekenkamp, I., Huisman, J., Bogena, H., Lin, H., Vereecken, H., 2016. Spatial and temporal occurence of preferential flow in a forested headwater catchment. J. Hydrol. 534, 139–149.

Winterdahl, M., Temnerud, J., Futter, M., Löfgren, S., Moldan, F., Bishop, K., 2011. Riparian Zone Influence on Stream Water Dissolved Organic Carbon Concentrations at the Swedish Integrated Monitoring Sites. AMBIO - J. Hum. Environ. 40, 920–930. https://doi.org/10.1007/s13280-011-0199-4

COMPRENHENSIVE BIBLIOGRAPHY

Amiotte-Suchet, P., Aubert, D., Probst, J.L., Gauthier-Lafaye, F., Probst, A., Andreux, F., Viville, D., 1999. δ13C pattern of dissolved inorganic carbon in a small granitic catchment: the Strengbach case study (Vosges mountains, France). Chem. Geol. 159, 129–145. https://doi.org/10.1016/S0009-2541(99)00037-6

Appling, A.P., Leon, M.C., McDowell, W.H., 2015. Reducing bias and quantifying uncertainty in watershed flux estimates: the R package loadflex., Ecosphere 6(12):269.

Bailey, S.W., Brousseau, P.A., McGuire, K.J., Ross, D.S., 2014. Influence of landscape position and transient water table on soil development and carbon distribution in a steep, headwater catchment. Geoderma 226–227, 279–289. https://doi.org/10.1016/j.geoderma.2014.02.017

Berner, E.K., Berner, R.A., 2012. Chemical Weathering: Minerals, Plants, and Water Chemistry, in: Global Environment: Water, Air, and Geochemical Cycles. Princeton University Press, pp. 151–184.

Bishop, K., Seibert, J., Köhler, S., Laudon, H., 2004. Resolving the Double Paradox of rapidly mobilized old water highly variable responses in runoff chemistry. Hydrol. Process. 18, 185–189. https://doi.org/10.1002/hyp.5209

Bonifacio, E., Zanini, E., Boero, V., Franchini-Angela, M., 1997. Pedogenesis in a soil catena on serpentinite in north-western Italy. Geoderma 75, 33–51. https://doi.org/10.1016/S0016-7061(96)00076-6

Brantley, S.L., Goldhaber, M.B., Ragnarsdottir, K.V., 2007. Crossing Disciplines and Scales to Understand the Critical Zone. Elements 3, 307–314.

Brimhall, G.H., Dietrich, W.E., 1987. Constitutive mass balance relations between chemical composition, volume, density, porosity, and strain in metasomatic hydrochemical systems: Results on weathering and pedogenesis. Geochim. Cosmochim. Acta 51, 567–587. https://doi.org/10.1016/0016-7037(87)90070-6

Burns, D.A., McHale, M.R., Driscoll, C.T., Roy, K.M., 2005. Response of Surface Water Chemistry to Reduced Levels of Acid Precipitation: Comparison of Trends in Two regions of New York, USA. Hydrol. Process. 20, 1611–1627.

Cerling, T.E., 1984. The stable isotopic composition of modern soil carbonateand its relationship to climate. Earth Planet. Sci. Lett. 71, 229–240.

Cronan, C.S., Schofield, C.L., 1979. Aluminum leaching response to Acid precipitation: effects on high-elevation watersheds in the northeast. Science 204, 304–306.

Dawson, J.J., Bakewell, C., Billett, M.F., 2001. Is in-stream processing an important control on spatial changes in carbon fluxes in headwater catchments? Sci Total Env. 265, 153–67.

de Wit, H., Skjelkvåle, B.L., Høgåsen, T., Clair, T., Colombo, L., Fölster, J., Jeffries, D., László, B., Majer, V., Monteith, D., Mosello, R., Rogora, M., Rzychon, D.,

Steingruber, S., Stivrina, S., Stoddard, J.L., Srybny, A., Talkop, R., Vesely, J., Vuorenmaa, J., Wieting, J., Worsztynowicz, A., 2007. Trends in surface water chemistry and biota; The importance of confounding factors: 2. Trends in surface water chemistry 1994-2004. NIVA Rep. 5385-2007, ICP Waters Report 87/2007 12–28.

Driscoll, C.T., Lawrence, G.B., Bulger, T.J., Cronan, C.S., Eagar, C., Lambert, K.F., Likens, G.E., Stoddard, J.L., Weathers, K.C., 2001. Acid Rain Revisited: Advances in Scientific Understanding Since the Passage of the 1970 and 1990 Clean Air Amendments 1.

Fanning, D.S., Fanning, M.C.B., 1989. Soil Morphology, Genesis, and Classification.

Ferry, J.M., 1991. Regional Metamorphism of the Waits River Formation, Eastern Vermont: Delineatoin of a New Type of Giant Metamorphic Hydrothermal System. J. Petrol. 33, 45–94.

Frisbee, M.D., Phillips, F.M., Campbell, A.R., Liu, F., Sanchez, S.A., 2011. Streamflow generation in a large, alpine watershed in the southern Rocky Mountains of Colorado: Is streamflow generation simply the aggregation of hillslope runoff responses? Water Resour. Res. 47.

Garmo, Ø.A., Skjelkvåle, B.L., de Wit, H.A., Colombo, L., Curtis, C., Fölster, J., Hoffmann, A., Hruška, J., Høgåsen, T., Jeffries, D.S., Keller, W.B., Krám, P., Majer, V., Monteith, D.T., Paterson, A.M., Rogora, M., Rzychon, D., Steingruber, S., Stoddard, J.L., Vuorenmaa, J., Worsztynowicz, A., 2014. Trends in Surface Water Chemistry in Acidified Areas in Europe and North America from 1990 to 2008. Water. Air. Soil Pollut. 225, 1880. https://doi.org/10.1007/s11270-014-1880-6

Hawkins, W.A., Graham, R.C., 2017. Soil Mineralogy of a Vernal Pool Catena in Southern California. Soil Mineral.

Hornbeck, J.., Bailey, S.., Buso, D.., Shanley, J.., 1997. Streamwater chemistry and nutrient budgets for forested watersheds in New England: variability and management implications. For. Ecol. Manag. 93, 73–89. https://doi.org/10.1016/S0378-1127(96)03937-0

Huang, Q.B., Qin, X.Q., Liu, P.Y., Zhang, L.K., Su, C.T., 2017. Impact of sulfuric and nitric acids on carbonate dissolution, and the associated deficit of CO2 uptake in the upper-middle reaches of the Wujiang River, China. J Contam Hydrol 203, 18–27. https://doi.org/10.1016/j.jconhyd.2017.05.006

Jenny, H., 1941. Factors of soil formation. McGraw-Hill, New York.

Jin, L., Ravella, R., Ketchum, B., Bierman, P.R., Heaney, P., White, T., Brantley, S.L., 2010. Mineral weathering and elemental transport during hillslope evolution at the Susquehanna/Shale Hills Critical Zone Observatory. Geochim. Cosmochim. Acta 74, 3669–3691. https://doi.org/10.1016/j.gca.2010.03.036

Johnson, C.E., Driscoll, C.T., Siccama, T.G., Likens, G.E., 2000. Element Fluxes and Landscape Position in a Northern Hardwood Forest Watershed Ecosystem. Ecosystems 3, 159–184. https://doi.org/10.1007/s100210000017

Johnson, N.M., Driscoll, C.T., Eaton, J.S., Likens, G.E., McDowell, W.H., 1981. "Acid rain", dissolved aluminum and chemical weathering at the Hubbard Brook Experimental Forest, New Hampshire. Geochim. Cosmochim. Acta 45, 1421–1437. https://doi.org/10.1016/0016-7037(81)90276-3

Kendall, K., Shanley, J., McDonnell, J., 1999. A hydrometric and geochemical approach to test the transmissivity feedback hypothesis during snowmelt. J. Hydrol. 219, 188–205. https://doi.org/10.1016/S0022-1694(99)00059-1

Kim, K., 1999. Geochemical evolution of groundwater along a flowpath determined from oxygen isotope analysis in a carbonate free, silicate aquifer. Geosci. J. 3, 191–200. https://doi.org/10.1007/BF02910490

Kopáček, J., Hejzlar, J., Kaňa, J., Porcal, P., Turek, J., 2016. The Sensitivity of Water Chemistry to Climate Forested, Nitrogen-Saturated Catchment Recovering from Acidification. Ecol. Indic. 63, 196–208.

Lagaly, G., 1993. Reaktionen des Tonminerale, in: Jasmund K, Lagaly G (Eds.), Tonminerale Und Tone: Struktur, Eigenschaften Und Einsatz in Industrie Und Umwelt. Steinkopff Verlag, Darmstadt, pp. 89–167.

Lawrence, G.B., Hazlett, P.W., Fernandez, I.J., Ouimet, R., Bailey, S.W., Shortle, W.C., Smith, K.T., Antidormi, M.R., 2015. Declining Acidic Deposition Begins Reversal of Forest-Soil Acidification in the Northeastern U.S. and Eastern Canada. Environ. Sci. Technol. 49, 13103–13111. https://doi.org/10.1021/acs.est.5b02904

Lidman, F., Boily, A., Laudon, H., Köhler, S.J., 2017. From soil water to surface water – how the riparian zone controls element transport from a boreal forest to a stream. Biogeosciences 14, 3001–3014. https://doi.org/10.5194/bg-14-3001-2017

Likens, G.E., Bormann, F.H., Johnson, N.M., 1972. Acid Rain. Environ. Sci. Policy Sustain. Dev. 14, 33–40. https://doi.org/10.1080/00139157.1972.9933001

Likens, G.E., Driscoll, C.T., Buso, D.C., 1996. Long-term effects of acid rain: response and recovery of a forest ecosystem. Science 272, 244–246.

Lybrand, R.A., Rasmussen, C., 2015. Quantifying Climate and Landscape Position Controls on Soil Development in Semiarid Ecosystems. Soil Sci. Soc. Am. J. 79, 104–116. https://doi.org/10.2136/sssaj2014.06.0242

Maher, K., 2011. The role of fluid residence time and topographic scales in determining chemical fluxes from landscapes. Earth Planet. Sci. Lett. 312, 48–58. https://doi.org/http://dx.doi.org/10.1016/j.epsl.2011.09.040

Matzner, E., Murach, D., 1995. Soil changes induced by air pollutant deposition and their implication for forests in central Europe. Water. Air. Soil Pollut. 85, 63–76. https://doi.org/10.1007/BF00483689

Mayer, B., Shanley, J.B., Bailey, S.W., Mitchell, M.J., 2010. Identifying sources of stream water sulfate after a summer drought in the Sleepers River watershed (Vermont, USA) using hydrological, chemical, and isotopic techniques. Appl. Geochem. 25, 747–754. https://doi.org/10.1016/j.apgeochem.2010.02.007

McIntosh, J.C., Schaumberg, C., Perdrial, J., Harpold, A., Vázquez-Ortega, A., Rasmussen, C., Vinson, D., Zapata-Rios, X., Brooks, P.D., Meixner, T., Pelletier, J., Derry, L., Chorover, J., 2017. Geochemical evolution of the Critical Zone across variable time scales informs concentration-discharge relationships: Jemez River Basin Critical Zone Observatory. Water Resour. Res. n/a-n/a. https://doi.org/10.1002/2016WR019712

McLeod, A.I., 2011. Kendall: Kendall rank correlation and Mann-Kendall trend test.

Meybeck, M., 1993. Riverine transport of atmospheric carbon: Sources, global typology and budget. Water. Air. Soil Pollut. 70, 443–463. https://doi.org/10.1007/BF01105015

Moore, D.M., Reynolds, R.C., 1997. X-Ray Diffraction and the Identification and Analysis of Clay Minerals, 2nd ed. New York: Oxford University Press.

Mulholland, P.J., Hill, W.R., 1997. Seasonal patterns in streamwater nutrient and dissolved organic carbon concentrations: Separating catchment flow path and in-stream effects. Water Resour Res 33, 1297–1306. https://doi.org/10.1029/97wr00490

Newell, A.D., Skjelkvåle, B.L., 1997. Acidification Trends in Surface Waters in the International Program on Acidification of Rivers and Lakes. Water. Air. Soil Pollut. 93, 27–57. https://doi.org/10.1023/A:1022126704750

Nezat, C.A., Blum, J.D., Klaue, A., Johnson, C.E., Siccama, T.G., 2004. Influence of landscape position and vegetation on long-term weathering rates at the Hubbard Brook Experimental Forest, New Hampshire, USA11Associate editor: K. L. Nagy. Geochim. Cosmochim. Acta 68, 3065–3078. https://doi.org/10.1016/j.gca.2004.01.021

Olson, K.R., Jones, R.L., Gennadiyev, A.N., Chernyanskii, S., Woods, W.I., Lang, J.M., 2003. SOIL CATENA FORMATION AND EROSION OF TWO MISSISSIPPIAN MOUNDS AT CAHOKIA ARCHAEOLOGICAL SITE, ILLINOIS. Soil Sci. 168.

Pavich, M.J., Obermeier, L., Estabrook, J.R., 1989. Investigations of the characteristics, origin, and residence time of the Upland residual mantle of the Piedmont of Fairfax County, Virginia. (U.S. Geological Survey professional paper No. 1352).

Perdrial, J., Thompson, A., Chorover, J., 2015. Chapter 6 - Soil Geochemistry in the Critical Zone: Influence on Atmosphere, Surface- and Groundwater Composition, in: John R. Giardino and Chris Houser (Ed.), Developments in Earth Surface Processes. Elsevier, pp. 173–201. https://doi.org/10.1016/B978-0-444-63369-9.00006-9

Perdrial, J.N., Warr, L.N., Perdrial, N., Lett, M.-C., Elsass, F., 2009. Interaction between smectite and bacteria: Implications for bentonite as backfill material in the disposal of nuclear waste. Chem. Geol. 264, 281–294. https://doi.org/10.1016/j.chemgeo.2009.03.012

Peters, N., Aulenback, B., 2009. Flowpath Contributions of Weathering Products to Stream Fluxes at the Panola Mountain Research Watershed, Georgia.

Pohlert, T., 2018. trend: Non-Parametric Trend Tests and Change-Point Detection.

Poppe, L.J., Paskevich, V.F., Hathaway, J.C., Blackwood, D.S., 2001. A Laboratory manua for X-Ray Powder Diffraction (Open-File No. 1–41). USGS.

R Core Development Team, 2017. R: A language and environment for statistical computing. R Foundation for statistical computing, Vienna, Austria.

Raddum, G.G., Fjellheim, A., Erikson, L., Fott, J., Halvorsen, G.A., Heegaard, E., Kohout, L., Kifinger, B., Schaumberg, J., Maetze, A., Zahn, H., 2007. Trends in surface water chemistry and biota; The importance of confounding factors: 5. Biological recovery. NIVA Rep. 5385-2007, ICP Waters Report 87/2007 50–63.

Ratcliffe, N., Stanley, R., Gale, M., Thompson, P., Walsh, G., 2011. Bedrock Geologic Map of Vermont. USGS Scientific Investigations Series Map 3184.

Rice, K.C., Herman, J.S., 2012. Acidification of Earth: An assessment across mechanisms and scales. Appl. Geochem. 27, 1–14. https://doi.org/10.1016/j.apgeochem.2011.09.001

Rogora, M., Colombo, L., Lepori, F., Marchetto, A., Steingruber, S., Tornimbeni, O., 2013. Thirty Years of Chemical Changes in Alpine Acid-Sensitive Lakes in the Alps. Water. Air. Soil Pollut. 224, 1746. https://doi.org/10.1007/s11270-013-1746-3

Runkel, R.L., Crawford, C.G., Cohn, T.A., 2004. Load estimator (LOADEST): a FORTRAN program for estimating constituent loads in streams and rivers. USGS Techniques and Methods Book 4, Chapter A5., U.S. Geological Survey, Reston, Virginia, USA.

Schimel D., Stillwell M. A., Woodmansee R. G., 1985. Biogeochemistry of C, N, and P in a Soil Catena of the Shortgrass Steppe. Ecology 66, 276–282. https://doi.org/10.2307/1941328

Schuster, P.F., Shanley, J., Marvin-Dipasquale, M., Reddy, M.M., Aiken, G.R., Roth, D.A., Taylor, H.E., Krabbenhoft, D.P., DeWild, J.F., 2007. Mercury and Organic

Carbon Dynamics During Runoff Episodes from a Northeastern USA Watershed. Water. Air. Soil Pollut. 187, 89–108.

Sebestyen, S.D., Boyer, E.W., Shanley, J.B., Kendall, C., Doctor, D.H., Aiken, G.R., Ohte, N., 2008. Sources, transformations, and hydrological processes that control stream nitrate and dissolved organic matter concentrations during snowmelt in an upland forest. Water Resour. Res. 44, W12410. https://doi.org/10.1029/2008WR006983

Shanley James B., Chalmers Ann T., Mack Thomas J., Smith Thor E., Harte Philip T., 2016. Groundwater Level Trends and Drivers in Two Northern New England Glacial Aquifers. JAWRA J. Am. Water Resour. Assoc. 52, 1012–1030. https://doi.org/10.1111/1752-1688.12432

Shanley, J.B., 2000. Sleepers River Watershed -- A USGS WEBB Program Site: U.S. Geological Survey Fact Sheet.

Shanley, J.B., Kram, P., Hruska, J., Bullen, T.D., 2004. A biogeochemical comparison of two well-buffered catchments with contrasting histories of acid deposition. Water Air Soil Pollut. Focus 4, 325–342. https://doi.org/10.1023/B:WAFO.0000028363.48348.a4

Skjelkvåle, B.L., 2003. The 15-year report: Assessment and monitoring of surface waters in Europe and North America; acidification and recovery, dynamic modelling and heavy metals. NIVA Rep. 4716-2003, ICP Waters Report 73/2003.

Skjelkvåle, B.L., Stoddard, J.L., Andersen, T., 2001. Trends in Surface Water Acidification in Europe and North America (1989–1998). Water. Air. Soil Pollut. 130, 787–792. https://doi.org/10.1023/A:1013806223310

Skjelkvåle, B.L., Stoddard, J.L., Jeffries, D.S., Tørseth, K., Høgåsen, T., Bowman, J., Mannio, J., Monteith, D.T., Mosello, R., Rogora, M., Rzychon, D., Vesely, J., Wieting, J., Wilander, A., Worsztynowicz, A., 2005. Regional scale evidence for improvements in surface water chemistry 1990–2001. Recovery Acidif. UK Evid. 15 Years Acid Waters Monit. Acidif. UK Evid. 15 Years Acid Waters Monit. 137, 165–176. https://doi.org/10.1016/j.envpol.2004.12.023

Smith, S., Aardenne, J., Klimont, Z., Andres, R., Volke, A., Delgado Arias, S., 2010. Anthropogenic sulfur dioxide emissions: 1850–2005. https://doi.org/10.5194/acpd-10-16111-2010

Sommer, M., 2006. Influence of soil pattern on matter transport in and from terrestrial biogeosystems—A new concept for landscape pedology. Adv. Landsc.-Scale Soil Res. 133, 107–123. https://doi.org/10.1016/j.geoderma.2006.03.040

Spence, J., Telmer, K., 2002. The Significance of Sulphuric Acid Induced Chemical Weathering on Long Term Fluxes of CO2 Between the Atmosphere-Ocean and Rocks: Evidence From River Chemistry and Carbon Isotopes in the Canadian Cordillera. AGU Fall Meet. Abstr.

Stoddard, J.L., Jeffries, D.S., Lukewille, A., Clair, T.A., Dillon, P.J., Driscoll, C.T., Forsius, M., Johannessen, M., Kahl, J.S., Kellogg, J.H., Kemp, A., Mannio, J., Monteith, D.T., Murdoch, P.S., Patrick, S., Rebsdorf, A., Skjelkvale, B.L., Stainton, M.P., Traaen, T., van Dam, H., Webster, K.E., Wieting, J., Wilander, A., 1999. Regional trends in aquatic recovery from acidification in North America and Europe. Nature 401, 575–578. https://doi.org/10.1038/44114

Strawn, D.G., Hinrich, B.L., O'Connor, G.A., 2015. Soil Chemistry, Fourth. ed. John Wiley & Sons, Ltd.

Taylor, A.B., Velbel, M.A., 1991. Geochemical mass balances and weathering rates in forested watersheds of the southern Blue Ridge II. Effects of botanical uptake terms. Weather. Soils 51, 29–50. https://doi.org/10.1016/0016-7061(91)90065-2

Vebel, M.A., 1985. Geochemical mass balances and weathering rates in forested watersheds of the southern Blue Ridge. Am. J. Sci. 285.

Vidon Philippe, Allan Craig, Burns Douglas, Duval Tim P., Gurwick Noel, Inamdar Shreeram, Lowrance Richard, Okay Judy, Durelle Scott, Sebestyen Steve, 2010. Hot Spots and Hot Moments in Riparian Zones: Potential for Improved Water Quality Management1. JAWRA J. Am. Water Resour. Assoc. 46, 278–298. https://doi.org/10.1111/j.1752-1688.2010.00420.x

White, A.F., Bullen, T.D., Schulz, M.S., Blum, A.E., Huntington, T.G., Peters, N.E., 2001. Differential rates of feldspar weathering in granitic regoliths. Geochim. Cosmochim. Acta 65, 847–869. https://doi.org/10.1016/S0016-7037(00)00577-9

Wiekenkamp, I., Huisman, J., Bogena, H., Lin, H., Vereecken, H., 2016. Spatial and temporal occurence of preferential flow in a forested headwater catchment. J. Hydrol. 534, 139–149.

Winterdahl, M., Temnerud, J., Futter, M., Löfgren, S., Moldan, F., Bishop, K., 2011. Riparian Zone Influence on Stream Water Dissolved Organic Carbon Concentrations at the Swedish Integrated Monitoring Sites. AMBIO - J. Hum. Environ. 40, 920–930. https://doi.org/10.1007/s13280-011-0199-4

APPENDIX A: ADDITIONAL SOIL DATA

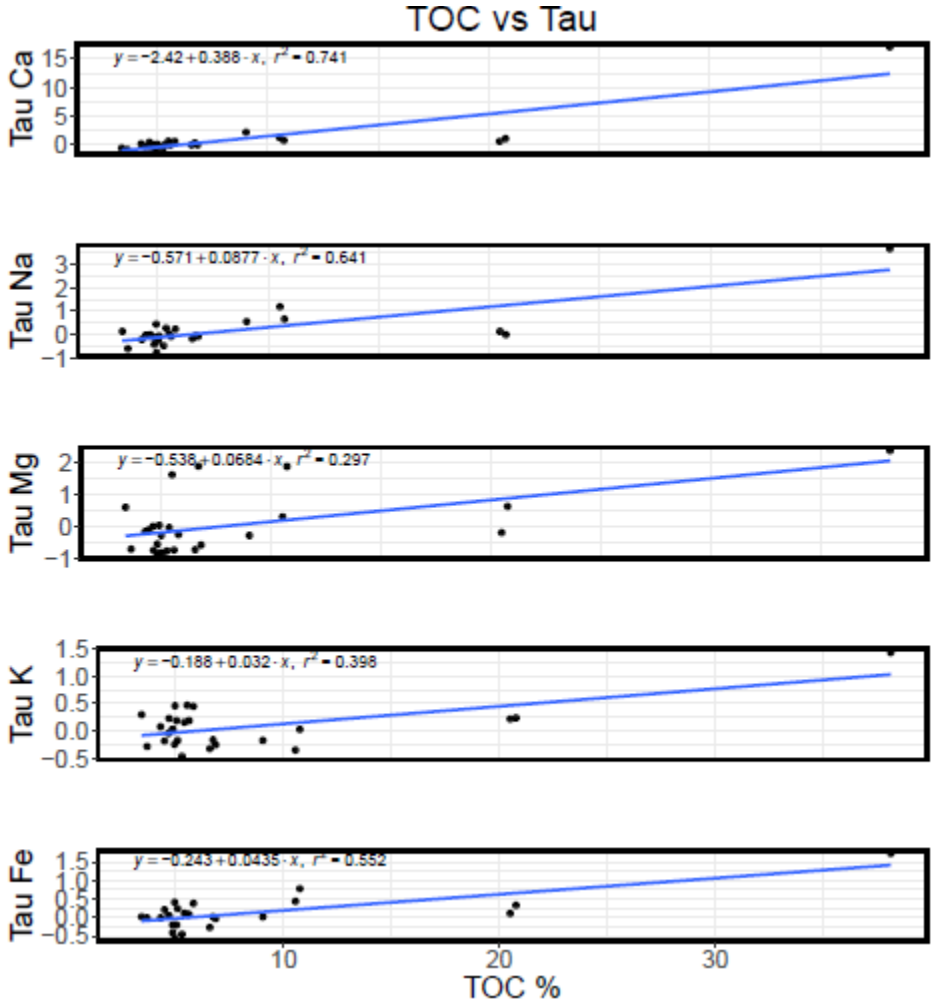

Appendix Figure A-1: *relationship between total organic carbon (TOC) content and tau values for base cations and iron indicating that base cations accumulate in areas that are rich in organic carbon. TOC data was provided by M. Cincotta from the top 15cm of soils taken on all 3 transects.*

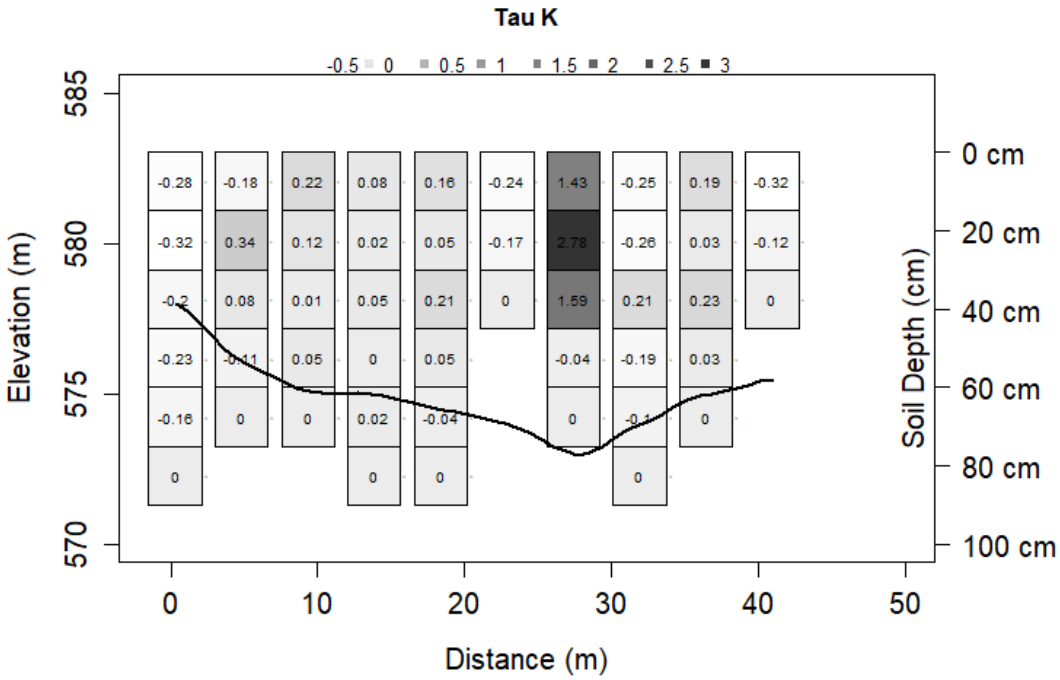

Appendix Figure A-2: *tau values for K along the transect with the greatest relief (compare to Fig. 2-4). As other base cations, K is depleted from all hilltop and some hillslope soils while it is enriched in riparian soil.*

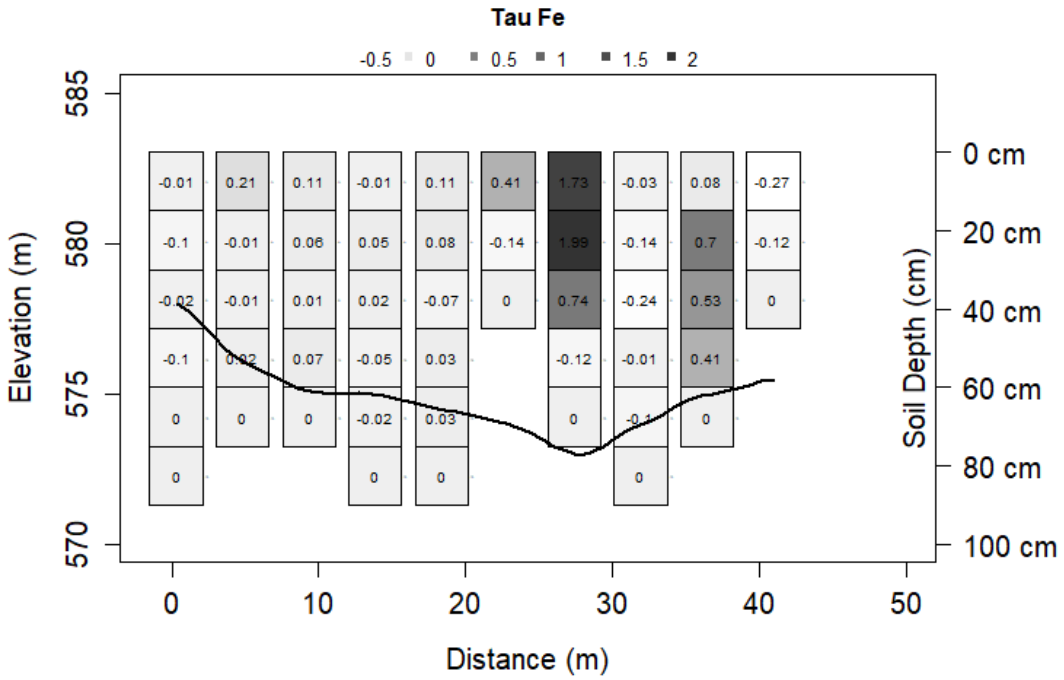

Appendix Figure A-3: t*au values for Fe along the transect with the greatest relief (Fig. 2-4). Fe is mildly depleted from hilltop soils, variable in hillslope soils, and accumulates in the upper horizons of riparian soils.*

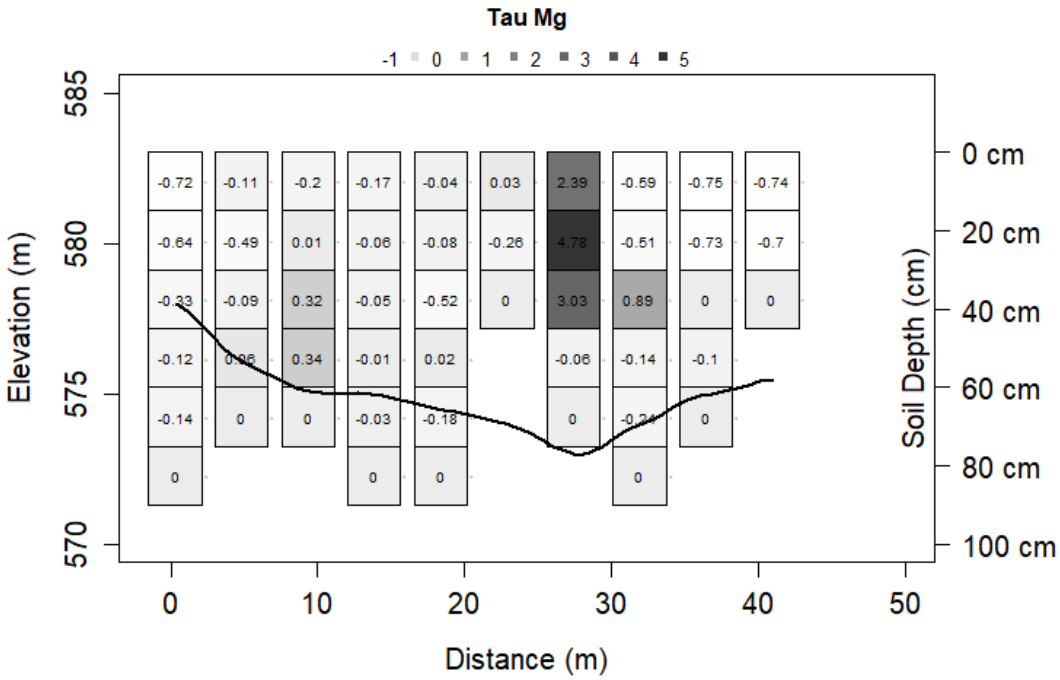

Appendix Figure A-4: *tau values for Mg along the transect with the greatest relief (compare to Fig. 2-4). Mg is strongly depleted from hilltop soils, mildly depleted in hillslope soils, and accumulates in riparian soils. Trends in Mg are consistent with trends in other base cations along this transect.*

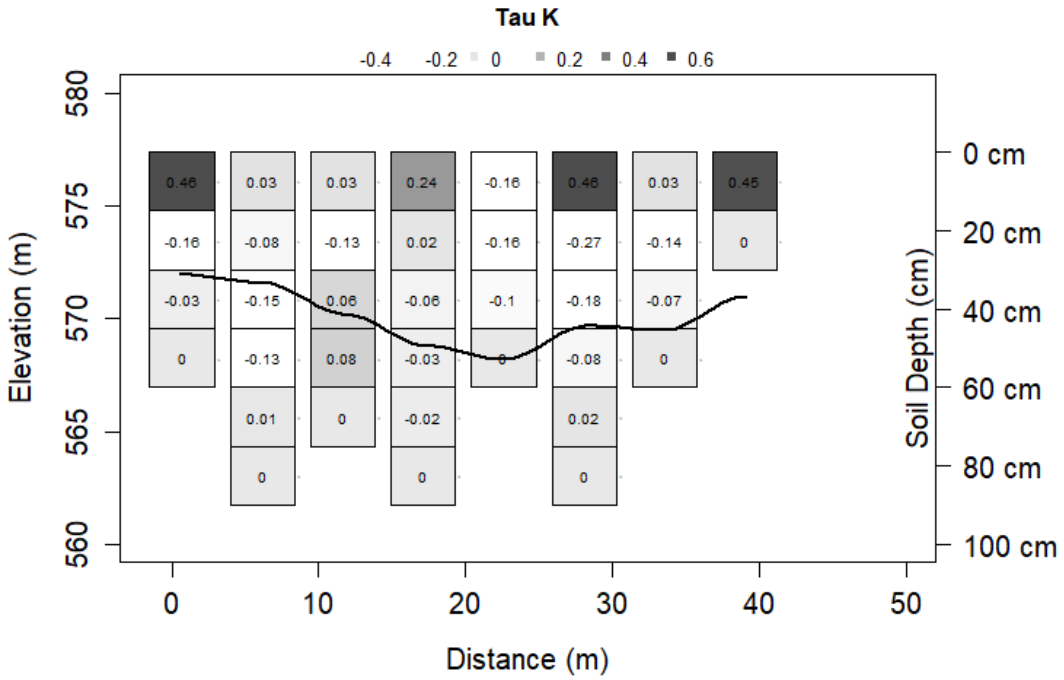

Appendix Figure A-5: *tau values for K along the transect with intermediate relief (supplementary materials Fig. 2-3). K tau values indicate a biogenic profile with depletions at depth and enrichments at the surface. Unlike the transect with the greatest relief, K is not accumulating with riparian soils on this transect. Unlike Ca and Na on this transect K is not accumulating with riparian soils but the variability in hilltop and hillslope soils is consistent with other base cations on this transect.*

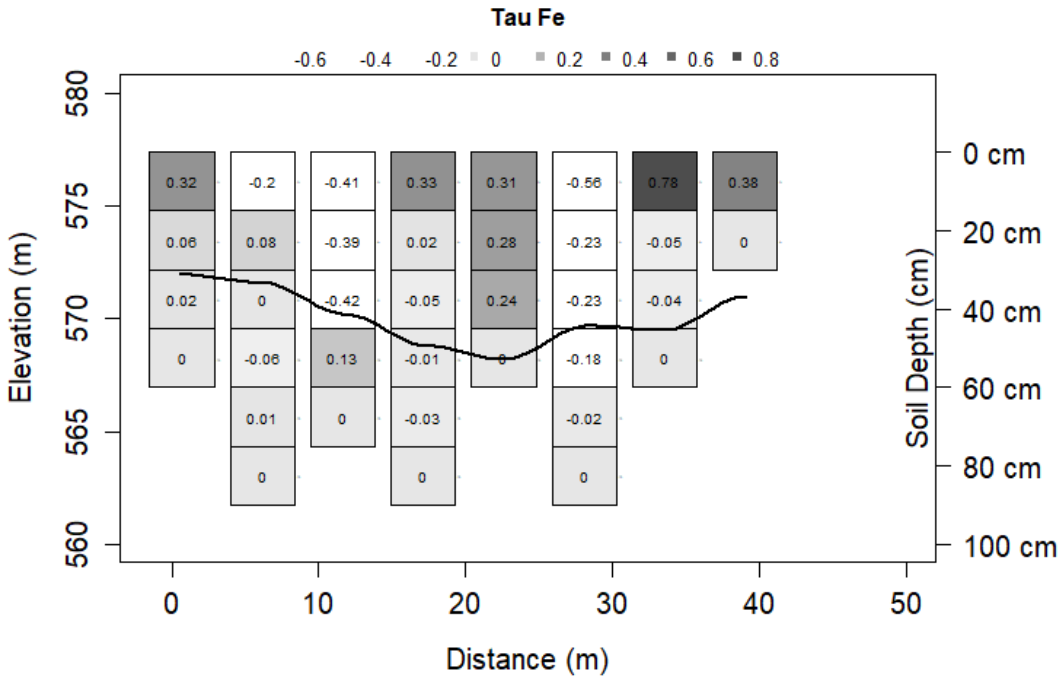

Appendix Figure A-6: *tau values for Fe along the transect with intermediate relief (supplementary materials Fig. 2-3). Hilltop soils are enriched in Fe, hillslope soils are highly variable, and riparian soils accumulate Fe. Trends in hilltop and hillslope soils differ from trends observed on the transect with the greatest relief.*

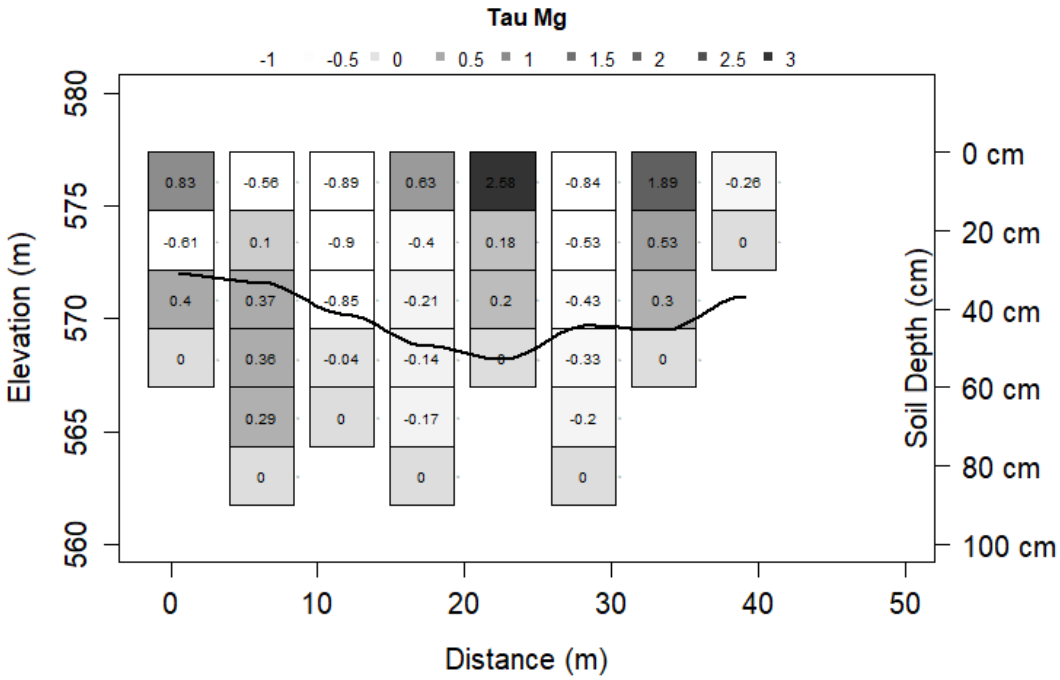

Appendix Figure A-7: *tau values for Mg along the transect with intermediate relief (supplementary materials Fig. 2-3). Mg is highly variable in hilltop and hillslope soils and accumulates in riparian soils. The variability in Mg in hilltop and hillslope soils as well as the accumulation in riparian soils is consistent with trends in other base cations in this transect.*

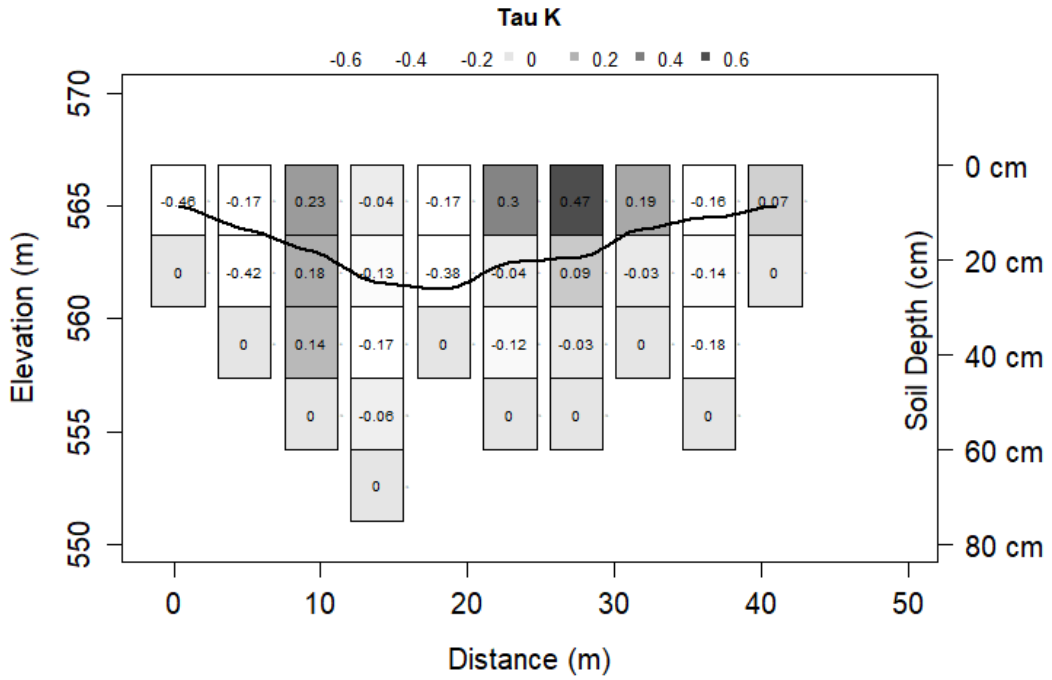

Appendix Figure A-8: *tau values for K along the transect with the least relief (supplementary materials Fig. 2-2). Unlike the transect with the greatest relief, K is not accumulating in riparian soils on this transect. Unlike Ca and Na on this transect K is not accumulating with riparian soils but the variability in hilltop and hillslope soils is consistent with other base cations on this transect.*

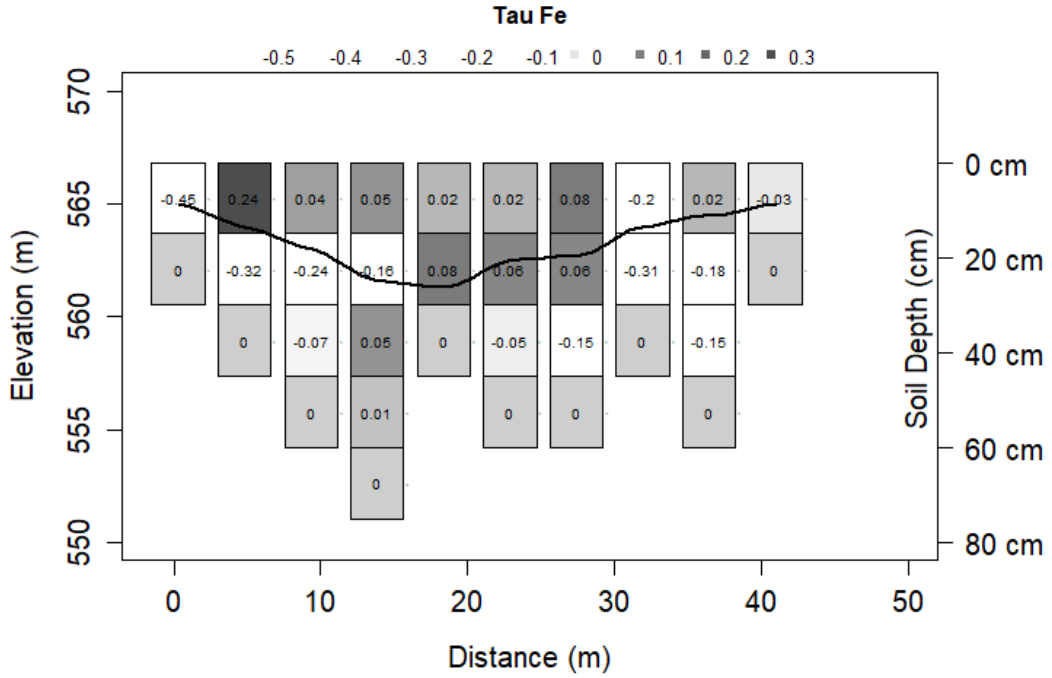

Appendix Figure A-9: *tau values for Fe along the transect with the least relief (supplementary materials Fig. 2-2). Hilltop tau values are variable, hillslope soils are generally mildly enriched close to the surface, and riparian soils accumulate Fe. Trends in hilltop and hillslope soils differ from trends observed on the transect with the greatest relief but trends in riparian soils agree.*

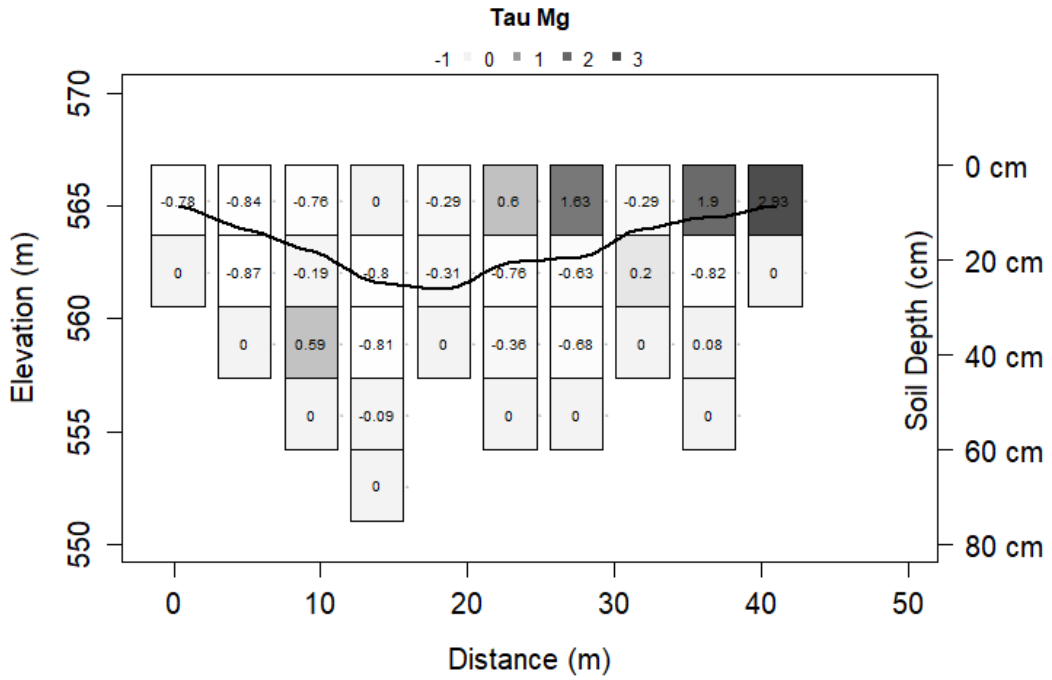

Appendix Figure A-10: *tau values for Mg along the transect with the least relief (supplementary materials Fig. 2-2). Hilltop and hillslope tau values are highly variable and depleted in riparian soils. The variability in Mg in hilltop and hillslope soils is consistent with trends in other base cations in this transect. Mg shows biogenic profiles on the east side of this transect and depleted profiles on the west side.*

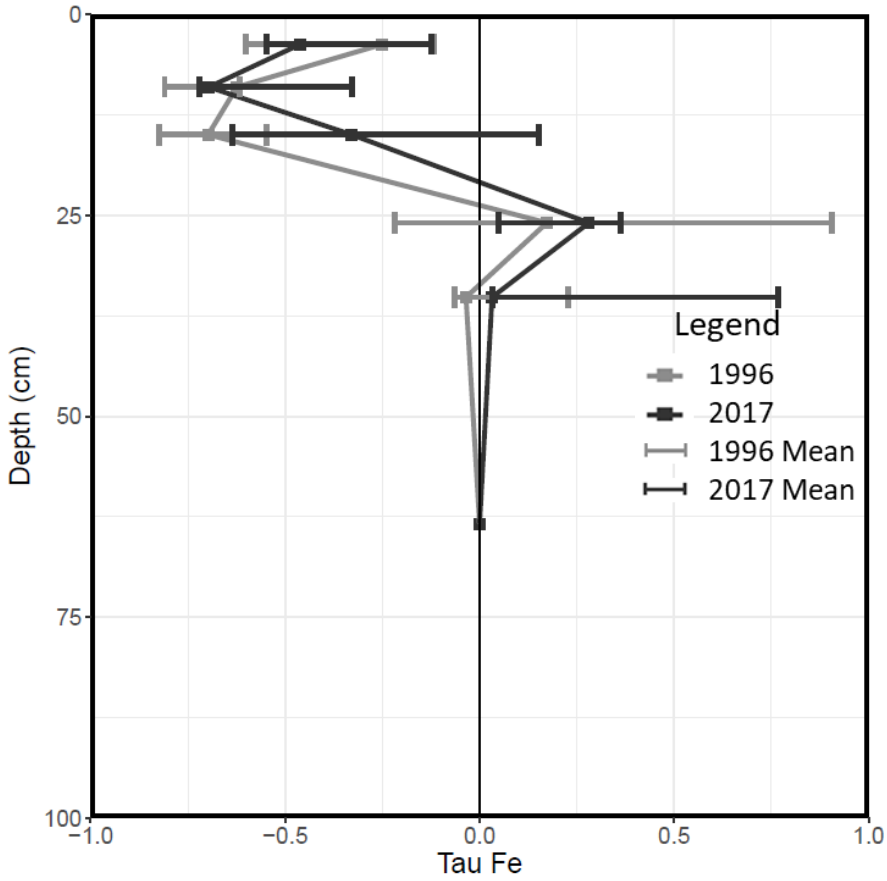

Appendix Figure A-11: *tau values for Fe in a typical hilltop soil (Spodosol, Fig. 2-5). Fe is depleted from upper soil horizons and enriched in the spodic horizon and in the underlying mineral soil. Tau values for Fe did not change significantly between archived and modern samples. Error bars in this figure represent the mean and standard error of all Spodosol samples taken in each sampling campaign.*

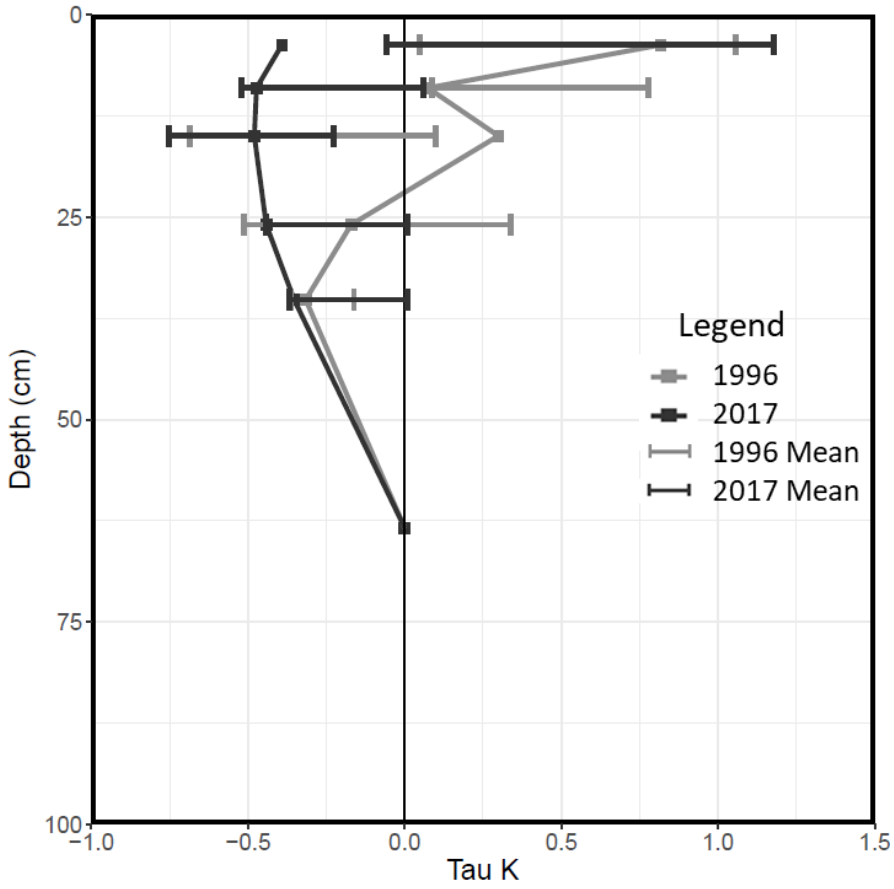

Appendix Figure A-12: *tau values for K in a typical hilltop soil (Spodosol, Fig. 2-5). K generally shows a biogenic profile (except in the resampled soil (2017)), which is consistent with other base cations in this soil. Mean tau values did not change significantly between archived and modern samples but the resampled pit showed consistently lower tau values for K than the archived pit. Error bars in this figure represent the mean and standard error of all Spodosol samples taken in each sampling campaign.*

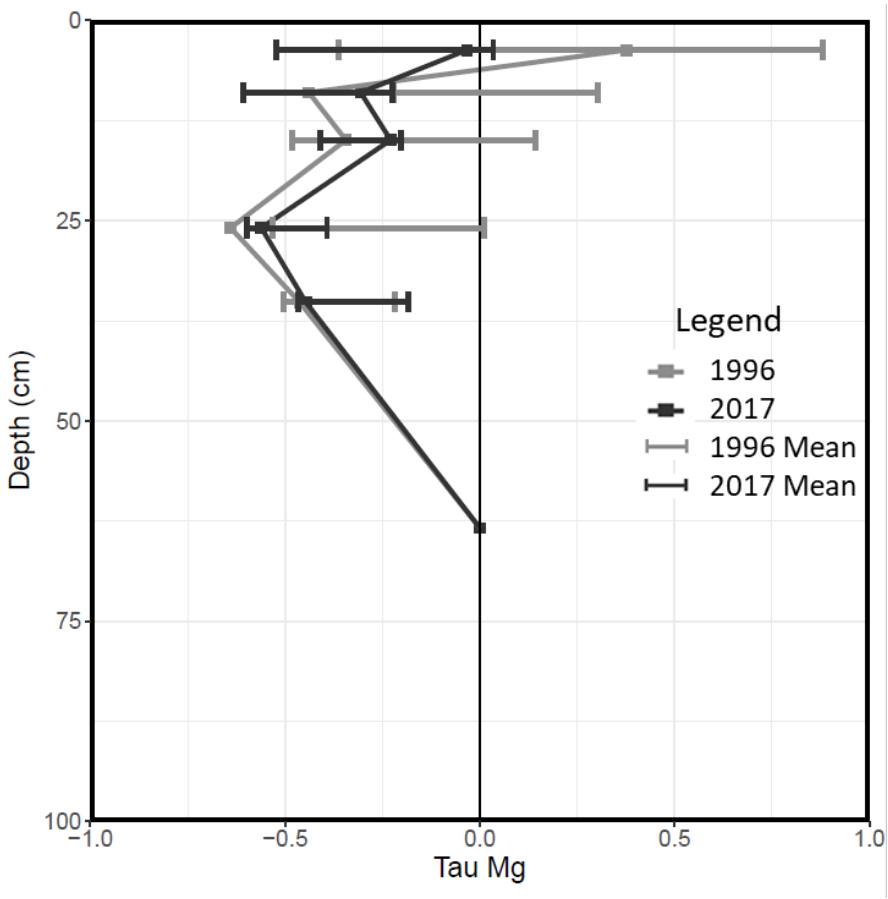

Appendix Figure A-13: *tau values for Mg in a typical hilltop soil (Spodosol, Fig. 2-5). Mg shows a biogenic profile in both the archived and modern soils which is consistent with other base cations in this soil. Values and means did not change significantly between archived and modern samples. Error bars in this figure represent the mean and standard error of all Spodosol samples taken in each sampling campaign.*

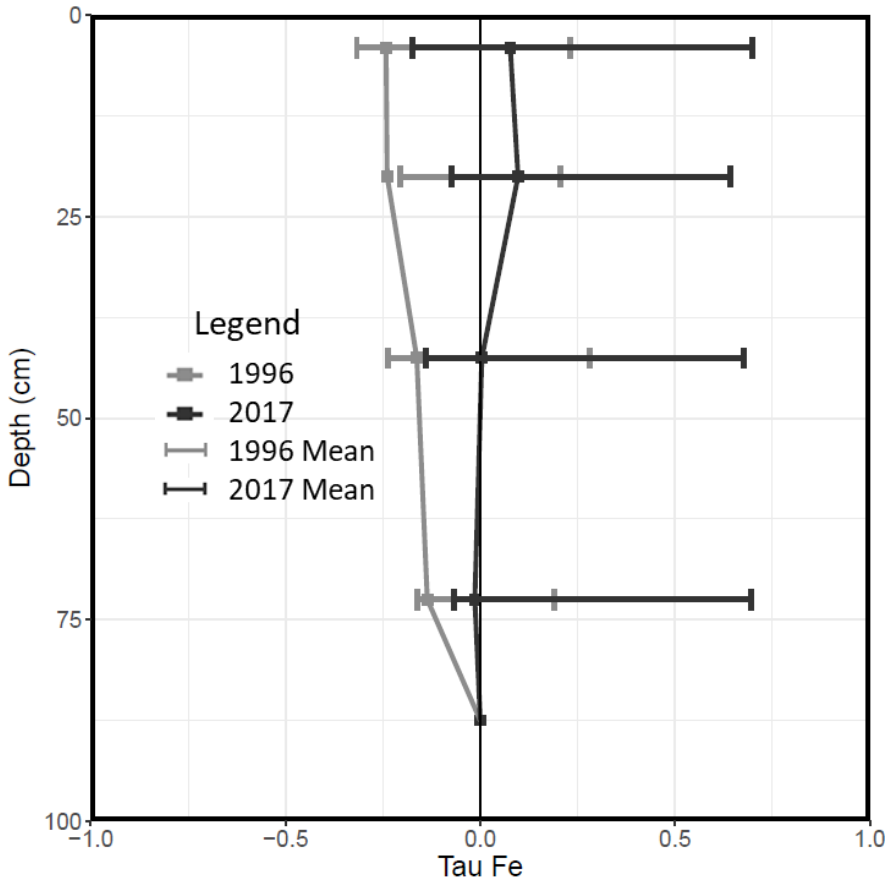

Appendix Figure A-14: *tau values for Fe in a typical hillslope soil (Inceptisol, Fig. 2-6). Fe shows a nearly immobile profile in this soil but is highly variable. Changes in tau values are not significant between archived and modern samples. Error bars in this figure represent the mean and standard error of all Spodosol samples taken in each sampling campaign.*

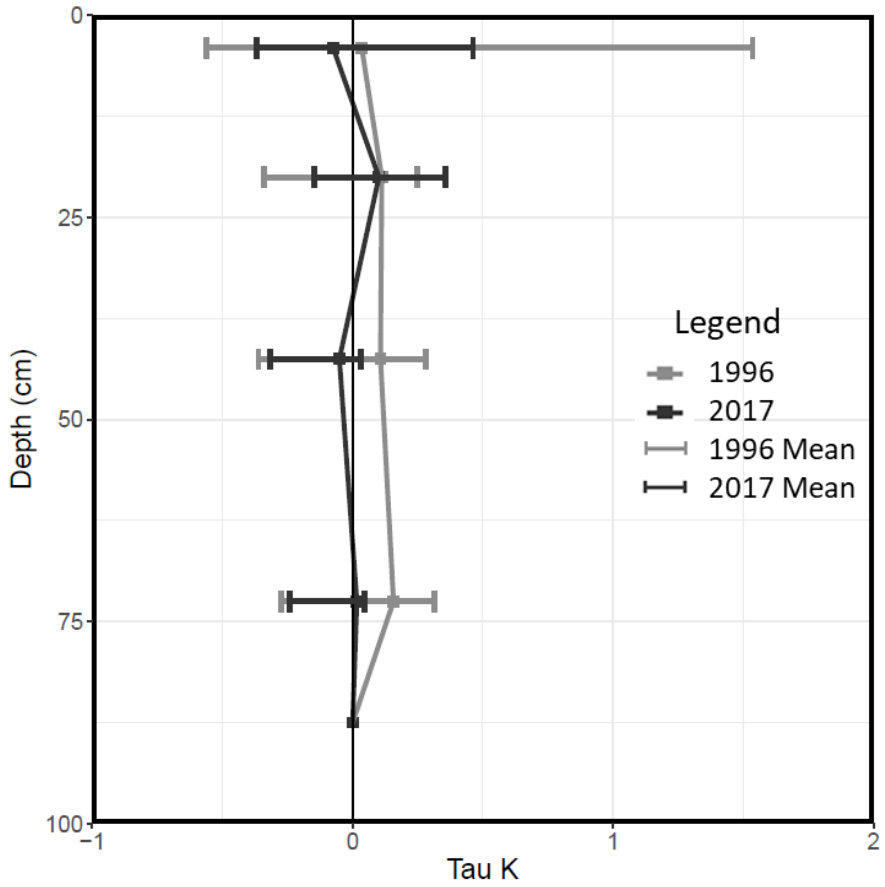

Appendix Figure A-15: *tau values for K in a typical hillslope soil (Inceptisol, Fig. 2-6). K shows a nearly immobile profile with no significant change between archived and modern data but shows some variability in the uppermost horizon. This pattern is consistent with other base cations in this soil. Error bars in this figure represent the mean and standard error of all Spodosol samples taken in each sampling campaign.*

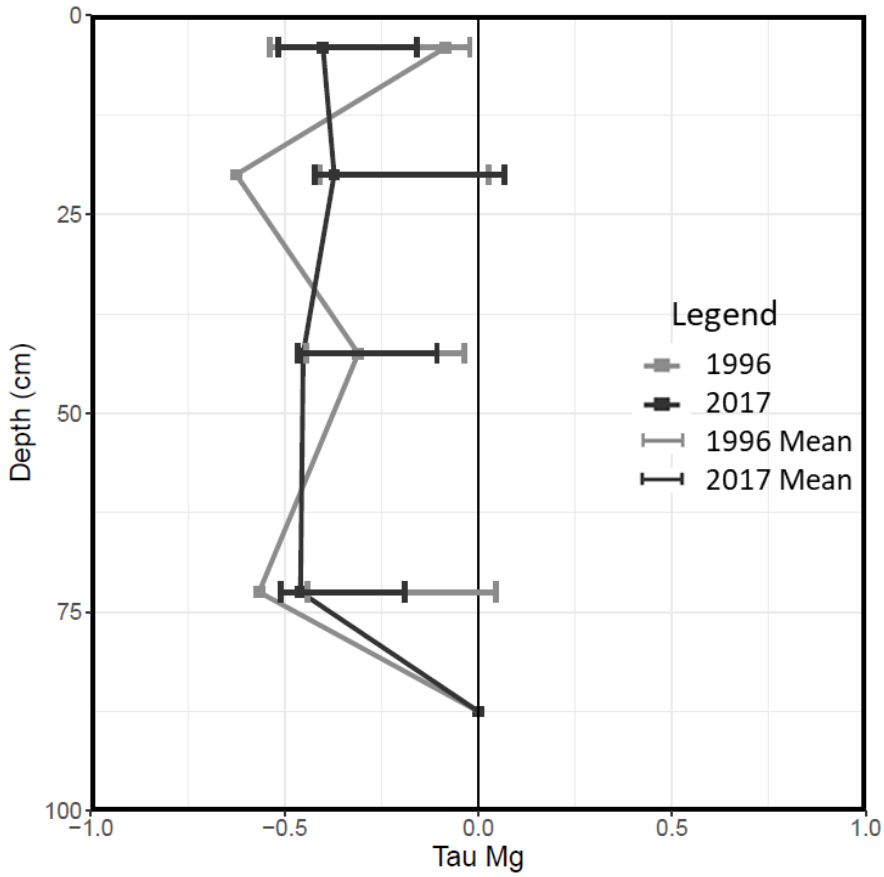

Appendix Figure A-16: *tau values for Mg in a typical hillslope soil (Inceptisol, Fig. 2-6). Mg shows a consistently depleted profile in all samples which is inconsistent with the nearly immobile profiles for other base cations in this soil. Error bars in this figure represent the mean and standard error of all Spodosol samples taken in each sampling campaign.*

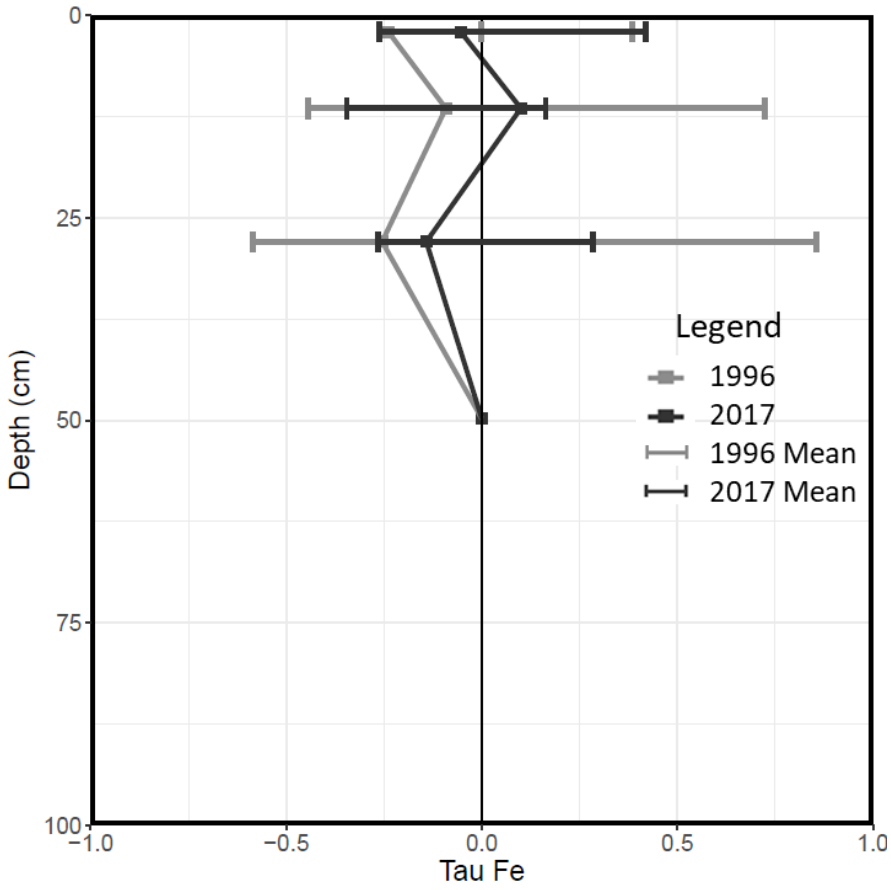

Appendix Figure A-17: t*au values for Fe in a typical riparian soil (Histosol, Fig. 2-7). Fe shows a highly variable profile in all samples and variability increases with depth. There are no significant changes between archived and modern samples, but archived samples have higher variability. Error bars in this figure represent the mean and standard error of all Spodosol samples taken in each sampling campaign.*

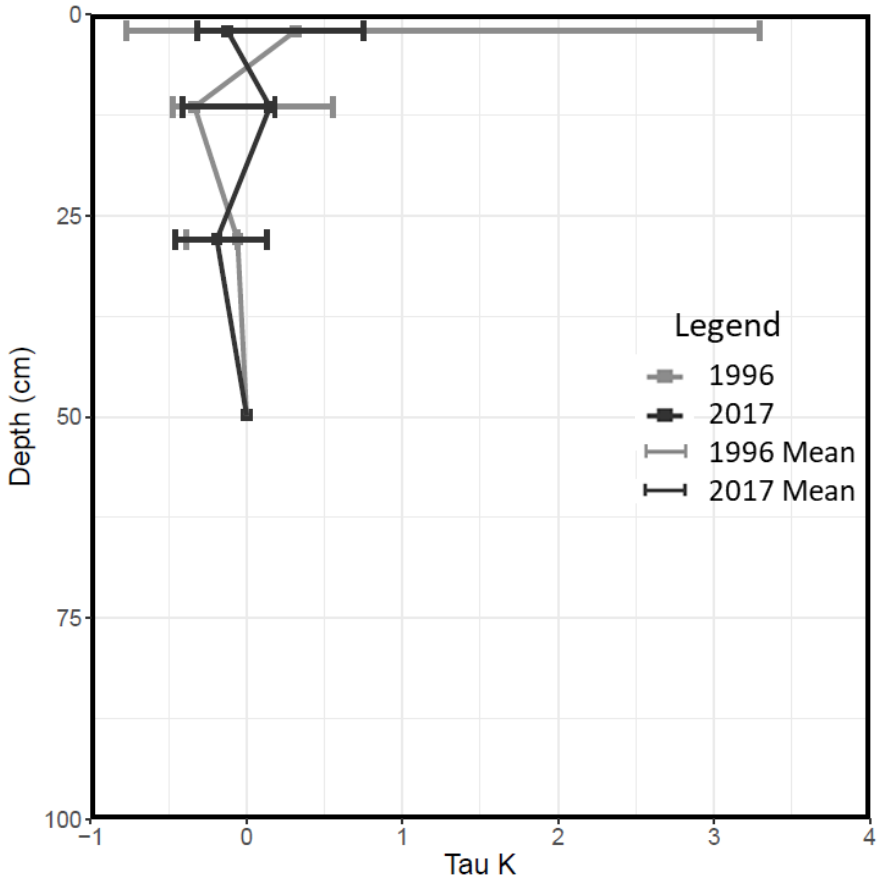

Appendix Figure A-18: *tau values for K in a typical riparian soil (Histosol, Fig. 2-7) showing a biogenic profile in all samples except the resampled pit in 2017, which is consistent with other base cations in this soil. The archived mean of the upper horizon is highly variable, but the modern mean shows less variability. Error bars in this figure represent the mean and standard error of all Spodosol samples taken in each sampling campaign.*

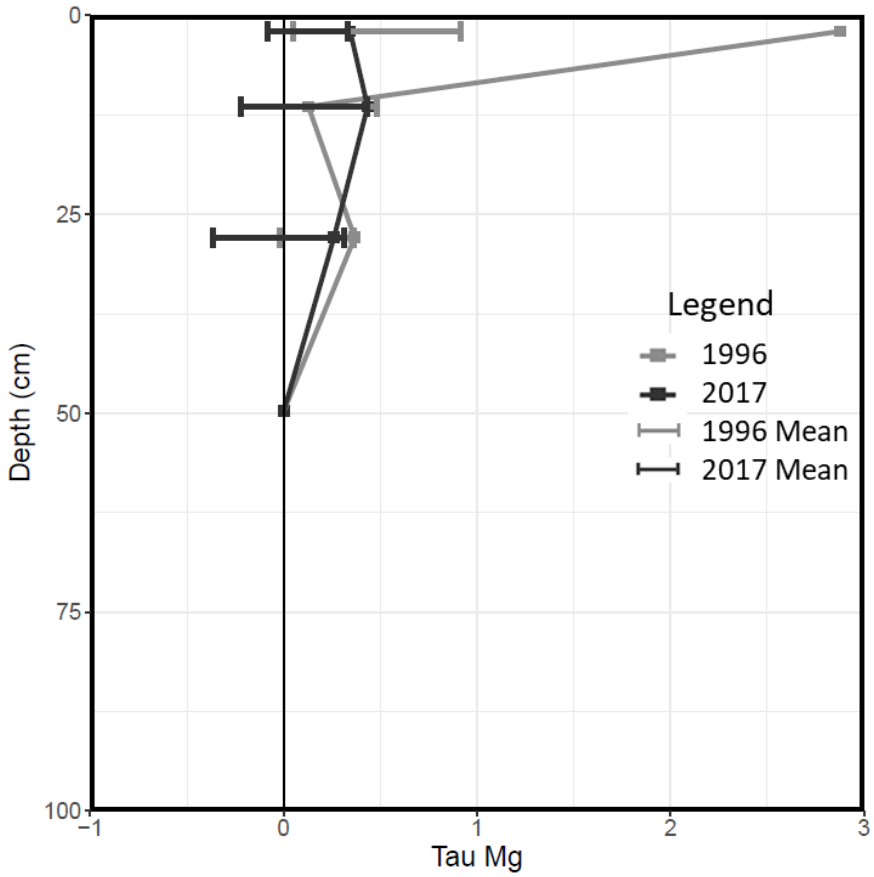

Appendix Figure A-19: *tau values for Mg in a typical riparian soil (Histosol, Fig. 2-7). Mg shows an addition profile with the highest enrichments at the surface which is likely due to biologic cycling but shows little signs of depletions at depth. This trend is consistent with other base cations in this soil. Error bars in this figure represent the mean and standard error of all Spodosol samples taken in each sampling campaign.*

APPENDIX B: ADDITIONAL AQUEOUS PHASE DATA

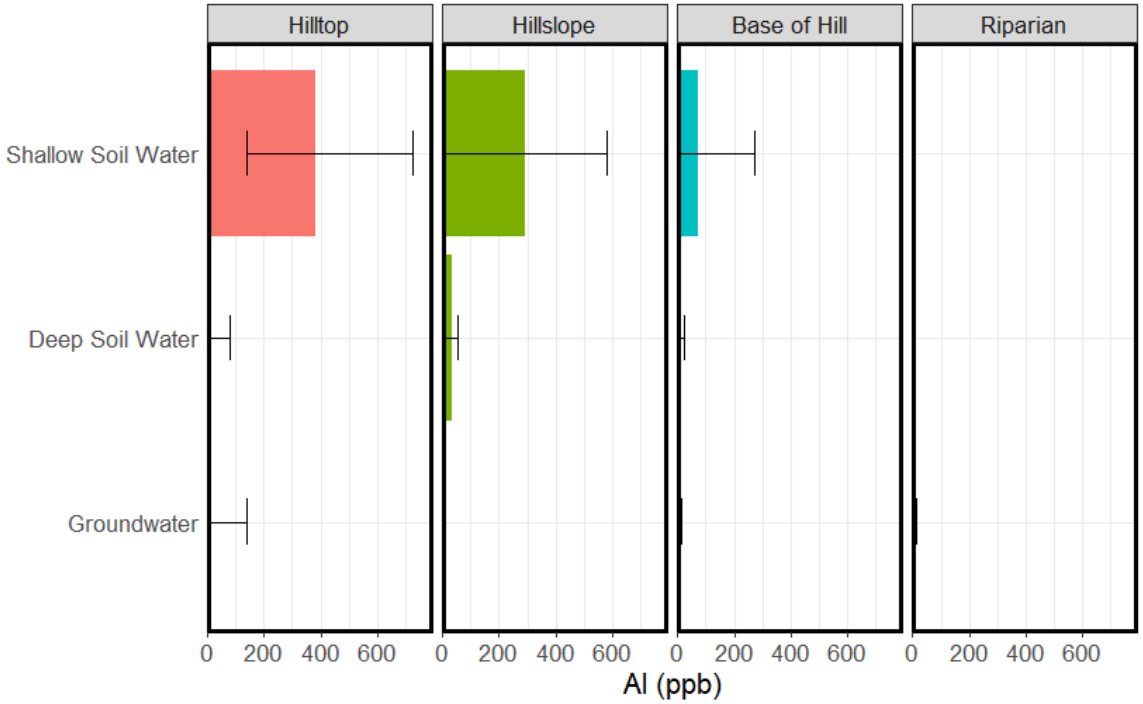

Appendix Figure B-1: *colored bars represent the mean Al concentration over the study period and error bars represent the range in measurement. Al is primarily released into shallow solution and concentrations decrease with depth and with proximity to the stream, presumably due to the increased buffering capacity in these locations limiting solubility.*

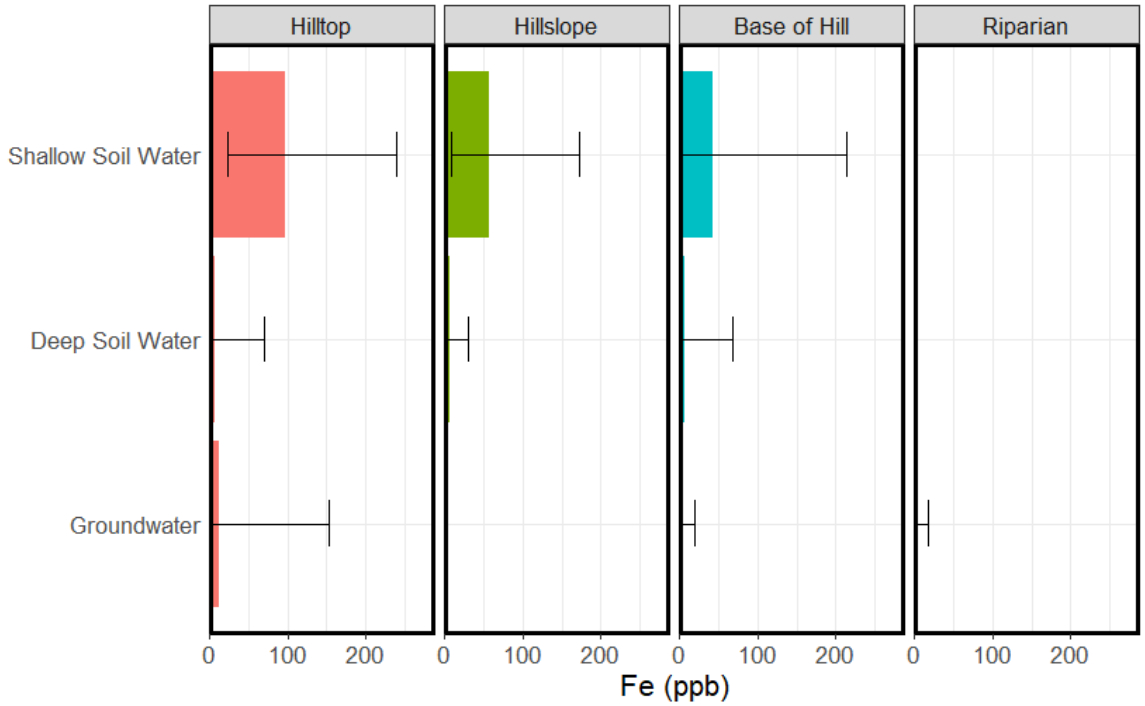

Appendix Figure B-2: *colored bars represent the mean Fe concentration over the study period and error bars represent the range in measurement. Fe is primarily released into shallow solution and concentrations decrease with depth and with proximity to the stream, presumably due to the increased buffering capacity in these locations limiting solubility and association with organic materials.*

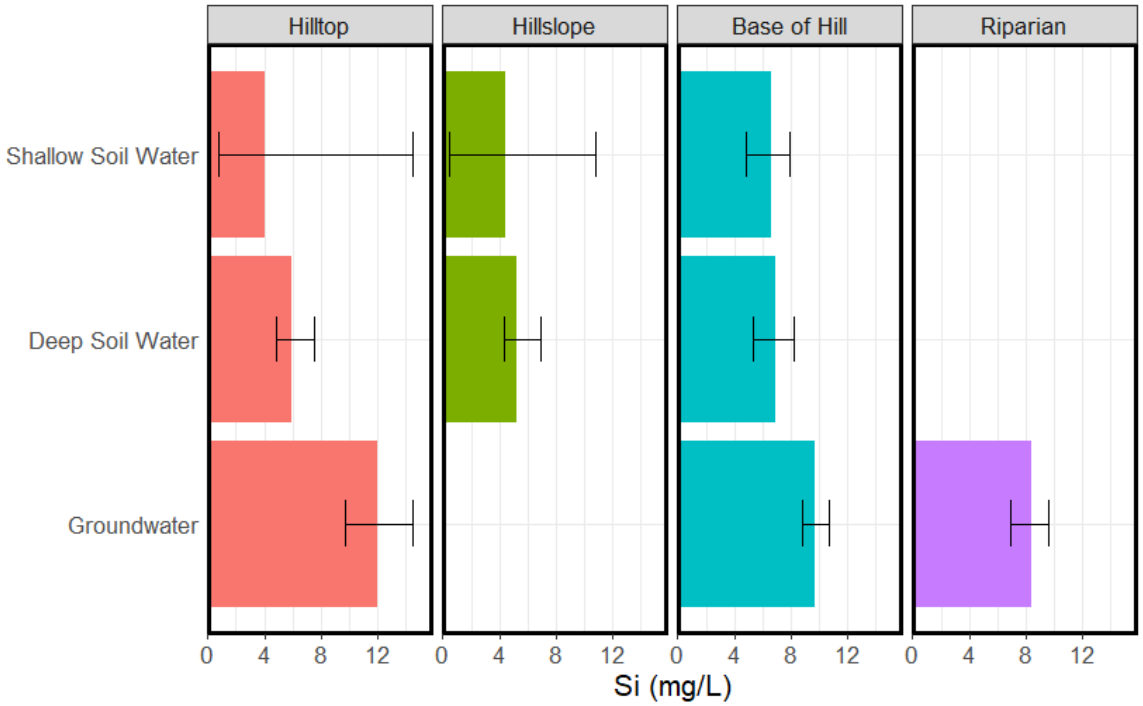

Appendix Figure B-3: *colored bars represent the mean Si concentration over the study period and error bars represent the range in measurement. Si is released into solution at all depths and landscape positions and values are highly variable in shallow soil water. Si is likely transferred laterally in soil solution as downslope soil solution has consistently higher mean concentrations. This also shows that Si is transferred vertically at each landscape position as deeper samples are consistently higher. Higher Si concentrations in GW could be due to vertical transfer but are also likely representative of a solution in equilibrium with the weathering front due to a longer fluid residence time. Si lost along the GW flowpath is consistent with solid phase results which suggest that clay minerals are forming in till. This result is also consistent with solid phase weathering data which suggests that the silicate weathering front is in the mineral soil.*

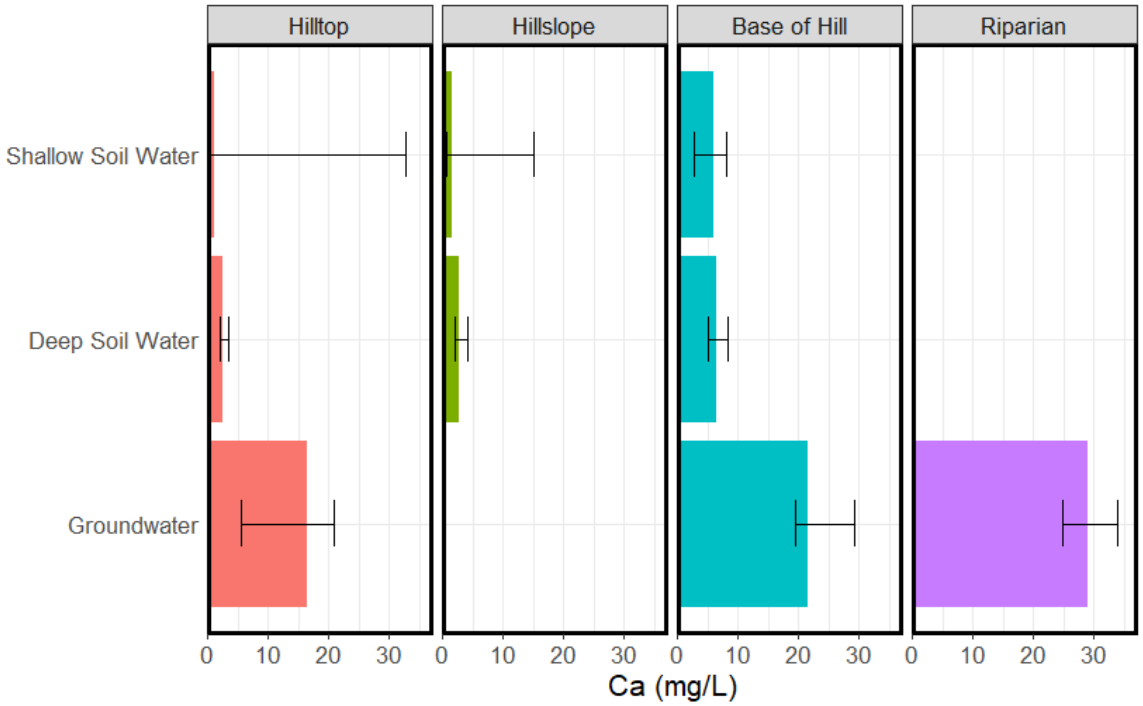

Appendix Figure B-4: *colored bars represent the mean Ca concentration over the study period and error bars represent the range in measurement. Ca is released into solution at all depths and landscape positions but is primarily released from weathered till. Ca values are highly variable in shallow soil water on the hilltop and slope likely due to acid driven weathering events and sampling during relatively dry conditions. Results could indicate that Ca is transferred laterally as downslope samples have consistently higher Ca concentrations. This also indicates that Ca is transferred vertically as deeper samples have consistently higher Ca concentrations. Higher Ca concentrations in GW are likely in part due to vertical transfer but more likely represent carbonate weathering from deep till.*

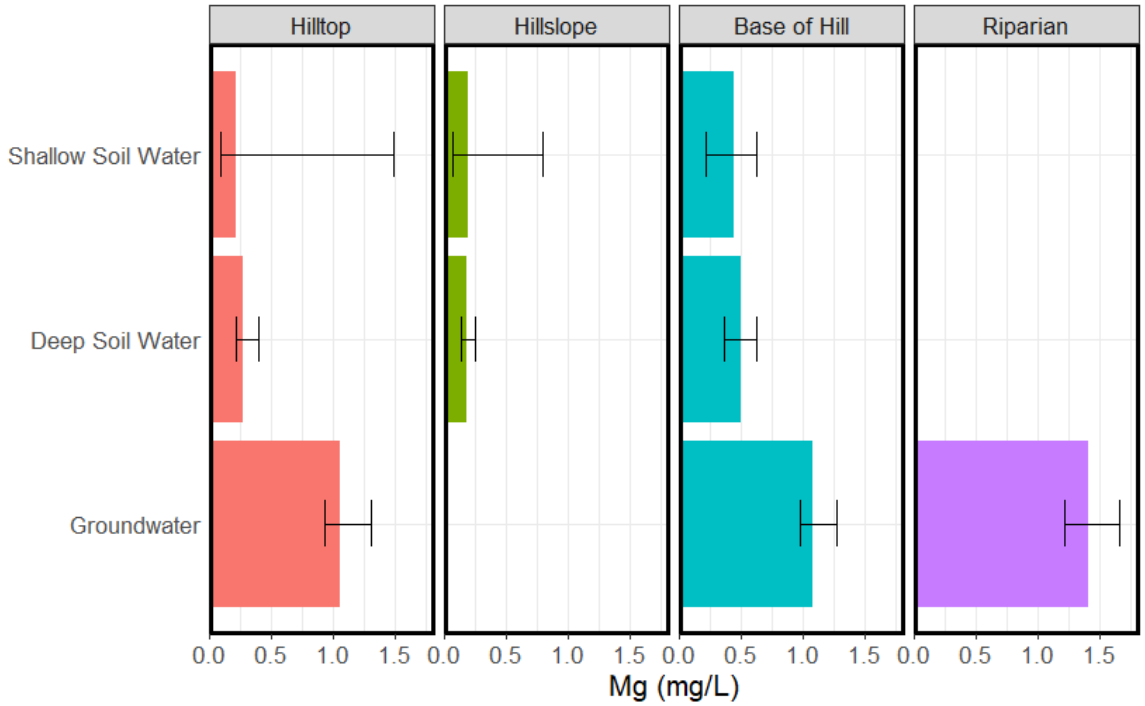

Appendix Figure B-5: *colored bars represent the mean Mg concentration over the study period and error bars represent the range in measurement. Mg is released into solution at all depths and landscape positions. Higher Mg concentrations in GW could be due to vertical transfer or could represent a solution in equilibrium with the weathering front due to a longer fluid residence time. Lateral transfer is likely responsible for the increased Mg concentrations at downslope locations.*

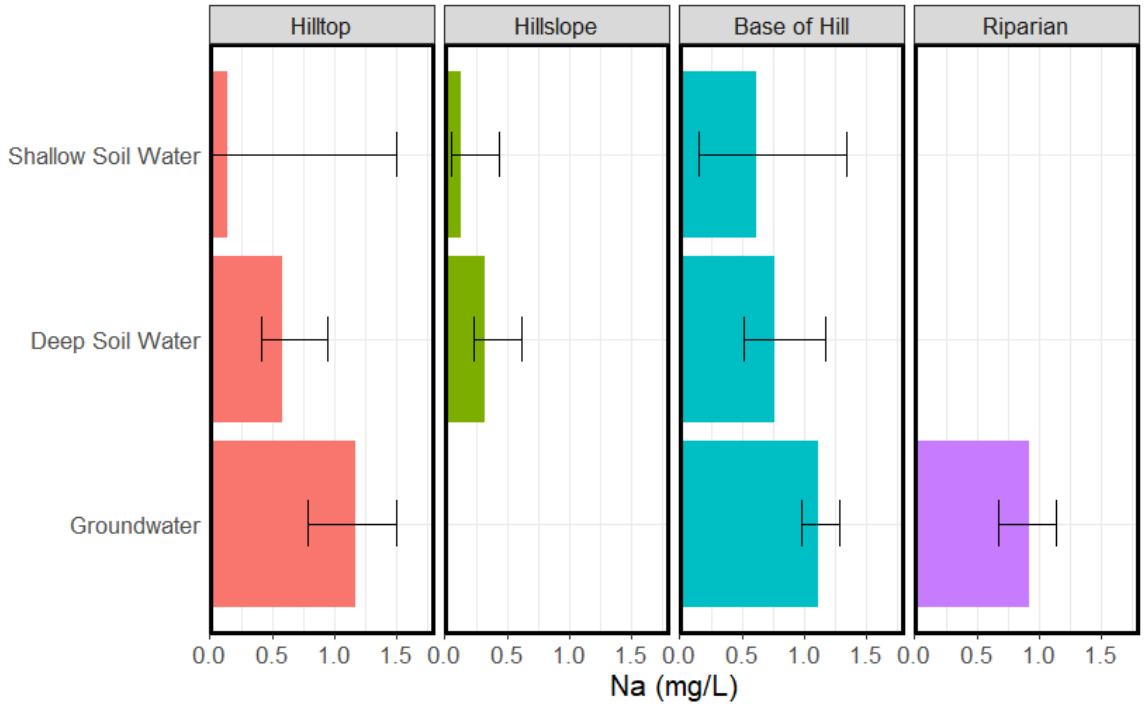

Appendix Figure B-6: *colored bars represent the mean Na concentration over the study period and error bars represent the range in measurement. Na is released into solution at all depths and landscape positions. Higher Na concentrations in GW could be due to vertical transfer or could represent a solution in equilibrium with the weathering front due to a longer fluid residence time. Lateral transfer is likely responsible for the increased Na concentrations at downslope locations.*

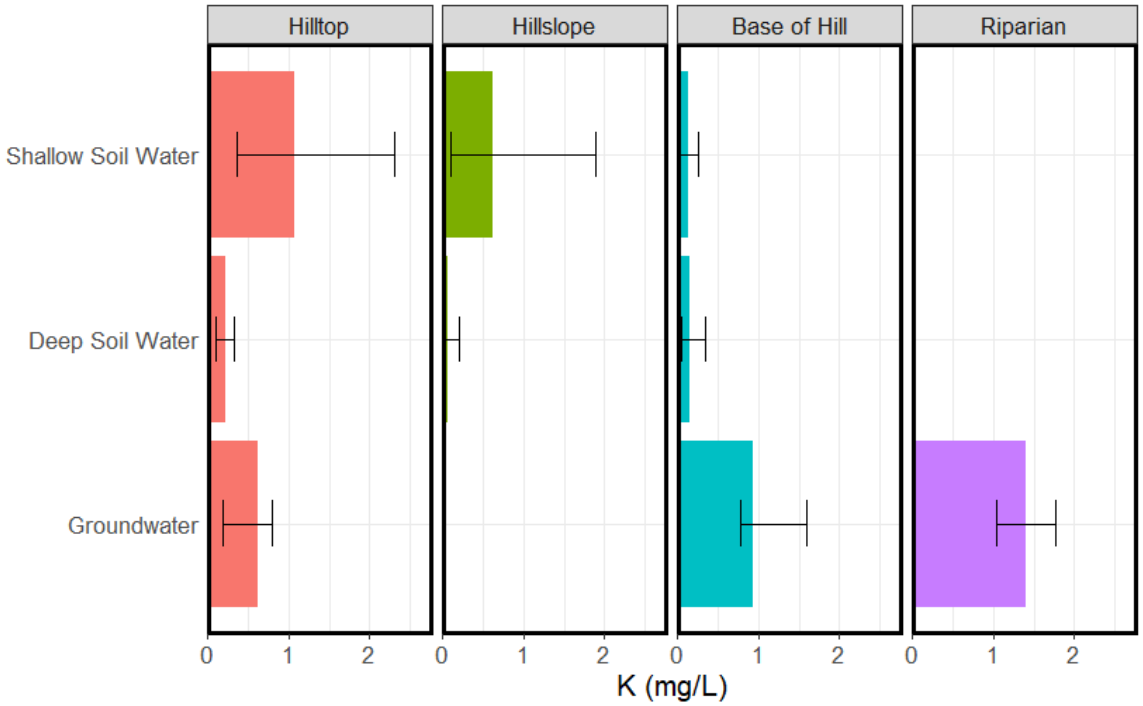

Appendix Figure B-7: *colored bars represent the mean K concentration over the study period and error bars represent the range in measurement. K is released into solution at all depths and landscape. Decreased K concentrations in shallow soil water with proximity to the stream are likely the result of biologic uptake.*

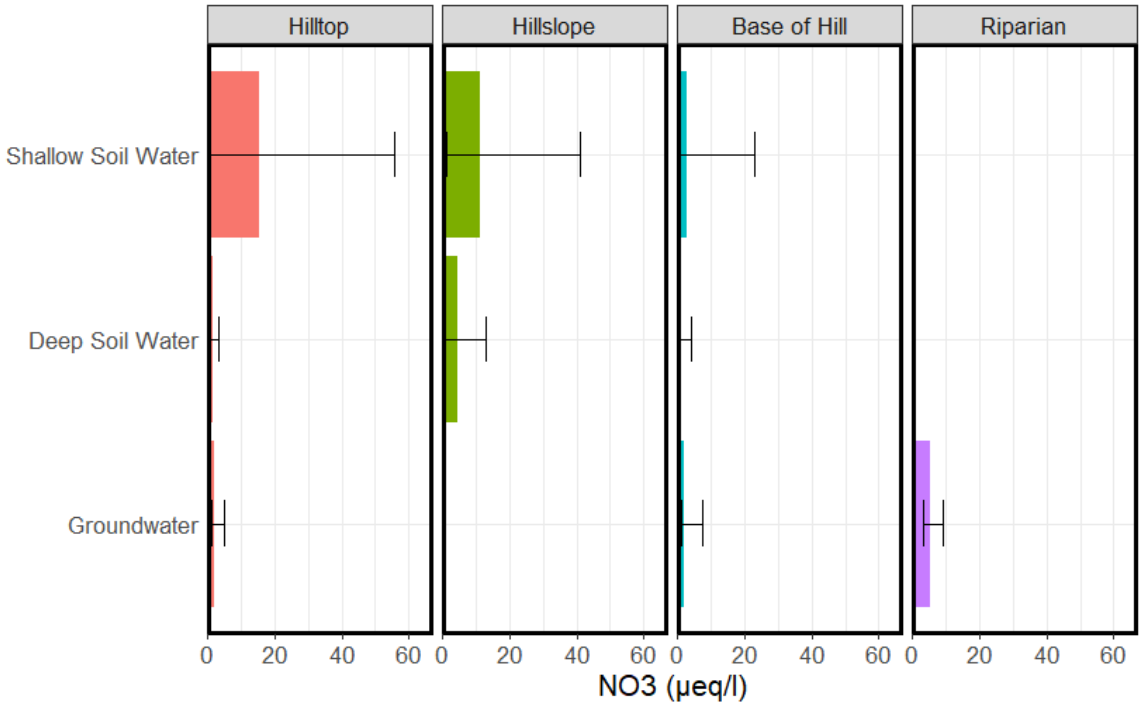

Appendix Figure B-8: *colored bars represent the mean nitrate (NO_3^-)concentration over the study period and error bars represent the range in measurement. Nitrate is likely delivered top down as concentrations in shallow soil water are significantly higher than deeper samples. Decreases in nitrate in shallow soil water with proximity to the stream are likely the result of biologic processing. Increases in nitrate along the GW flowpath are likely due to a substrate that is impenetrable for roots so once nitrate is transferred to GW the concentration increases with increasing residence time.*

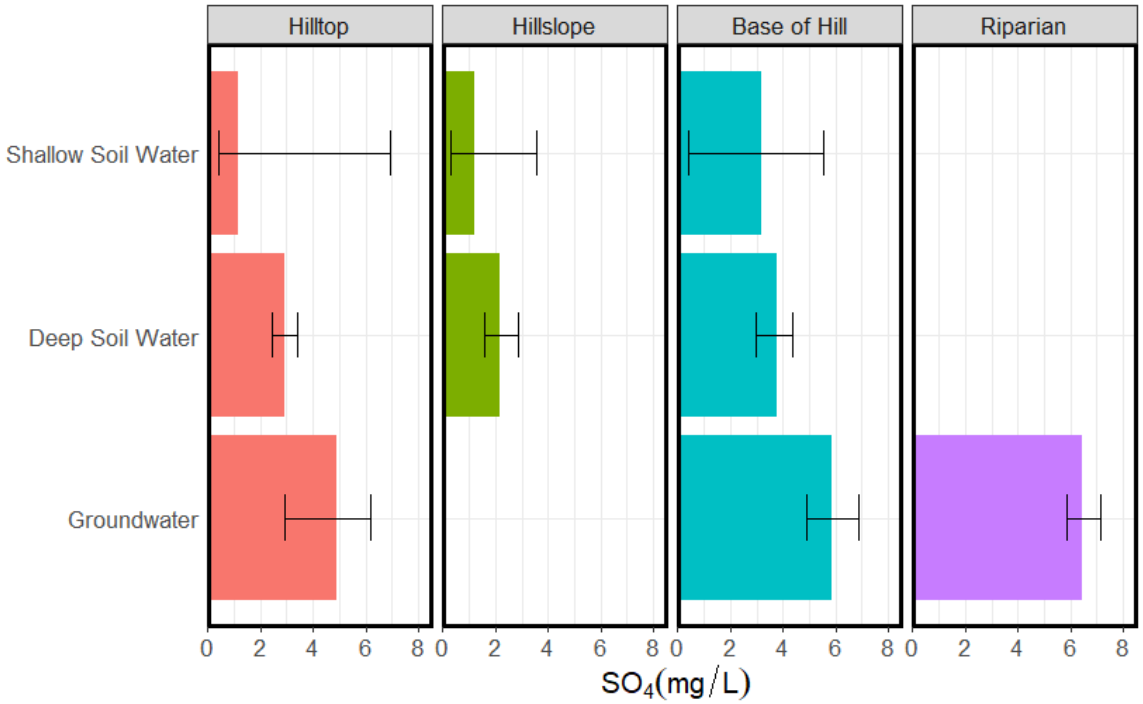

Appendix Figure B-9: *colored bars represent the mean sulfate (SO_4^{2-}) concentration over the study period and error bars represent the range in measurement. Increasing sulfate concentrations with depth are likely the result of both vertical transfer, storage in Histosols and pyrite oxidation at depth. Increasing sulfate concentrations with proximity to the stream are likely a result of lateral transfer in soil solution and pyrite oxidation in GW.*

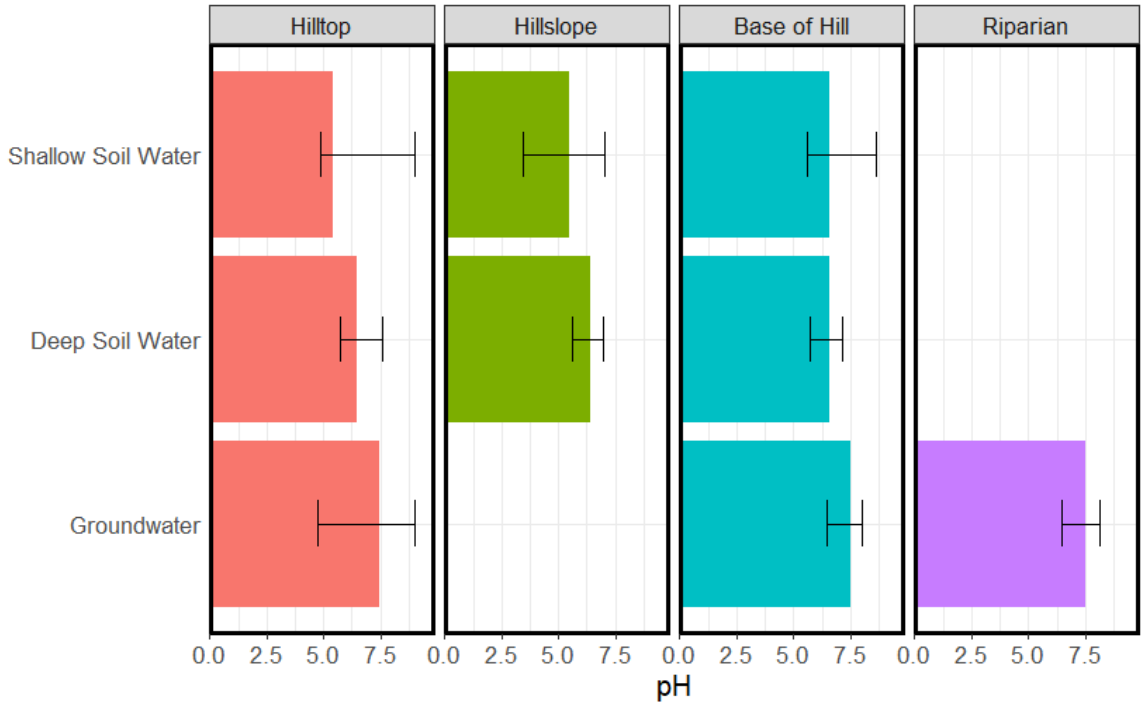

Appendix Figure B-10: *colored bars represent the mean pH over the study period and error bars represent the range in measurement. pH is lowest and highly variable in shallow soil solution, but variability decreases, and pH increases with depth and proximity to the stream.*

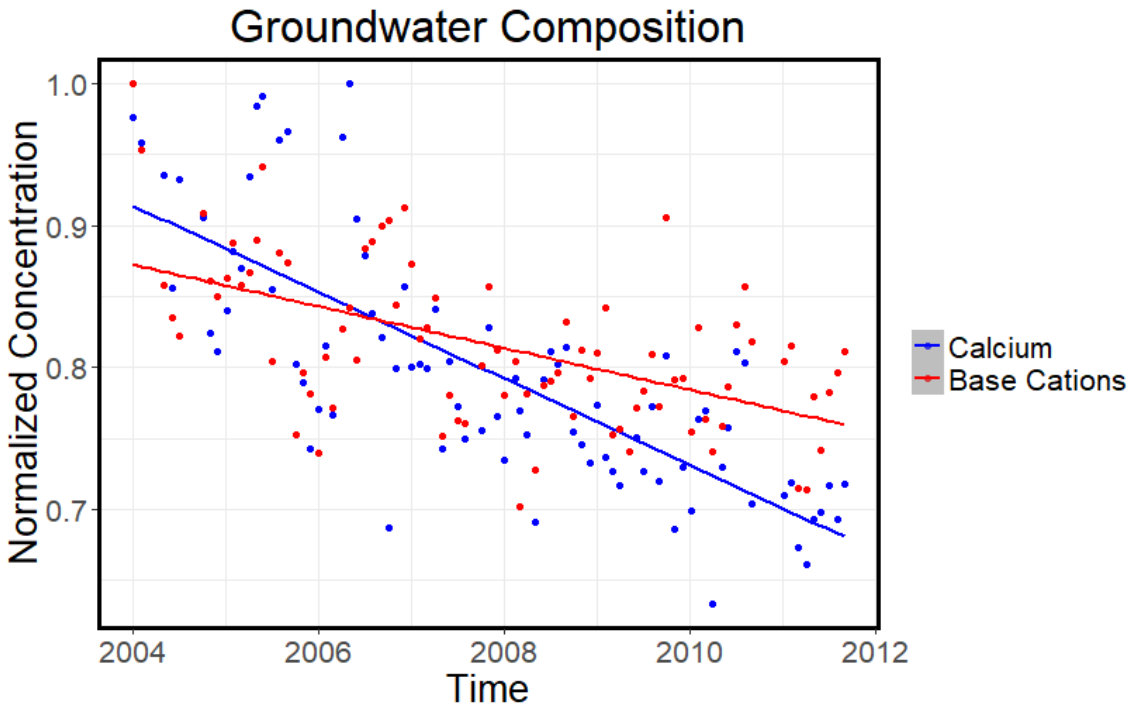

Appendix Figure B-11: *normalized concentrations (observed/max) of Ca and other base cations (Σ[K], [Mg], [Na]) over time in GW at the hilltop well. Linear fits show that Ca concentrations have declined more rapidly than that of other base cations, likely a result of decreased carbonate weathering due to decreased acid inputs.*

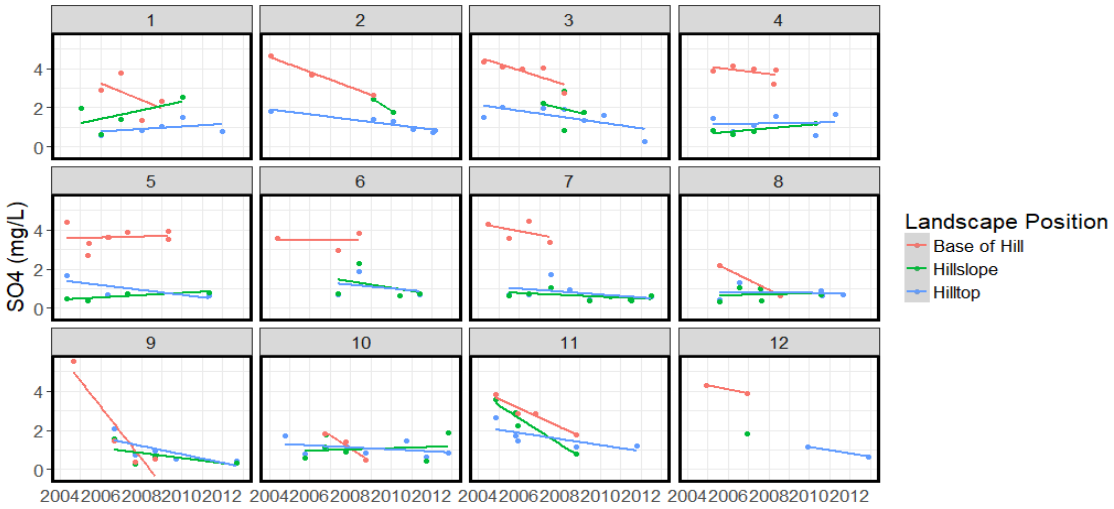

Appendix Figure B-12: *raw sulfate (SO_4^{2-}) concentrations in shallow soil solution by month (1=Jan, 2=Feb. etc.) for each year since 2004 (chosen to eliminate seasonal effects) and landscape position. This figure generally shows negative trends in sulfate content with time.*

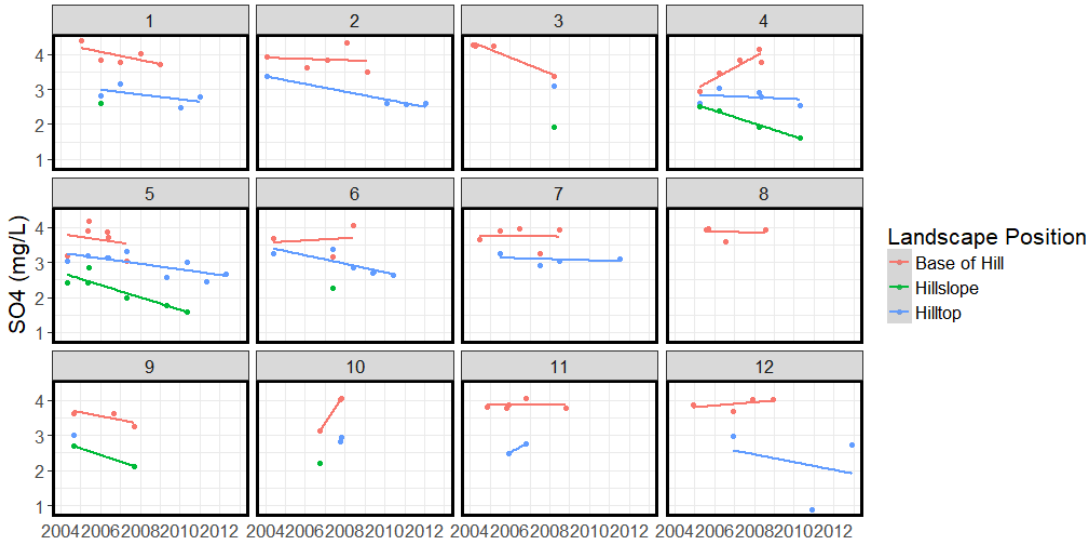

Appendix Figure B-13: *raw sulfate (SO_4^{2-}) concentrations in deep soil solution by month (1=Jan, 2=Feb. etc.) for each year since 2004 (chosen to eliminate seasonal effects) and landscape position. This figure generally shows negative trends in sulfate content with time.*

	R^2	P	Sig?	Direction	Min	Max	Range	Years
pH	0.0532	> 0.05	Yes	Positive	6.9	8.1	1.2	2004-2013
Sulfate	0.9215	< 0.05	Yes	Negative	4.4	5.3	0.9	2004-2013
Nitrate	0.1087	> 0.05	No	N/A	0	0.035	0.018	2004-2013
Silicon	0.015	> 0.05	No	N/A	12	12.3	0.6	2004-2012
Total Base Cations	0.649	< 0.05	Yes	Negative	17	21.4	4.1	2004-2012
Calcium	0.9597	< 0.05	Yes	Negative	15	18.8	4.2	2004-2012
Sodium	0.2749	> 0.05	No	N/A	1.1	1.22	0.09	2004-2012

Appendix Table B-1: *summary statistics for trends in GW presented in Supplementary Materials Figure 2-1. Significant trends are indicated by the column with the header: Sig? Direction indicates whether trends are positive or negative, Min indicates the minimum measured value (mg/L for all but pH), Max indicates the maximum measured value, range indicates the range of values measured, Years indicates the range of years included in the analysis.*

	R^2	P	Sig?	Direction	Min	Max	Range	Years
pH	0.8405	< 0.05	Yes	Negative	6.1	6.8	0.7	2004-2008
Sulfate	0.2569	> 0.05	No	N/A	69.9	72.2	2.3	2004-2008
Nitrate	0.9916	< 0.05	Yes	Positive	1.4	4.3	2.9	2004-2008
Silicon	0.2278	> 0.05	No	N/A	6.2	6.7	0.5	2004-2008
Total Base Cations	0.2429	> 0.05	No	N/A	5.8	6.2	0.4	2004-2008
Calcium	0.4808	> 0.05	No	N/A	4.7	5	0.3	2004-2008

Appendix Table B-2: *summary statistics for trends in deep soil solution independent of landscape position. Significant trends are indicated by the column with the header: Sig? Direction indicates whether trends are positive or negative, Min indicates the minimum measured value (mg/L for all but pH), Max indicates the maximum measured value, range indicates the range of values measured, Years indicates the range of years included in the analysis.*

	R^2	P	Sig?	Direction	Min	Max	Range	Years
pH	0.7661	= 0.05	Yes	Negative	5.5	6.3	0.8	2004-2008
Sulfate	0.6966	~=.05 (.08)	Yes	Negative	1.55	3.22	1.67	2004-2008
Nitrate	0.6564	> 0.05	No	N/A	0.1	0.2	0.1	2004-2008
Silicon	0.1825	< 0.05	No	N/A	4.6	5.7	1.1	2004-2008
Total Base Cations	0.6576	> 0.05	No	N/A	3.4	5.8	2.4	2004-2008
Calcium	0.6739	> 0.05	No	N/A	2.4	4.2	1.8	2004-2008

Appendix Table B-3: *summary statistics for trends in shallow soil solution independent of landscape position. Significant trends are indicated by the column with the header: Sig? Direction indicates whether trends are positive or negative, Min indicates the minimum measured value (mg/L for all but pH), Max indicates the maximum measured value, range indicates the range of values measured, Years indicates the range of years included in the analysis.*